
# Program and Abstract Volume

LUNAR AND PLANETARY INSTITUTE

LPI Contribution No. 1559

# Nördlingen 2010

## The Ries Crater, the Moon, and the Future of Human Space Exploration

June 25–27, 2010

Nördlingen, Germany

## Sponsors

Museum für Naturkunde –
Leibniz-Institute for Research on Evolution and Biodiversity at the Humboldt University Berlin, Germany
Institut für Planetologie, University of Münster, Germany
Deutsches Zentrum für Luft- und Raumfahrt DLR (German Aerospace Center) at Berlin, Germany
Institute of Geoscience, University of Freiburg, Germany
Lunar and Planetary Institute (LPI), Houston, USA
Deutsche Forschungsgemeinschaft (German Science Foundation), Bonn, Germany
Barringer Crater Company, Decatur, USA
Meteoritical Society, USA
City of Nördlingen, Germany
Ries Crater Museum, Nördlingen, Germany
Community of Otting, Ries, Germany
Märker Cement Factory, Harburg, Germany

## Local Organization

City of Nördlingen
Museum für Naturkunde –
Leibniz- Institute for Research on Evolution and Biodiversity at the Humboldt University Berlin
Ries Crater Museum, Nördlingen
Center of Ries Crater and Impact Research (ZERIN), Nördlingen
Society Friends of the Ries Crater Museum, Nördlingen
Community of Otting, Ries
Märker Cement Factory, Harburg

## Organizing and Program Committee

Prof. Dieter Stöffler, Museum für Naturkunde, Berlin
Prof. Wolf Uwe Reimold, Museum für Naturkunde, Berlin
Dr. Kai Wünnemann, Museum für Naturkunde, Berlin
Hermann Faul, First Major of Nördlingen
Prof. Thomas Kenkmann, Freiburg
Prof. Harald Hiesinger, Münster
Prof. Tilman Spohn, DLR, Berlin
Dr. Ulrich Köhler, DLR, Berlin
Dr. David Kring, LPI, Houston
Dr. Axel Wittmann, LPI, Houston
Gisela Pösges, Ries Crater Museum, Nördlingen
Ralf Barfeld, Chair, Society Friends of the Ries Crater Museum
Lunar and Planetary Institute

LPI Contribution No. 1559

Compiled in 2010 by
LUNAR AND PLANETARY INSTITUTE

The Lunar and Planetary Institute is operated by the Universities Space Research Association under a cooperative agreement with the Science Mission Directorate of the National Aeronautics and Space Administration.



Abstracts in this volume may be cited as

Author A. B. (2010) Title of abstract. In *Nördlingen 2010: The Ries Crater, the Moon, and the Future of Human Space Exploration,* p. XX. LPI Contribution No. 1559, Lunar and Planetary Institute, Houston.

This volume is distributed by

ORDER DEPARTMENT
Lunar and Planetary Institute
3600 Bay Area Boulevard
Houston TX 77058-1113, USA
Phone: 281-486-2172
Fax: 281-486-2186
E-mail: order@lpi.usra.edu

*A limited number of copies are available for the cost of shipping and handling.*
*Visit the LPI Online Store at https://www.lpi.usra.edu/store/products.cfm.*

ISSN No. 0161-5297

# Preface

This volume contains abstracts that have been accepted for presentation at Nördlingen 2010: The Ries Crater, the Moon, and the Future of Human Space Exploration, June 25–27, 2010, Nördlingen, Germany.

Administration and publications support for this meeting were provided by the staff of the Publications and Program Services Department of the Lunar and Planetary Institute.

# Contents

# Program

**Friday, June 25, 2010**
**OPENING CEREMONY**
**3:00 p.m.**

3:00 p.m. Welcome

3:15 p.m. Dr. Stanley G. Love, NASA Astronaut
*Exploratory Planetary Science: Today and Tomorrow*

4:00 p.m. Dr. Gerhard Thiele, ESA Astronaut, European Space Policy Institute
*The Quest for Knowledge — Impact Craters and Human Space Exploration?*

**Friday, June 25, 2010**
**POSTER SESSION**
**4:30 p.m.**

**Moderator: Ralf Jaumann**

**Ries Crater**

Schmieder M. Buchner E.
*How 'Dry' was the Ries-Steinheim Impact Event?* **[#7001]**

Willmes M. Sturm S. Hiesinger H. Kenkmann T. Pösges G.
*Detection of Subsurface Megablocks in the Ries Crater, Germany: Results from a Field Campaign and Remote Sensing Analysis* **[#7002]**

Sapers H. M. Osinski G. R. Banerjee N. R.
*Enigmatic Tubular Textures Hosted in Impact Glasses from the Ries Impact Structure, Germany* **[#7024]**

Reimold W. U. Hansen B. K. McDonald I. Koeberl C. Jacob J. Stöffler D. Meyer C.
*Detailed Investigations of the SUBO 18 (Enkingen) Drill Core from the Ries Crater, Southern Germany* **[#7026]**

Meyer C. Stöffler D. Jébrak M. Reimold W.-U.
*Stratigraphy of the Ries Suevite, Germany, from Stereometric Analysis* **[#7032]**

Osinski G. R. Grieve R. A. F.
*Comparison of Mid-Size Complex Terrestrial Impact Structures* **[#7038]**

Pontefract A. Osinski G. R. Flemming R. Southam G.
*Characterization of Polymict Crystalline Breccias, Ries Crater, Germany* **[#7039]**

**Terrestrial Craters and Impactites**

Danilin A. N.
*On a Possible Association of Giant Ore Districts with Marks of Meteoroid Impacts on the Earth's Surface* **[#7005]**

Dypvik H. Claeys P. Deutsch A. Kyte F. T. Matsui T. Smelror M.
*The Late Jurassic Mjølnir Impact Crater in the Barents Sea-Drilling Proposal* **[#7009]**

Magna T. Deutsch A. Skála R. Mezger K. Adolph L. Seitz H.-M. Wasson J. T. Mizera J. Randa Z.
*Lithium Isotopes in Tektites — Tales of Sources, Histories and Impacts* **[#7017]**

Mader M. M. Osinski G. R. Marion C. L. Dammeier R. Shankar B. Sylvester P. J.
*Mistastin Impact Structure, Labrador: A Geological Analogue for Lunar Highland Craters* **[#7018]**

Peate D. W. Ukstins Peate I. A. Chung Wan L. Kloberdanz C.
*Compositional Variations and Petrography of Metallic Spherules in Melt Rock at Monturaqui Crater, Chile* **[#7019]**

Berlin J. Cohen B. A. Newsom H. E. Tagle R.
*Another Anniversary: 5 Years Since the K/P Boundary Sample Started its Journey from Starkville/Colorado to the Riescrater-Museum in Nördlingen* **[#7022]**

Mohr-Westheide T. Reimold W. U. Gibson R. L. Mader D. Koeberl C.
*Formation of Pseudotachylitic Breccias from the Archean Gneiss of the Vredefort Dome, South Africa* **[#7025]**

**Moon and Lunar Impactites**



**Mars and Martian Rocks**



**Human-Robotic Exploration of the Moon and Mars**

**Saturday, June 26, 2010**
**KEYNOTE LECTURES:**
**RIES CRATER — MESSAGES FOR CRATER FORMATION,**
**SHOCK METAMORPHISM, AND IMPACTITE CLASSIFICATION**
**9:00 a.m.**

**Chairs:** **Wolf Uwe Reimold**
**Kai Wünnemann**

9:00 a.m. Stöffler D. *
*Introduction to the Topic of the Workshop*

9:15 a.m. Stöffler D. * Reimold W. U.
*The Impact of Ries Crater Research on the Recognition and Classification of Impact-Metamorphosed Planetary Rocks* **[#7011]**

9:50 a.m. Langenhorst F. *
*Shock Metamorphism at the Ries and Implications for Lunar Rocks and Martian Meteorites* **[#7043]**

10:25 a.m. BREAK

10:40 a.m. Wünnemann K. * Artemieva N. A. Collins G. S.
*Modeling the Ries Impact: The Role of Water and Porosity for Crater Formation and Ejecta Deposition* **[#7008]**

**Saturday, June 26, 2010**
**KEYNOTE LECTURES:**
**RIES CRATER — MESSAGES FOR CRATER AND IMPACT FORMATIONS ON THE MOON AND MARS**
**11:15 a.m.**

**Chairs:** **Falko Langenhorst**
**David Kring**

11:15 a.m. Arp G. *
*Post-Impact Sedimentary and Geomicrobiological Processes in the Ries Crater with Implications for Search of Possible Microbial Life on Mars* **[#7003]**

11:45 a.m. Buchner E. * Schmieder M.
*Post-Impact Erosion and Redeposition of Impactites at the Ries Crater and Implications for Similar Processes on Mars* **[#7004]**

12:15 p.m. Kenkmann T. * Wittmann A.
*The Ries Crater and the Interpretation of Ejecta Deposits at Impact Craters on Mars* **[#7010]**

12:50 p.m. LUNCH

2:00 p.m. Jolliff B. L. * Korotev R. L. Zeigler R. A.
*Provenance of Impact-Melt Breccias Collected at the Apollo Landing Sites: What Did We Learn and What Are the Implications for Future Exploration?* **[#7040]**

**Saturday, June 26, 2010**
**KEYNOTE LECTURES:**
**FUTURE LANDING SITES ON THE MOON AND MARS:**
**WHAT DO ASTRONAUTS NEED TO KNOW?**
**2:35 p.m.**

**Chairs:** **Ulrich Koehler**
**Brad Jolliff**

2:35 p.m. Pieters C. M. *
*Future Landing Sites on the Moon: What is New and What Do We Need to Know?* **[#7014]**

3:10 p.m. Head J. W. III *
*Potential Landing Sites for Robotic-Human Exploration on Mars* **[#7016]**

3:45 p.m. Kring D. A. *
*What can Astronauts Learn from Terrestrial Impact Craters for Operations on the Moon and Mars?* **[#7036]**

**Saturday, June 26, 2010**
**GENERAL DISCUSSION**
**4:20 p.m.**

**Chairs and Moderators:**
**James W. Head III**
**Tilman Spohn**

Discussion Focus:

- Relevance of Ries and terrestrial crater research to the Moon and Mars
- Strategies and boundary conditions for sampling rocks on planetary bodies by human-robotic exploration

**Saturday, June 26, 2010**
**CELEBRATION OF THE THREE RIES ANNIVERSARIES**
**6:30 p.m.**

Celebration of the three Ries anniversaries hosted by the City of Nördlingen
with invited lectures by astronaut Dr. Dr. h.c. Ernst Messerschmid, Stuttgart
("Die Internationale Raumstation – und was folgt danach?")
and the former director of the Natural History Museum at Berlin,
Dr. Dieter Stöffler ("Was hat das Ries mit dem Mond und der Landung von Astronauten auf benachbarten Himmelskörpern zu tun?")

City brass band of Nördlingen

Celebration will be held in German

**POST-IMPACT SEDIMENTARY AND GEOMICROBIOLOGICAL PROCESSES IN THE RIES CRATER WITH IMPLICATIONS FOR SEARCH OF POSSIBLE MICROBIAL LIFE ON MARS.**

Gernot Arp, Geowissenschaftliches Zentrum, Geobiologie, Georg-August-Universität Göttingen, Goldschmidtstrasse 3, D-37077 Göttingen, Germany (garp@gwdg.de).

**Introduction:** In the shadow of the spectacular cosmic event of the Ries impact, the water body that accumulated subsequently in the bowl attained slightly less attention. However, research since about 1975 successively revealed that the Ries crater lake, which initially has been recognized as a lively subtropical habitat [1], demonstrating recovery after a catastrophe, had a changeful history with prolonged phases of ecologically extreme conditions [2]. Moreover, it became obvious that the Ries crater lake is distinctly different from the simultaneously formed Steinheim crater lake with its highly diverse fauna comprising endemic gastropod lineages [3] and attempts to find similar radiations in the Ries basin were unsuccessful [4].

**Evolution of the Ries crater lake:** As a consequence of the high diameter/depth ratio of the crater basin, the low precipitation/evaporation ratio, and the composition of rocks successively available for weathering and ion supply, the Ries crater lake developed from (i) a playa lake, to (ii) a soda lake with stratified water column, and to (iii) an alkaline halite lake rich in $Mg^{2+}$ and $Sr^{2+}$ [2, 5]. Superimposed climatic fluctuations caused evaporation cycles and instable ecological conditions in the shallow lake. Processes that lead to a $Na^{+}$-$HCO_3^{-}$-rich lake water are silicate weathering and intense bacterial sulfate reduction, the latter being substantiated by the occurrence of sulfurized organic components [6]. Bacterial sulfate reduction was fueled by the high primary production in the eutrophic, salinity-stratified water column. Minor $Ca^{2+}$ influx was detracted by microbial carbonate precipitation at subaquatic springs and green algal bioherms flourishing at lake margins due to the eutrophic conditions [5]. A successive change from instable silicates to Jurassic limestones and dolomites as primary source of inorganic dissolved ions is indicated by a unidirectional trend in $^{87}Sr/^{86}Sr$ from 0.7119 to 0.7112, i.e., a trend from crystalline basement [7] to Jurassic marine values [8]. Hence, $Ca^{2+}$, $Mg^{2+}$ and $Cl^{-}$ increased and $Sr^{2+}$ further accumulated in the lake water, whereas $Na^{+}$ and $HCO_3^{-}$ were extracted by authigenic silicate minerals [2] and biogenic carbonate deposition, respectively. $Mg^{2+}$-rich lacustrine fluids mixing with meteoric groundwater [5] may be responsible for the dolomitization of the porous algal bioherms and the precipitation of unusual $Sr^{2+}$-rich dolomite cement [9] late in the lake history. Planorbid gastropods and charophytes in latest preserved lake sediments finally indicate oligotrophic freshwater conditions [4, 5], a development possibly related to a change to humid climate and/or formation of an outflow [9].

**Microbial deposits:** A number of different microbial rocks formed in the Ries crater lake [5], which can be regarded as a small-scale palaeo-ocean showing the relation of hydrochemical evolution and microbial carbonate deposition. Specifically, non-skeletal stromatolites in early algal bioherms were replaced by stromatolites with dolomitized cyanobacterial filaments and finally stromatolites with cyanobacterial filament tubes in late algal bioherms. This development that can be explained by a decreasing concentration in inorganic dissolved carbon, which determines the relative effect of photosynthetic $CO_2$ fixation and exopolymer degradation [10]. Further deposits of geomicrobiological significance, which highlight extreme ecological conditions, are (i) analcime-bearing bituminous shales and claystones, (ii) sublacustrine spring deposits similar to present-day soda lakes, (iii) possible thermal spring deposits, and (iv) deep subsurface calcite veins of the crater basement.

**Implications for search of possible extra-terrestrial life:** The recognition of microbial rock fabrics and morphological and molecular traces of fossil microbial life in such deposits may serve as a test for tracing potential fossil life on Mars or other extraterrestrial bodies. Besides layered lake basin sediments, subsurface mineral veins as well as spring deposits could be promising targets for search of signatures of former life. However, the hypothesis that carbonate spring deposits similar to that of alkaline lakes on Earth may have formed in Martian lakes [11] turned out to be inconsistent with acidic water bodies on Mars, displaying sulphate not carbonate mineral deposits [12].

**References:** [1] Seemann (1941) *Jh. Ver. vaterländ. Naturk. Württemberg*, *94*, 49-62; [2] Jankowski (1981) *Bochumer geol. geotech. Arb.*, *6*, 1-315; [3] Gorthner (1990) *Stuttgarter Beitr. Naturk.*, *B 190*, 1-173; [4] Bolten (1977) Thesis München, 228 pp.; [5] Arp (1995) *Facies*, *33*, 35-90; [6] Rullkötter et al. (1990) *ACS Symp. Ser.*, *429*, 149-169; [7] Horn et al. (1985) *EPSL*, *75*, 384-392; [8] Pache et al. (2001) *Facies*, *45*, 211-230; [9] Wolff and Füchtbauer (1976) *Geol. Jb.*, *D 14*, 3-53; [10] Arp et al. (2001) *Science*, *292*, 1701-1704; [11] Kempe and Kazmierczak (1997) *Planet. Space Sci.*, *45*, 1493-1499; [12] Fairén et al. (2004) *Nature*, *431*, 423-426.

**ARE ALL LUNAR HIGHLAND PRISTINE ROCKS REALLY PRISTINE?** A. T. Basilevsky[1,2] and G. Neukum[2], [1]Vernadsky Institute, RAS, 119991 Moscow, Russia atbas@geokhi.ru; [2]Freie Universitaet Berlin, D-12249 Berlin, Germany. gerhard.neukum@fu-berlin.de

**Introduction:** This paper has appeared as a result of attempts to resolve the well known controversy: If in the early history of the Moon there was a ***terminal cataclysm*** when within a short time period ~3.9 Ga ago a majority of now observed impact craters and basins of lunar highlands formed, or did they form over a longer time since the time of formation of the lunar crust till 3.9 Ga ago. One of the strongest arguments favoring the idea of a terminal cataclysm was advanced by G. Ryder [1]. He paid special attention to the fact that impact melts older than ~4.0 Ga (actually 4.2 Ga) are practically absent in the lunar sample collections and concluded that this rules out extensive basin formation during the earlier times. His logic was that formation of lunar basins should produce abundant impact melts and if the earlier basins were numerous, some of their melts should be among the collected samples. In the collections there are samples older than 4.2 Ga and these are ***pristine*** highland igneous rocks showing 4.2 -4.5 Ga ages of crystallization [2, 3] We explore a possibility if **s*ome of the alleged pristine highland rocks may indeed be remnants of impact melts from the large basin-forming impacts*.**

**Analysis of the problem:** Pristine rocks of lunar highlands are distinguished on the basis of two criteria: 1) they have structures typical of igneous rocks; and 2) they are not polluted with meteoritic matter that is determined from the low contents of siderophile elements, of which the most indicative is considered to be iridium [e.g., 2]. The usual view of impact melts based on experience of their study in the majority of terrestrial impact craters implies poorly crystallized fine-grained rocks often with admixture of target rocks clasts. The majority of samples of lunar impact melts are indeed rocks of that sort. This is true, however, for the melts of not very large impact craters. Impact melts of the Sudbury astrobleme, which is the largest known terrestrial impact crater (D ~250 km) petrographically are normal medium- to coarse-grained igneous rocks: norites, quartz gabbro and granophyres [e.g., 4].

1) Lunar impact basins should contain very large pools of impact melt. The study [5] shows that as impact magnitude increases, the volume of created melt relative to that of the crater should grow. At the 20-30 km crater diameters the depth of melting should exceed the depth of excavation and this should progressively decrease a proportion of larger rock clasts (which effectively cool the melt) incorporated into the melt. At the sizes corresponding to the smallest basins incorporation of the clasts into the created melt pool should be insignificant and the melt pool, as it cools, should be able to evolve into a differentiated unit [5]. Recent numerical modeling by [6] demonstrated that impacts of large asteroid-like projectiles result in the formation of a central pool of impact melt (complete melting) of hundreds to more than a thousand kilometers in diameter and tens of kilometers thick. These should crystallize as normal large igneous massifs.

2) To consider a possibility if some lunar impact melts could have low contents of Ir and thus be classified as pristine rocks we compared Ir contents in 4 varieties of lunar materials (mare basalts, pristine highland monomict rocks, soils and regolith breccias and highland polymict breccias) with those in terrestrial impact melts: from 12 terrestrial impact craters the smallest of which was crater Aouelloul, D = 0.37 km and the largest, Sudbury, 250 km. The comparison showed that impact melts of the majority of the terrestrial craters considered have very variegated contents of Ir. The high contents are obviously due to admixture of meteoritic material, while the low contents may be due to low Ir contents in the projectiles responsible for these impacts: most achondrites and some iron meteorites have low iridium contents . The Sudbury impact melts, however, especially in the upper part of the body, have low Ir contents although the Sudbury projectile projectile had high siderophile contents [e.g., 7]. But Ni, Co and platinum group elements including Ir were extracted from the silicate melt into the sulfide melt which sank and formed ore deposits at the lower contact zone and in some dikes [e.g., 8] .

**Conclusions:** Some lunar highland “pristine” rocks having 4.2 to 4.5 Ga crystallization ages may indeed be not pristine but products of crystallization of large bodies of melt fomed by the basin-forming impacts. This suggests that the above mentioned argument of Ryder (2002) may not be valid and terminal lunar cataclysm might not be the case.

We acknowledge help of B. Ivanov, C. Koeberl, M. Lesher and R. Grieve.

**References:** [1] Ryder (2002) *JGR, 107,* (e4). [2] Tailor et al. (1991) *Lunar Source Book.* 183-284. [3] Stoffler et al. (2006) *Rev. Miner. Geochem.*. 60, 519-596 [4] Therriault et al. (2002) *Econ. Geology*, 87, 1521-1540. [5] Cintala and Grieve (1998) *MPS*, 33, 889-912. [6] Ivanov et al. (2010) GSA Special Paper *in press*. [7] Grieve (1994) Ontario Geol. Surv. Spec. Vol. 5,119-132. [8] Lightfoot (2004) Mineral. Petrol. 82, 217-258.

**EXPERIMENTAL SHOCK TRANSFORMATION OF GYPSUM TO ANHYDRITE: A POSSIBLE LOW PRESSURE REGIME SHOCK INDICATOR.** M. S. Bell[1], [1]Jacobs@NASA/Johnson Space Center, m.s.bell@nasa.gov.

**Introduction:** The shock behavior of gypsum is important in understanding the Cretaceous/Paleogene event and other terrestrial impacts that contain evaporite sediments in their targets (e.g., Mars Exploration Rover Spirit detected sulfate at Gusev crater, [1]). Most interest focuses on issues of devolatilization to quantify the production of $SO_2$ to better understand its role in generating a temporary atmosphere and its effects on climate and biota [2,3]. Kondo and Ahrens [4] measured induced radiation emitted from single crystal gypsum shocked to 30 and 40 GPa. They observed greybody emission spectra corresponding to temperatures in the range of 3,000 to 4,000 K that are a factor of 2 to 10 times greater than calculated pressure-density energy equation of state temperatures (Hugoniot) and are high enough to melt gypsum. Chen *et al*. [5] reported results of shock experiments on anhydrite, gypsum, and mixtures of these phases with silica. Their observations indicated little or no devolatilization of anhydrite shocked to 42 GPa and that the fraction of sulfur, by mass, that degassed is ~$10^{-2}$ of theoretical prediction. In another report of shock experiments on calcite, anhydrite, and gypsum, Badjukov *et al*. [6] observed only intensive plastic deformation in anhydrite shock loaded at 63 GPa, and gypsum converted to anhydrite when shock loaded at 56 GPa but have not experimentally shocked gypsum in a stepwise manner to constrain possible incipient transformation effects. Schmitt and Hornemann [7] shock loaded anhydrite and quartz to a peak pressure of 60 GPa and report the platy anhydrite grains were completely pseudomorphed by small crystallized anhydrite grains. However, no evidence of interaction between the two phases could be observed and they suggested that recrystallization of anhydrite grains is the result of a solid-state transformation. They concluded that significant decomposition of anhydrite requires shock pressures higher than 60 GPa. Gupta *et al*. [8] reanalyzed the calcite and anhydrite shock wave experiments of Yang [9] using improved equations of state of porous materials and vaporized products. They determined the pressures for incipient and complete vaporization to be 32.5 and 122 GPa for anhydrite GPa which is a factor of 2 to 3 lower than reported earlier by Yang [9].

Impactites produced in dominately evaporate targets lack quartz, a commonly used shock indicator with well documented effects induced over a range of shock pressures beginning as low as ~10 GPa [10,11,12]. Bell [13] reports preliminary identification of gypsum transforming to anhydrite in systematic step-wise shock experiments from 10 to 47 GPa and documents a calibration scheme of shock effects in calcite and gypsum relative to those in quartz. The transformation of gypsum to anhydrite as evidenced by high relief and high birefringence is observed in the 18.4 GPa shock experiment and the effect is continuous through the 40.7 GPa experiment but whether or not calcium sulfate remains birefringent cannot be resolved in the 47.7 GPa experiment. The transition of gypsum to anhydrite (a stable polymorph) + $H_2O$ is monotropic (irreversible) in which the temperature required to initiate the transformation is lowered with increasing pressure (200 $^oC$ at 1 atm). The shock-induced transformation effects in gypsum could provide a new low pressure regime shock indicator for impact deposits lacking quartz or other crystalline rock-forming minerals. Raman spectroscopy can be used to detect the presence of water in gypsum which is characterized by a peak in the spectral region near 3500 $cm^{-1}$. Results of Raman analyses have been used to verify the transformation of gypsum to anhydrite and preliminary results of that study are reported here.

**Experimental:** Details of the shock experiments can be found in Bell, 2010. Pure gypsum (Sigma Aldrich 255548-100G) was used for the experiments. Raman spectra were collected using the Jobin-Yvon LabRAM HR800 at the Johnson Space Center Astromaterials Research and Exploration Science Directorate. The spectrometer is equipped with an argon ion (Ar+) gas laser using the 514.5$cm^{-1}$ plasma line of that laser. Laser power was 80 mW at the sample to maximize spectral quality and minimize beam damage. The slit width was set at 100 µm and a data collection interval of 1 $cm^{-1}$ was used in recording Raman spectra. Ten spectra were acquired per sample for each shock interval.

**Results and Conclusions:** The gypsum used in this study was characterized by Raman spectroscopy in the range 50 to 4000 $cm^{-1}$ and peaks were assigned according to [14] . In the Raman spectra, the peaks around 3500 $cm^{-1}$ ($\nu_1$ and $\nu_3$) are the result of stretch vibration modes of water, and no peaks for these modes of water were observed in any spectra from the shocked gypsum samples. The spectral peak for the $\nu_1$ ($SO_4$) symmetric stretch vibration mode of SO4 tetrahedra is consistently located near 1017$cm^{-1}$ which is upshifted from the gypsum peak at 1008 $cm^{-1}$. These results indicate that all gypsum samples shocked in the pressure range 10 to 47 GPa have been transformed to anhydrite. Thus, deformation effects observed in these shock experiments on gypsum are solid-state reactions and by comparison to solid-state shock effects in quartz from the same experiments, can provide a low pressure calibration scheme for shock effects in naturally shocked rocks lacking quartz under certain conditions - if those effects have not been overprinted by subsequent processes such as thermal annealing or alteration.

**References:** [1] Ming, et al. (2008) *Science* v [2] Silver, L.T. and Schultz, P.H., eds. (1982) GSA Special Paper 190. 528 p.[3] Brett, R. (1992) *GCA* 56, 3603-3606. [4] Kondo, K.-I. and Ahrens, T.J. (1983) *Phys Chem of Mins* 9, 173-181.[5] Chen, G., Tyburczy, J.A., and Ahrens, T.J. (1994) *E & PSL* 128, 615-628. [6] Badjukov, D.D., Dikov, Yu P., Petrova, T.L., and Pershin, S.V. (1995) *LPSC XXVI* (abs.) 63-64.

[7] Schmitt, R.T. and Hornemann, U. (1998) *LPSC XXIX*-abst. #1019, CD-ROM. [8] Gupta, S.C., Ahrens, T.J., and Yang, W. ( 1999) *in* Shock Compression of Condensed Matter,1259-1262. [9] Yang, W. and Ahrens, T.J. (1998) *E & PSL Letters* 156, 125-140. [10] Stöffler, D. and Langenhorst, F. (1994) *Meteoritics* 29, 155-181.[11] Grieve, A.F., Langenhorst, F., and Stoffler, D. (1996) *MAPS* 31, 6-35 [12] Bell, M.S. (2010) *GSA Special Paper* 465, in Press. [13] Sarma et al. (1998) *J. Raman Spec.* 29, 851-856.

**Another anniversary: 5 years since the K/P boundary sample started its journey from Starkville/Colorado to the Riescrater-Museum in Nördlingen.** J. Berlin[1,2], B. A. Cohen[1,3], H. E. Newsom[1] and R. Tagle[2], [1]University of New Mexico, Albuquerque, NM 87131, USA, [2]Bruker Nano GmbH, Schwarzschildstrasse 12, 12489 Berlin, Germany, [3]NASA Marshall Space Flight Center, Huntsville, AL 35806, USA (jberlin@daad-alumni.de).

In May 2005, a group of scientists and students of the University of New Mexico went on a field trip (led by B. Cohen) to Northern New Mexico and Southern Colorado to observe the K/P boundary layer at different locations. For four of us (B. Cohen, R. Coker, H. Newsom, and J. Berlin), the journey was not over until we had dug out two larger K/P boundary samples (Fig. 1a,b) at the Starkville/South site [1] – one intended for the Meteorite Museum at UNM and one for the Riescrater-Museum in Nördlingen.

One of the pieces we had dug out did not actually survive as a whole; it was so brittle that it simply fell apart when we opened the wrapping after transport to UNM (Fig. 1c). Therefore, we decided to stabilize the other piece with plaster of Paris and epoxy (Fig. 1d). Finally, the latter sample was cut into three slabs at La Tierra Interiors in Bernalillo, NM (Fig. 1e). One of the slabs (Fig. 1f) travelled to Germany in a carry-on suitcase in December 2005 and was installed in room F in the Riescrater-Muesum in Nördlingen.


**Fig. 1.** Sampling and preparation of the K/P boundary sample that can be seen at exhibition room F in the Riescrater-Museum in Nördlingen. A sample from the broken piece shown in Fig. 1c was analyzed by µ-XRF (refer to Fig. 2).

Several small samples containing the K/P boundary clay were recovered from the piece that fell apart (Fig. 1c). Figure 2 shows one of these samples, consisting of the K/P boundary clay and overlying coal deposits, next to selected element distribution maps that were obtained with a recently developed µ-XRF scanner (M4 Tornado). The scans represent 919 x 168 pixel with a step size of 60 µm and measurement time of 50 ms per pixel adding up to a total area of 55 by 10 mm and ~2.5 hours total measurement time.

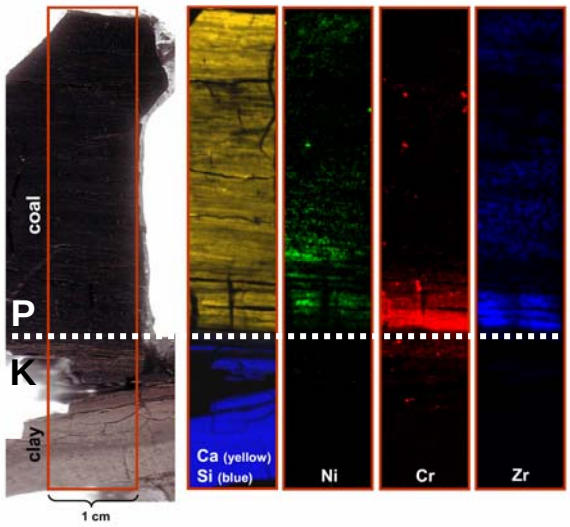


**Fig. 2.** Sample of the K/P boundary clay and overlying coal deposits (recovered from the broken piece in Fig. 1c) and element maps of Ca+Si, Ni, Cr, and Zr obtained by µ-XRF.

The element scans illustrate the chemical transition during the deposition of the sediments across the K/P boundary (abrupt change from silicates to carbonates). Iridium is below the detection limit of the µ-XRF, but elements like Ni and Cr (probably from the projectile) and Zr (indicating the presence of shocked zircons in the distal Chicxulub ejecta? [2]) appear to be good indicators for the location of the K/P boundary.

**References:** [1] Pillmore C. L. et al. (1984) *Science, 223,* 1180-1183. [2] Krogh T. E. et al. (1993) *EPSL, 119,* 425-429.

**Acknowledgements:** The UNM meteorite museum thanks Gisela Pösges and the Riescrater-Museum for donating a wonderful slab of suevite in response to the K/P sample. We also thank Rob Coker for his help digging out the K/P samples at the Starkville/South site and La Tierra Interiors in Bernalillo, NM for cutting the slabs.

**IMPLICATION RESULTING FROM SEIFERTITE FORMATION IN SHERGOTTITES.** U. W. Bläß[1] and F. Langenhorst[2], [1]Institut für Geowissenschaften, Friedrich-Schiller-Universität Jena, Burgweg 11, 07749 Jena, Germany (Ulrich.Blaess@uni-jena.de), [2]Bayerisches Geoinstitut, Universität Bayreuth, 95440 Bayreuth, Germany (Falko.Langenhorst@uni-bayreuth.de).

**Introduction:** High-pressure silica polymorphs are used as crucial indicators for impact processes in terrestrial bedrocks (e.g., formation of coesite in suevites from the Ries) and serve as pressure and temperature markers in several meteorites. These phases commonly crystallise as tiny crystals during the short shock pulse from silicate melts or glasses at high-pressure.

The discovery of more than 100 µm large post-stishovite polymorphs like seifertite ($\alpha$-$PbO_2$ structured silica) in the Martian meteorites Shergotty and Zagami [1; 2], however, point to a completely different and unknown mechanism of formation. Equilibrium pressures for the formation of observed post-stishovite phases are substantially higher [3; 4] than previously estimated shock pressures of ~30 GPa for the meteorites embedding these phases [5]. In addition fast solid state transformation processes are not known for the $SiO_2$-system, which transforms extremely sluggish at low pressures. In order to get a more profound understanding of the formation of seifertite crystals and resulting implications for the shock history of the host meteorite, we investigated their petrographic characteristics and defect microstructures by using scanning and transmission electron microscopy.

**Results:** The occurrence of seifertite in Shergotty and Zagami is restricted to the mesostasis of our samples. These mesostasis regions exhibit sometimes an approximately rectangular or even tetragonal shape and show severe radial cracks penetrating far into adjacent phases indicating a strong volume expansion of these regions. However, TEM analyses reveal that all these regions correspond to late stage magmatic differentiation products composed predominantly of a fine-grained (1-5 µm) mixture of seifertite plus maskelynite and tiny accessory minerals like tranquillityite or titanomagnetite.

Seifertite has been characterized by electron diffraction pattern, which can be indexed as a orthorhombic phase with lattice constants of $a$ = 4.45 Å, $b$ = 4.05 Å and $c$ = 5.05 Å, but not by any other known silica polymorphs. Chemical compositions are close to pure silica but contain 1.1 - 1.5 % of aluminum and < 1% sodium indicating cristobalite or tridymite as potential precursor phases. The crystals are only a few microns large and are pervaded by characteristic sets of amorphous lamellae as described e.g. by [2]. The lamellae divide the entire phase into 50 - 200 nm large blocks of roughly equal crystallographic orientation. In contrast accessory phases like tranquillityite exhibit a strongly shock-deformed microstructure.

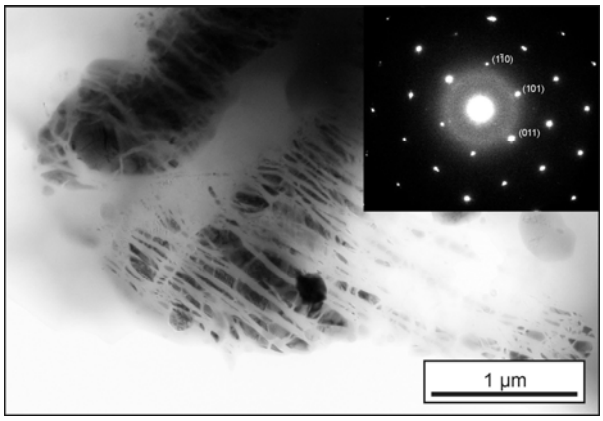


Fig.: TEM bright field image and diffraction pattern (inset) of seifertite showing characteristic lamellae.

**Discussion:** Shock induced deformation features in tranquillityite indicate that the mesostasis could not be remolten during the shock event. Hence embedded seifertite crystals must have been transformed by a solid state process, independent of their size. The transition occurred likely metastable at pressures far below the stability of seifertite, because no features were observed justifying the assumption of shock-pressures considerably above the previously estimated 30 GPa. Substantially higher shock-pressures would cause severe melting and the resulting high post-shock temperatures would likely prohibit the crystallisation of a high pressure paragenesis like in the Shergottite Dhofar 378.

These investigations demonstrate therefore, that in contrast to high pressure phases crystallised from a melt, solid state transformation processes do not unambiguously indicate minimum shock pressures, but could be misleading due to their metastable nature.

**References:** [1] Sharp T. G. et al. (1999) *Science 284*, 1511-1513. [2] El Goresy A. et al. (2004) *J. Phys. Chem. Sol. 65*, 1597-1608. [3] Dubrovinsky L. S. et al. (1997) *Nature 388*, 362-365. [4] Teter D. M. et al. (1998) *Phys. Rev. Let. 80*, 2145-2148. [5] Stöffler D. et al. (1986) *Geochim. Cosmochim. Act. 50*, 889-903.

**POST-IMPACT EROSION AND REDEPOSITION OF IMPACTITES AT THE RIES CRATER AND IMPLICATIONS FOR SIMILAR PROCESSES ON MARS.** E. Buchner[1,2] and M. Schmieder[1], [1]Institut für Planetologie, Universität Stuttgart, Herdweg 51, 70174 Stuttgart, elmar.buchner@geologie.uni-stuttgart.de, [2]HNU – Hochschule Neu-Ulm, University, Wileystraße 1, 89231 Neu-Ulm.

**Introduction:** Impact ejecta reworked by various sedimentary processes have been reported from a number of impact structures on Earth [1]. Tsunami-reworked layers of impact glass/spherules and shocked mineral grains at K/P boundary sections associated with the Chicxulub impact structure, Mexico, were described by [2]. At marine impact structures, such as Lockne, Sweden, impact ejecta are commonly reworked within submarine turbiditic 'resurge breccia/arenite' deposits [3]. At impact structures degraded by glacial erosion, e.g., Paasselkä, Finland, glacial float may contain proximal ejecta material [4]. In contrast to the marine and glacial processes mentioned above, impact ejecta reworked by fluvial processes are sparsely mentioned in the literature.

The ~14.5 Ma [5] Nördlinger Ries impact structure in southern Germany is unique in terms of the state of preservation of its ejecta that is conserved as a contiguous blanket surrounding mainly the southern part of the crater. Whereas a great portion of the ejecta is preserved in situ, a certain amount of proximal Ries ejecta material was reworked, fluvially transported and deposited far from its original position. Similarily, distal ejecta were redistributed by Miocene fluvial systems.

**Results and Discussion:** The rare documentation of fluvially reworked impact ejecta may suggest that shocked mineral grains and impact glasses are unstable when eroded and transported in fluvial systems.

*Fluvial reworking of proximal ejecta:* Here we report impact ejecta that show sedimentological evidence for at least three steps of high-level fluvial reworking [6]. Well-rounded Ries ejecta material (suevite-derived shocked quartz grains, diaplectic quartz/feldspar glass, and lithic clasts of Bunte Breccia and suevite within multi-generation sandstone pebbles) is distributed within post-impact fluvial sandstones locally known as the 'Monheimer Höhensande'; the latter were carried and deposited within a water distribution network that incised into the eastern part of the Ries ejecta blanket soon after the impact event. Our findings document that shocked quartz grains and diaplectic glass can survive short-range multiple fluvial reworking [6].

A fluvial sediment body at the northern rim of the North Alpine Foreland Basin, locally known as 'Grimmelfingen Formation', consists mainly of coarse-grained fluvial sands ('Graupensande'). [7] reported shocked quartz and other impact-related phenomena in mineral grains and rock fragments ('suevite pebbles') collected from several outcrops of the 'Graupensande'. The sediment body contains material reworked from the Ries ejecta blanket and redeposited within a distance of up to ~150 km from the Ries crater. A prae-impact fluvial structure was probably buried by the impact ejecta and reincised into the southern part of the Ries ejecta blanket soon after the impact event.

*Fluvial reworking of distal ejecta:* Isolated angular to poorly rounded boulders of Upper Jurassic limestones and some (Middle Jurassic?) mudstone fragments are distributed within fluvial sediments of the Middle to Late Miocene Obere Süßwassermolasse of the North Alpine foreland basin, locally known as 'Reutersche Blöcke' or 'Brockhorizont', respectively. Numerical simulations by [8] suggested that these boulders were ejected during the Ries impact, balistically transported over a distance of up to ~200 km, and subsequently reworked within a fluvial system.

Tektites of the Central European strewn field, distributed within a distance of up to 450 km from the Ries crater that even survived multiple fluvial reworking have been reported from the Czech Republic and from Lusatia (moldavites) [e.g., 6].

**Implications for Mars:** Soon after the Ries impact event, an initial water distribution network developed in a landscape shaped by the Ries ejecta blanket. Proximal impact ejecta became eroded, transported over considerable distances, and redeposited by local watercourses, in multiple steps. On Mars, the development of initial water distribution networks in impact ejecta blankets can be studied in many cases. The distinct water distribution network that incised the ejecta blanket of the Huygens carter on Mars [e.g., 9] may serve as an analogon to the Nördlinger Ries crater.

**Acknowledgements:** The authors are grateful to Julia Lanz, Stuttgart, for providing Mars data.

**References:** [1] Simonson B. M. and Glass B. P. (2004) *Ann. Rev. Earth Planet. Sci., 32,* 329-361. [2] Smit J. (1999) *Ann. Rev. Earth Planet. Sci., 27,* 75-113. [3] Sturkell E. F. F. (1998) *Geol. Rdsch., 87,* 253-267. [4] Schmieder M. et al. (2008) *Meteoritics & Planet. Sci., 43,* 1189–1200. [5] Buchner E. et al. (2010) *Meteoritics & Planet. Sci.* (in press). [6] Buchner E. and Schmieder M. (2009) *Meteoritics & Planet. Sci. 44,* 1051–1060. [7] Buchner E. et al. (2003) *Int. J. Earth Sci., 92,* 1–6. [8] Buchner E. et al. (2007) *Icarus, 191,* 360–370.[9] Irvin R. P. et al. (2005) *J. Geophys. Res., 110, E12S15,* 38 p.

**MODELLING THE SOUTH POLE-AITKEN BASIN IMPACT.** G. S. Collins[1], R. W. K. Potter[1], D.A. Kring[2], W. S. Kiefer[2], P. J. McGovern[2], [1]Impacts and Astromaterials Research Centre, Dept. Earth Science and Engineering, Imperial College London, London, SW7 2AZ, UK, ross.potter04@imperial.ac.uk; [2]Lunar and Planetary Institute, 3600 Bay Area Blvd, Houston, TX, 77058, USA

**Introduction:** The 2500km diameter [1] South Pole-Aitken (SPA) basin is the largest and oldest impact structure on the Moon. The scale of the impact suggests that normally inaccessible lunar material, such as deep crust or mantle, was excavated or uplifted to the lunar surface, making SPA a strong candidate for possible sample return missions [2]. Analysis of originally deep-seated material would help further our understanding of planetary differentiation and early Solar System processes.

Crater scaling arguments [3] and previous numerical modeling of giant impacts on the Moon [4, 5, 6] suggest that an SPA-scale impact would bring impact-processed mantle material to the lunar surface either by ejection or by uplift as part of the rebounding crater floor. SPA-scale impact models also predict the production of a large melt pool underneath the central crater basin. Many spectroscopic studies of the basin have been undertaken [7, 8, 9], with [8] suggesting that the basin floor has a composition best described as a mixture of lower crustal and mantle material. Gravity data, tied to constraints on crustal structure from Apollo seismic data, suggest that the SPA basin is underlain by a ~10-30km-thick layer, less dense than the mantle, which thins toward the crater center [10]. Here, we use these observational constraints to refine hydrocode simulations of the SPA impact based on model predictions of the volume, dimensions and final location of the melt pool and crustal deformation.

**Methods:** We used the two-dimensional iSALE hydrocode [12,13] to simulate vertical impacts at 10-20 km/s of asteroids 100-200-km diameter into a spherical Moon with a resolution of 2.5-5 km per cell (20-80 CPPR). The Moon was modelled as a three-layer globe, 1750 km in radius (slightly larger than the true radius of 1737 km), consisting of a 50-km thick crust, a 1350-km thick mantle and a 350-km radius core. ANEOS-derived equation of state tables for dunite [14] and iron [15] were used to represent the mantle and core, respectively. A Tillotson equation of state, with parameters determined for gabbroic anorthosite [16], was used to model the crust. Dunite was also used to represent the impacting asteroid. Strength and thermal model parameters for both dunite and gabbroic anorthosite were derived from fits to experimental data [17, 18].

Self-consistent initial gravity, pressure, strength and density fields within the Moon were computed based on a prescribed radial thermal profile, representing lunar conditions at the time of impact. As a first approximation, the temperature in the Moon was assumed to increase with depth by 25K/km in the crust and upper mantle, and follow an adiabatic temperature gradient in the mantle and core, pinned at a temperature of 1740K at a depth of 560km.

**Results:** Numerical model results show two distinct zones created by the impact. The inner zone contains a deep pool of mantle material melted by shock heating and decompression melting. This zone is approximately equal in diameter to the transient crater and contains little, if any, crustal material. In the outer zone, which extends from the approximate location of the transient crater rim to the final crater rim, crustal material underlies mantle material heated above the solidus that is exhumed to the lunar surface by both ejection and run-off from the central uplift.

**Discussion:** The compositional anomaly at SPA is approximately equal to its topographic diameter (2500 km). Moreover, analysis of Clementine data suggests that later impacts in the outer part of the SPA basin have exposed buried upper crustal anorthosite; whereas, there is no evidence of upper crustal anorthosite exposures within an inner diameter of 1260 km. Assuming the compositional anomaly is related to the presence of (partially) molten upper mantle on the lunar surface, our numerical models are in best agreement with observations for an SPA impact energy of about $4\text{-}5 \times 10^{26}$ J.

**Acknowledgements:** RWKP and GSC are grateful for NSLI travel support allowing them to carry out research at the LPI-JSC Center for Lunar Science and Exploration, NASA Lunar Science Institute. We thank Boris Ivanov, Jay Melosh, Kai Wünnemann and Dirk Elbeshausen for their work in the development of iSALE. RWKP and GSC were both funded by NERC.

**References:** [1] Wilhelms, D. E. (1987) *The Geologic History of the Moon*, U.S Government Printing Office, Washington, D. C. [2] National Research Council (2007) *The scientific context for the exploration of the moon*, National Academies Press, Washington D.C. [3] Croft, S.K. (1978), *Proc. LPSC. IX*, 3711-3733. [4] Collins, G.S & Melosh, H.J. (2004) *LPSC XXXV*, abstract #1375. [5] Ivanov, B.A. (2007) *LPSC. XXXVIII*, abstract #2003. [6] Hammond, N.P. et al (2009) *LPSC XL*, abstract # 1455. [7] Pieters et al (1997) *GRL*, 24, 1903-1906 [8] Lucey, P.G. et al (1998) *JGR.* 103, 3701-3708. [9] Spudis, P. D. & Bussey, D. B. J. (2003) *LPSC* XXXIV, abstract #1693. [10] Hikida, H. & Wieczorek, M.A. (2007) *Icarus*, 192, 150-166. [12] Collins, G.S. et al (2004) *MAPS* 39, 217-231 [13] Amsden, A. A., et al (1980) *Los Alamos National Laboratory Report LA-8095* [14] Benz, W. et al (1989) *Icarus*, 81, 113-131 [15] Thompson, S.L. & Lauson, H.S. (1972) *Sandia National Laboratory Report SC-RR-71 0714* [16] O'Keefe, J.D. & Ahrens, T.J. (1982) *Geol. Soc. Am. Spec. Pap.*, 190, [17] Azmon, E. (1967) *NSL 67-224.* [18] Stesky R. M. et al (1974) *Tectonophys.* , 23, 177–203.

**ON A POSSIBLE ASSOCIATION OF GIANT ORE DISTRICTS WITH MARKS OF METEOROID IMPACTS ON THE EARTH'S SURFACE.** A.N. Danilin, Karpinsky Geological Research Institute (VSEGEI), St. Petersburg, Russia.

Impacts of large (more than one kilometer) meteoroids (asteroids and nuclei of large comets) on the surface of continental Earth's crust in different geological epochs were accompanied by intense fragmentation of rocks below the floor of the explosion-generated crater attenuating with depth and sidewards. Post-impact recoil of socle rocks caused their additional fragmentation; moreover, as a result of isostasy, the Earth's crust area emerged, its lower boundary uplifted relative to the environment as well. In a meteorite crater (astrobleme), the Earth's crust is thinned, crushed and easily penetrable. Subsequent geological processes distorted the primary picture of the astrobleme structure. Only preservation of its crushed "roots" often overlapped by deposits of different age is most probable.

It is known that formation of various mineral deposits is more easily realized in a permeable environment with large deposition surface, as each rock degradation has a catalytic effect, reducing the activation energy in solutions saturated with mineral components. It is obvious that all other conditions being equal, both endo- and exogenic fluids, crustal and mantle magmatism centers – ancestors of mineral deposits – prepared or taking place in crustal migration "life" of the given territory will use the preserved space impact mark. In the areas of hydrocarbons formation, the latter will prefer to form accumulations in prepared (crushed) cavities of the Earth's crust.

Thus, socle astrobleme complexes represent giant chemical reservoirs-reactors, where intense processes of hydrothermal synthesis take place, extraction and concentration of migration-capable occurrence forms of different atoms is in progress. The most well-known and characteristic example of such synthesis is Witwatersrand gold-uranium deposits located in fractured rocks of Vredefort astrobleme (South Africa) socle.

In our opinion, the Olympic Dam (Australia) group of deposits and their genetic analog the Central Aldan District (Russia) could be associated to a set of giant deposits formed in a sequence of fractured rocks of the socle complex of ancient astroblemes.

Intensely crushed "roots" of the Polar Urals (Russia) circular structure assigned by us to astroblemes comprise a number of so far discovered deposits of different minerals. The territory is estimated as very prospective for discoveries of new large deposits – construction of a branch railway is planned here under the federal program.

**A RECONSIDERATION OF AN IMPACT MODEL FOR THE RIES CRATER BASED ON COMPARISONS BETWEEN THE RIES-STEINHEIM AND CLEARWATER LAKE PAIRED CRATERS.**

Michael R. Dence, 824 Nesbitt Place, Ottawa, Ontario, Canada, K2C 0K1, e-mail: mrdence@rogers.com

**Introduction:** Terrestrial impact craters provided examples of craters of different sizes formed in a broad range of target materials ranging from crystalline rocks to stratified sedimentary rocks with variable physical properties. There are corresponding variations in the structure and topographic expression of the craters: those formed largely or entirely in crystalline rocks show morphological similarities to craters formed on other rocky planets while those where sedimentary rocks predominate comprise a subset not readily matched elsewhere in the Solar System. Steinheim crater[1], the smaller 3.4km diameter companion to the Ries, is representative of complex craters formed in sedimentary rock targets that have a central uplift that has risen from a depth (d) approximately 1/10th the diameter (D) of the final crater. A general expression $d = 0.086\ D^{1.03}$ has been derived from these craters [2]. As the central uplift has typically risen to within 50-100m of the original surface, d has also been accepted as the approximate depth of the excavated transient cavity (or primary crater) prior to any late stage modification. However drilling at the 3.8km Brent simple crater formed in crystalline rocks shows a transient cavity depth of about 1km [3], about three times that for Steinheim. From a consideration of shock metamorphism in the central uplifts of larger crystalline rock craters an alternative expression $d = 0.4\ D^{0.84}$ has been developed [4]. As the 24km Ries crater is formed in a mixed target of sedimentary rocks ~700m thick overlying a crystalline basement the question of which formula is more appropriately applied in such a case is open.

**Current Ries model:** Pohl et al. [5] provide a model of the Ries crater based on geological, geophysical and drilling information available in 1977 that appears to remain the current standard. It infers that the crater has a relatively subdued central peak 4 to 5km in diameter that may in part rise to within ~500m of the surface, has significant magnetic expression, and may be covered by 100 to 400m of suevite breccia as found in the Nördlingen drillhole of 1973. The hole was placed 3.5km from the center and thus outside the inferred central peak. The primary crater (transient cavity) is estimated to have been 2 to3 km deep, apparently by using the sedimentary crater formula. Interpretations of seismic and gravity data indicate that fracturing of the underlying basement extends to a depth of 6km. Note, however, that fracturing at Brent largely dies out within about 150m of the base of the transient cavity.

**The Clearwater Lake paired craters:** The two craters at Clearwater Lake, northern Quebec, [6] bear comparison with the Ries-Steinheim pair, being also about 40km apart (center to center), though their larger size (32 and 18-20 km) brings their rims closer together. They were formed in crystalline rocks overlain by an estimated 50-100m of Paleozoic limestone`275Ma ago and have been eroded by approximately 500m since formation. The larger West crater resembles the Ries in having a topographically subdued central peak with a significant magnetic signature and a distinct ring uplift half the diameter of the final crater but has a weaker gravity anomaly. The smaller East crater is substantially deeper, has distinct central peak as demonstrated by drilling near the center, and a bowl-shaped gravity anomaly similar to that at the Ries. Drilling has shown that, after allowance for erosion, the East crater was about 400-500m deeper than the West crater. If the latter was similar in depth to the Ries, the East crater was approximately 700-800m deep when fresh, perhaps the deepest known crater on Earth.

**Alternative Ries model:** The Ries has much in common with the Clearwater crystalline rock craters and has characteristics that are intermediate between them. Application of the transient cavity depth formula for crystalline rocks to the Ries gives a depth of 4 to 5 km**,** comparable to the estimated depth of fracturing and similar to the stratigraphic uplift at the 24km Gosses Bluff crater [7]. Only further drilling at the center will clarify the question.

**References:** [1] W. Reiff (1977) *in Roddy, D. et al. Impact and Explosion Cratering.* Pergamon, 309-320. [2] M.J. Cintala and R.A.F. Grieve (1998) *Meteorit.& Planet. Sci. 33,* 889. [3] M.R. Dence (2004) *Meteorit.& Planet. Sci.39,*267-286. [4] M.R. Dence (2010) *in preparation*.[5] j. Pohl et al. (1977) *in Roddy, D. et al. Impact and Explosion Cratering.* Pergamon, 343-404.[6] M.R. Dence (1965) *Ann. NY Acad. Sci.123,* 941-969. [7] D.J. Milton et al.(1996) *AGSO Journ. Austral. Geol & Geophys. 16* 487-527.

**THE LATE JURASSIC MJØLNIR IMPACT CRATER IN THE BARENTS SEA– DRILLING PROPOSAL.**

H. Dypvik[1], P. Claeys[2], A. Deutsch[3], F.T. Kyte[4], T. Matsui[5], M. Smelror[6], [1]Department of Geosciences, University of Oslo, P.O.Box 1047 Blindern, NO 0316 Oslo, Norway (henning.dypvik@geo.uio.no) ,[2]Earth System Science, Vrije Universiteit Brussel, Pleinlaan 2, B-1050 Brussels, Belgium, [3]Institut für Planetologie, Westfälische Wilhelms-Universität Münster Wilhelm-Klemm-Str. 10, D-48149 Münster, Germany,[4]Institute of Geophysics and Planetary Physics, UCLA University of California Los Angeles, CA 90095-1567, USA, [5]Chiba Institute of technology (Chitech), 2-17-1 Tsuda-numa, Chiba 275-0016, Japan, [6]Geological Survey of Norway, NO 7491 Trondheim, Norway.

**Introduction:** The Mjølnir impact structure is a 40 km in diameter crater, localized on the Bjarmeland Platform in the Barents Sea below 350 m of water and 50 to 150 m of post-impact sediments. The impact happened close to the Jurassic/Cretaceous boundary (about 142 million years ago), in a time when a wide, shallow (300- 400m deep) epicontinental sea covered the area [1,2,3]. The Mjølnir crater is presently situated between Bear Island and the mainland Norway. It is one of few, large marine impact structures on the Earth and one of the very few were crater and proximal ejecta can be correlated [4].

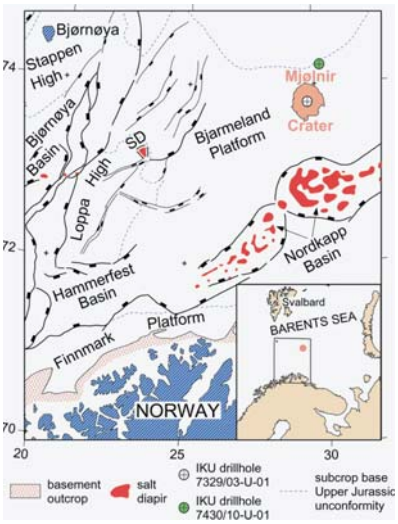


**Figure 1.** The location of the Mjølnir Impact structure in the Barents Sea is shown on the Bjarmeland Platform between the mainland Norway and Svalbard.

**Background:** During the last 30 years the Barents Sea and the Mjølnir structure area have been well mapped geophysically. One shallow core (7329/03-U-01)(121 m) (Figure 1) drilled inside the crater and a few shallow drillholes in its neighborhood (a few tens to hundreds of kilometers away) provide a fairly good overview of the main phases of the impact event. Moreover, interesting results have been achieved in combination with numerical simulations [5,6].

Impacts, particularly in marine environments, can significantly affect Earth's geological and biological evolution. However, detailed knowledge of the marine impact cratering process is still limited [4]. Among the 176 terrestrial craters, Mjølnir and its well preserved proximal ejecta deposits are unique; as these ejecta deposits always remained under water in calm conditions, consequently their preservation is most likely excellent.

The Barents Sea has been opened for petroleum exploration south of the Bjarmeland Platform. The development of the Mjølnir research program is consequently carried out in full cooperation with the Norwegian authorities (Norwegian Petroleum Direcotrate) and the active petroleum industry in the area.

**The coring program:** One of Mjølnir's great scientific advantages is the clear correlation between the crater and the proximal ejecta, accessible by shallow drilling (<300 meters). Consequently, Mjølnir is an ideal target for scientific drilling to document ejecta generation and distribution, and the relationship between a midsize marine impact event and biotic evolution. Moreover, Mjølnir's ejecta may serve as a stratigraphic marker to correlate Boreal and Tethyan faunal provinces near the Jurassic/Cretaceous boundary; a problem that has puzzled stratigraphers for years. Impact- induced tsunami generation, and ignition of organics and subsequent soot distribution, provide further research opportunities.

The coring is planned for 2011. Finacially support has been applied for; possible sources include, the integrated Ocean Drilling Program (IODP) og International Continental Scientific Drilling Program (ICDP), Norwegian Research Council (NRC) and the petroleum industry active in the area.

**References:** [1] Dypvik H., Gudlaugsson S.T., Tsikalas F, Attrep M.Jr., Ferrell R.E.Jr, Krinsley D.H., Mørk A., Faleide J.-I., and Nagy J.,(1996) *Geology* 24, 779 – 782. [2] Gudlaugsson S.T.(1993). *Geology*, 21, 291-294. [3] Tsikalas F.,Gudlaugsson S.T. and Faleide J.-I. (1998). *Journal of Geophysical Research,* 103: 30,469 – 30,483. [4] Dypvik H. and Jansa, L. (2003). *Sedimentary Geology*, 161, 309 – 337. [5]Shuvalov V., Dypvik H. and Tsikalas F. (2002) *Journal of Geophy ical Research,* 107, E7, 10.1029: 1-1 to 1-13. [6] Shvalov V. and Dypvik H. (2004).*Metoritics and Planeta Sciences* 39(3), 467 – 478.

**LUNAR METEORITES: SHOCK EFFECTS VS. $^{40}$AR-$^{39}$AR AGES.** V. A. S. M. Fernandes[1,2], J. P. Fritz[3], K. Wünnemann[3], U. Hornemann[4]; [1]CREMINER/LA-ISR, Univ. Lisbon , Portugal, veraafernandes@yahoo.com; [2]Univ. Manchester, Manchester, UK; [3]Museum für Naturkunde, Leibniz Institut an der HU-Berlin; [4]Ernst Mach Institut für Kurzzeitdynamik, Fraunhofer Institut, Germany.

**Introduction:** The moon recorded the impact flux since the early history of the solar system, and allows to deduce the lunar crater production rates; the most important chonological standart for dating planetary surfaces in the inner solar sytem. Lunar impact events can be dated by measuring different isotopic systems in rocks. In contrast to Sm-Nd and Rb-Sr ages which date the solidification of the rock (e.g. impact melt), the Ar-Ar dating technique can also determine the resetting ages of thermal events induced by impacts. These thermal/impact events can in some cases cause partial Ar-loss (affect only the low temperature steps of the Ar-release patterns). Therefore this dating technique can be applied to a broad range of rock types (not only impact melts). This is particularly relevant to the large number of lunar meteorites considered as more representative of the average lunar crust, compared to the Apollo and Luna mission samples which were limited to equatorial and nearside localities. Here we investigate on the influence of shock pressure and temperature on the Ar budget of lunar meteorites.

**Methods:** Shock reverberation experiments on calcium rich plagioclase ($An_{94}$) shocked to 20, 24, 28 and 36 GPa, respectively, were conducted at the Ernst Mach Institute in Freiburg [1]. The recovered samples were studied macroscopically, by optical microscopy, and Raman spectroscopy.

**Results:** Shock recovery experiments showed that calcium rich plagioclase ($An_{94}$) transformes into maskeynite at shock pressures >24 GPa. Using calcium rich plagioclase as an experimentally calibrated pressure barometer allows to determine the shock pressures recorded in lunar meteorites. As a preliminary result we present the optical properties of plagioclase in lunar meteorites and the deduced shock pressures in Table 1.

Partial and complete resetting of Ar-ages were determined by 1) measuring Ar-release during step heating experiments, and 2) compare the derived ages with literature data on crystallization ages obtained by other isotopic chonometers, including Sm/Nd, Pb/Pb Th/Pb, U-Pb. (Tab. 1) [2-14].

**Discussion:** Preliminary investigation show that 1) formation of maskelynite, e.g. in Asuka 881757 is not leading to a loss of Ar, and even impact melt bearing samples (EET 96008) are not completely reset. In co-trast partial or complet resetting of Ar ages were observed in some meteorites shocked to relatively low pressures of 22-25 GPa. This indicates that Ar loss is not a result of weak to moderate shock pressures. It appears that rock need to kept at elevated temperatures for extended times allowing for the diffusion of Ar. Different radiogenic ages in rock can be explained by a two stage cooling history, e.g exhumation by mega-impacts of hot deep seated crustual rocks onto the cool lunar surface, or reheating by a later emplacement of cool rocks into a hot ejecta blanket.

Table 1. Investigated lunar meteorites, including information on pertological type, shock metamorphic features, deduced shock pressures, and completely or partially reset Ar-ages.

| Name | type | plag | shock pressure [GPa] | melt veins | reset Ar-age | partial loss |
|---|---|---|---|---|---|---|
| Asuka 881757 | b | C | >25 | Yes | No | No |
| Yamato 793169 | b | B | 22-25 | Yes | No | Yes |
| MIL 05035 | b | B | >25 | | No | Yes |
| LAP 02205 | b | C | 21-25 | Yes | No | No |
| NWA 032/479 | b | | | | No | No |
| Dhofar 287-A | b | C | >25 | Yes | Yes | - |
| NWA 2977 | b | B | 21–25 | Yes | | |
| EET 96008 | bb | | | | ? (No) | |

Type b = basalt, bb = basaltic breccia; shock features in plagioclase are A = birefringent, B = partially isotropic, and C = completely isotropic maskelynite.

**Acknowledgements:** **F**unding provided by the Synthesis Programm (EU FP7) and the Helmholtz Alliance HA-203 "Planetary Evolution and life" WP3200 is acknowledged. We thank H. Schneider and H. R. Knöfler for preparing the shock experiment assemblies and sample preparation, respectively, and H.-R. Wenk for providing the Grass Valley rock sample used in the shock experiments.

**References:** **[1]**Müller W. F and Hornemann U. (1969) Earth Planet. Sci. Lett., 1969; 3: 251-264; **[2]**Misawa et al. (1993) GCA, 57, 4687–4702; **[3]**Fernandes et al. (2009) MaPS 44, 805-821; **[4]** Torigoye-Kita el al. (1995) GCA,59, 2621–2632; **[5]**Nyquist et al. (2007) XXXVIII LPSC, abst. #1702; **[6]**Rankenburg et al. (2007) GCA, 71, 2120–2135; **[7]**Nyquist et al. (2005) XXXVI LPSC, abst.# 1702; **[8]**Anand et al. (2006) GCA, 70, 246–264; **[9]**Nyquist et al (2009) 72nd MetSoc, abst.# 5347; **[10]**Burgess et al (2007) XXXVIII LPSC, abst.# 1603; **[11]**Borg et al (2009) GCA, 73, 3963-3980; **[12]**Fernandes et al. (2003) MaPS, 58, 555-564; **[13]** Fernandes et al 2008, Goldschmidt abst.# A264; **[14]**Anand et al (2003) MAPS 38, 485-499.

**POTENTIAL LANDING SITES FOR ROBOTIC-HUMAN EXPLORATION ON MARS.** J. W. Head, III, Dept. of Geological Sciences, Brown University, Providence, RI 02912 USA (james_head@brown.edu)

**Introduction:** Apollo exploration of the Moon showed the importance of robotic precursors for establishing the nature of the surface at high resolution (Ranger), for undertaking reconnaissance of global geologic features and certifying engineering properties of the surface for landing site selection (Lunar Orbiter), and obtaining information on the physical properties of the lunar soil and analyzing the geology and composition of surface materials (Surveyor). Furthermore, during Apollo, human-robotic partnerships were used to advantage with the Lunar Roving Vehicle (LRV) to significantly enhance the range of human exploration and to carry tools and experiments up to ~7 km away from the Lunar Module. Astronauts deployed complex and comprehensive lunar experiment packages (ALSEP) that could not be deployed robotically. Astronauts also deployed complex geophysical experiments such as Heat Flow Experiments, Active Seismic Experiments, a Surface Electrical Properties Experiment, a Portable Magnetometer, a Traverse Gravimeter, as well as drilling cores into the lunar regolith. Indeed, Dual-Mode Lunar Roving Vehicles (DMLRV) were planned for later Apollo missions, in which the rover from a completed Apollo mission would robotically traverse to the next landing site, making observations and sampling along the way. Thus, the importance of human-robotic partnerships for planetary exploration was demonstrated over 35 years ago. These approaches were applied to addressing the most fundamental questions in lunar science: Was the Moon hot or cold? What were the origins and ages of the major geologic units on the Moon? Of what was the crust made and how did it form and evolve? What was the origin and evolution of the major basins such as Imbrium and Serenitatis? What is the nature of the basic geological time scale and how have processes varied during history?

Return to the Moon and exploration of Mars requires the same type of human-robotic partnerships to accomplish the major exploration goals. In this contribution the importance of this approach to the exploration of Mars is documented.

**Scientific Goals for the Exploration of Mars:** The basic outlines of the history of Mars have been derived from data returned from Mariner and Viking images, and augmented and clarified by many subsequent orbital and rover missions (Fig. 1). Thus, the human-robotic partnership in exploring Mars has already begun; key to the success of human exploration is the in-depth traversing of each of the three main periods of geological history, the Noachian (Fig. 2), Hesperian (Fig. 3) and Amazonian (Fig. 4) as shown in sample traverse maps.

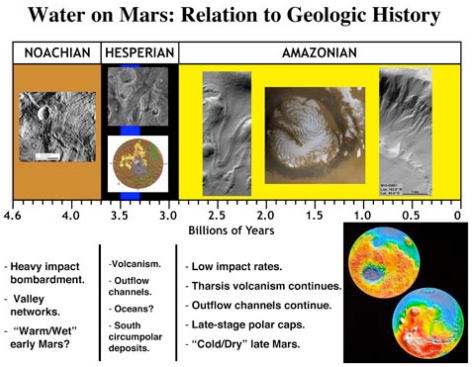


Fig. 1. Major processes during Mars' history.

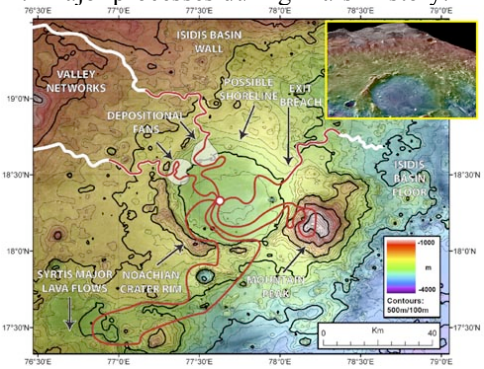


Fig. 2. Noachian Jezero crater and fluvial channels.

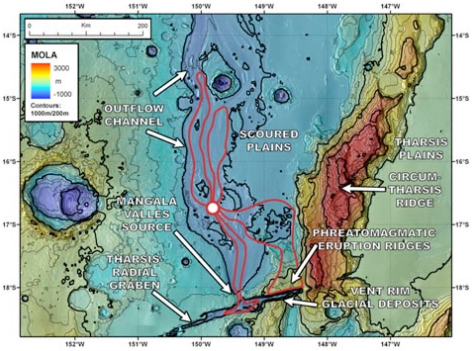


Fig. 3. Hesperian Mangala Valles outflow channel.

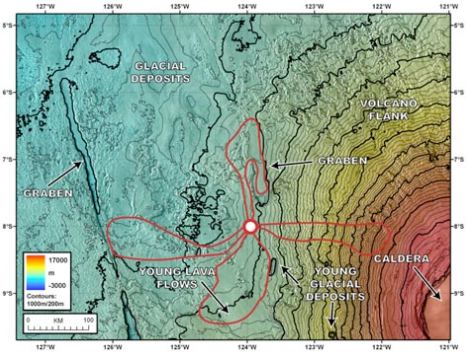


Fig. 4. Amazonian tropical mountain glacier on the NW flank of Arsia Mons volcano.

**SHOCK NEOFORMATION OF HIGHLY MAGNETIC NANO PARTICLES IN "BROWN" COLOUR OLIVINES IN MARTIAN METEORITES AND IMPLICATIONS FOR THE MAGNETIZATION OF MARS SOILS AND SURFACE ROCKS.** V.H. Hoffmann[1,2], T. Mikouchi[3], T. Kurihara[3], M. Funaki[4], M. Torii[5], [1]Institute for Geosciences and ZAG, University of Tuebingen, Sigwartstrasse 10, 72076 Tuebingen, and [2]Department of Geo- and Environmental Sciences, University of Muenchen, Theresienstrasse 41, 80333 Muenchen, Germany, [3]Dept. of Earth and Planetary Science, University of Tokyo, Japan, [4]National Institute of Polar Research, Tachikawa, Tokyo, Japan. [5]Dept. of Geosphere-Biosphere System Science, Okayama Univ. of Science, Okayama, Japan.

**Introduction:** During the last years, brown-coloured olivines are frequently observed in moderately-highly shocked Martian meteorites (SNC), specifically in lherzolitic and olivine-phyric shergottites. TEM studies revealed that Fe-Ni metal nano-particles are responsible for the dark "brown" colour of olivine in the NWA 2737 chassignite, a shocked dunite, which is interpreted to have formed by reduction of olivine due to heavy shock events [1,2]. Similar brown colour olivine seems to be fairly common among Martian meteorites and thus the widespread presence of Fe-Ni metal nano-particles in these olivine grains can be expected. The formation of nano phases in olivine matrix could be related to shock metamorphism in a degree of at least 40 GPa [2]. Native Fe-Ni or magnetite nano particles in brown/ black Fe-bearing olivines or pyroxenes could be detected in ALH 77005 (Fe-Ni), Y000097 (Fe-Ni), LEW 88516 ($Fe_3O_4$), NWA 1950 (Fe-Ni), LAR 06319 (Fe-Ni) [2-7] and DaG 476 (in olivine and pyroxene [this study]). [2] reported the results of laboratory shock experiments on natural San Carlos olivines: depending on the sample properties (olivines with/without graphite) and the degree of shock (20–46 GPa) magnetite (Ni free) or Ni-bearing Fe nano phases were found in the olivine matrix by TEM and EDS analyses. Recently the same authors could demonstrate that Fe-Ni metal nano-particles can be produced instead of magnetite nano phases by preheating olivine before performing shock experiments [9,10]. Most likely, temperature difference during shock might control the formation of Fe-rich nano-particles either Fe-Ni metal or magnetite.

The aims of our study are to investigate and to better understand the magnetic signature and record of the "brown" colour olivine bearing Martian meteorites.

**Samples and experiments:** The magnetic properties of a series of laboratory-shocked olivines were investigated systematically. We used selected samples of the set as described by [2]. All data are compared with the results of a systematic search on the magnetic signature of the forsterite-fayalite series (synthetic material) as reported by [8] and additional systematic low-temperature investigations [this study]. For a detailed description of the samples and their preparation as well as of the shock experiments we refer to [2].

**Results:** The high sensitivity of our magnetic methods allows very detailed view to the effects of shock, especially dynamics and kinetics of this process, on the magnetic properties of olivines and consequently the shock-induced neoformation of nano sized ferri(o)magnetic phases. The 40 GPa sample (with graphite) behaves differently from all others because it contains a significant amount of native Fe (only neglectible Ni according to our results) while both the 20 GPa and the 40GPa samples without graphite are mainly dominated by magnetite like phases (eventually also maghemite or Mg-ferrite). Our data clearly indicate that already at 20 GPa the magnetic signature and phase composition is significantly modified. In a next step, the olivine samples which have been preheated before the shock experiments, shall be the target of a similar set of magnetic tests.

**Conclusions:** Presently it is speculated about the potential of these highly magnetic nano particles, native Fe-Ni or magnetite, to act as recorders of stable and reliable magnetic remanences in Martian surface rocks and crust. Large parts of the Mars surface are covered by impact craters, and consequently we should expect to find thick layers of impactites on the Mars surface. [12, 13] reported the finding of high concentrations of strongly magnetic material in the soils around the Phoenix lander. The origin of the different classes of particles is uncertain, only comparison with suitable terrestrial Mars analogue materials could provide some hints in terms of both spectral and magnetic properties [see also 11].

**References:** [1] Treiman A.H. et al. (2007) J. Geophys. Res. E (112), 2007. [2] Kurihara T. et al. (2008a) 39th LPSC, #2505. [3] Kurihara T. et al. (2008b) MAPS 43, #5177. [4] Kurihara T. et al. (2008c) 39th LPSC, #2478. [5] Hoffmann V. et al. (2008a) MAPS 43, #5233. [6] Hoffmann V. et al. (2008b) Contrib. Geophys. Geod., 100-101. [7] Hoffmann V.H. et al. (2008c) Paneth Colloquium PC2008#021. [8] Hoffmann V. & Soffel H.C. (1986) J. Geophys. Res. 60, 41-46. [9] Kurihara T. et al. (2009) 40th LPSC, #1049. [10] Kurihara T. et al. (2010) 41st LPSC, #1655. [11] Koizumi E. et al. (2010) 41st LPSC, #1575. [12] Goetz W. et al. (2009a) Workshop Microstructure of Martian Surface, #9012. [13] Goetz W. et al. (2009b) Jour. Geophys. Res. (submitted).

**PROVENANCE OF IMPACT-MELT BRECCIAS COLLECTED AT THE APOLLO LANDING SITES: WHAT DID WE LEARN AND WHAT ARE THE IMPLICATIONS FOR FUTURE EXPLORATION?** B. L. Jolliff, R. L. Korotev, and R. A. Zeigler. Department of Earth and Planetary Sciences and the McDonnell Center for the Space Sciences, Washington University, St. Louis, MO, 63130, USA (blj@wustl.edu).

In the past four decades, much has been learned about samples returned from the Moon by Apollo and Luna, and more recently, from the study of lunar meteorites. One of the legacies of the lunar samples is the correlation between ages of rocks that were created in or affected by impact events and the locations where they were sampled. From such correlations, precise ages have been assigned to events that seemed most logical according to geologic relationships. Moreover, with a few accurately determined ages, an entire relative chronology was developed according to stratigraphic relationships and impact crater size-frequency distributions [reviewed by 1].

Still, after 40+ years of study, the provenance of samples and ages of key events continue to be a focus of research and a topic of debate. Central to the argument are the formation ages of the impact basins and the implications of those ages. From geologic relationships, we infer that (1) noritic impact-melt breccias and crystalline melt rocks from Apollo 14 and 15 record the formation age of the Imbrium Basin, (2) those from the boulders of the highland massifs at Apollo 17 record the age of Serenitatis, (3) those from the KREEP-poor impact-melt-breccia groups at Apollo 16 record the age of Nectaris, and (4) similar materials from Luna 24 record the age of Crisium. Ejecta from such prominent craters as Copernicus and Tycho were sampled at Apollo 12 and 17, respectively, and local craters such as Cone at Apollo 14, and North Ray and South Ray at Apollo 16 were also sampled and ages determined for those events. Much of what we understand about the impact flux is based on these ages.

One fundamental conclusions from the data is that impact basin ages point to a late, heavy bombardment or "cataclysm," with a pronounced spike in large impact events ~4.0–3.8 Ga. The paucity of impact melt rocks older than 4.0 Ga has been interpreted to mean that either (1) most impact basins formed at this time, or (2) the large, near-side, relatively late basins whose ejecta deposits dominate the Apollo samples simply obscured or reset impact rocks formed earlier [2].

To complicate matters, different age-dating methods can yield different ages of formation. In some cases, the information is complementary, for example, Sm-Nd or Rb-Sr isotopes might give a crystallization age whereas an Ar-Ar age from the same rock might record an event that reset the isotopes but did not completely melt the rock. Recent data from the sensitive, high-resolution ion microprobe (SHRIMP) date zircons in impact-melt rocks has given a precise age determination of a Th-rich lunar meteorite, SaU-169 [3], and a group of very similar Apollo 12 impact-melt breccias [4] of 3.91 Ga. The simplest interpretation is that these samples were produced by Imbrium. What does this mean for the more commonly cited age of Imbrium of 3.86 Ga [5]?

Although the origin of the impact-melt breccias from Apollo 17 has been called into question [2], samples from boulders that have clear origins in the massif deposits were most likely formed by the Serenitatis event. Their ages, determined mainly by Ar geochronology, point to 3.89 Ga.

Impact-melt rocks from Apollo 16 span a range of geochemical characteristics and ages. The Cayley Plains and most of the mafic impact-melt groups likely have an Imbrium origin. KREEP-poor melt rocks may come from Nectaris; and still others may even come from Serenitatis. Ages, mostly by $^{40}$Ar-$^{39}$Ar, have proven difficult to interpret [6].

What is needed is to sample directly impact melt rocks from within a basin, i.e., its melt sheet. The deposition of basin ejecta deposits is largely ballistic, so distal deposits have mixed provenance. Direct sampling of a basin such as Orientale or Schrodinger, where basin melt deposits are unambiguous, or sampling the ejecta of a young crater that penetrates mare to excavate underlying impact deposits is needed.

A high-priority goal of impact basin chronology on the Moon is to test the Cataclysm hypothesis. Perhaps the best approach is to determine the chronology of the South Pole-Aitken Basin, the oldest and largest recognized basin on the Moon. Its location far from the large and late, nearside basins coupled with impact ejecta modeling indicating that rocks of the original impact-melt sheet should still be the dominant component of the regolith in the Basin interior makes it a prime exploration target for sample return. Confirming or refuting the Cataclysm hypothesis will have implications for the early bombardment history of the Solar System at a critical time for surface evolution of the Earth and other planets of the inner Solar System.

**Acknowledgements:** Support is from the NASA Cosmochemistry program, # NNX07AI44G.

**References:** [1] Stöffler et al. (2006) *RIM-G,* **60**, 519-596; [2] Haskin et al. (2003) *Meteorit. Planet. Sci.*, **38**, 13-33; [3] Gnos et al. (2004) *Science*, **305**, 657-659; [4] Liu et al. (2002) *LPS 41,* Abstract #2477; [5] Dalrymple and G. Ryder (1993) *JGR*, **98**, 13,085-13,095; [6] Norman (2009) *Elements*, **5**, 23-28.

**FORMATION AGES OF THE APOLLO 16 REGOLITH BRECCIAS: IMPLICATIONS FOR ACCESSING THE BOMBARDMENT HISTORY OF THE MOON.** K. H. Joy[1,2], D. A. Kring[1,2], D. D. Bogard[2,3], M. E. Zolensky[2,3], and D. S. McKay[2,3]. [1]CLSE, LPI/USRA, 3600 Bay Area Blvd., Houston, Texas 77058, USA (joy@lpi.usra.edu). [2]NASA Lunar Science Institute. [3]ARES, NASA Johnson Space Center, Houston, TX 77058, USA.

**Regolith breccia 'formation' ages:** Regolith breccias are lithified samples of the regolith that have been fused together by impact shock and thermal metamorphism. In lunar regolith samples, the ratio of trapped $^{40}Ar/^{36}Ar$ is a useful indicator of antiquity and can be used to model the closure age / lifithication event of the regolith (i.e. the apparent time when Ar became trapped [1]), thus providing important insights into specific times when that regolith was being gardened by impacting asteroids and comets [2-4].

**The Apollo 16 regolith breccias:** McKay et al. [5] used this method to identify two groups of regolith breccias at the Apollo 16 (A16 RB) landing site: (i) the 'ancient' group, representative of immature (i.e. <30 $I_s$/FeO: Table 1) pre-3.9 Ga regolith, and (ii) the 'younger' group that generally have higher levels of maturity (Table 1) and were formed after 3.9 Ga (see also [6-8]). We have used the relationship between trapped $^{40}Ar/^{36}Ar$ and sample isotopic age as shown in Fig. 6 of McKay et al. [5] to calculate the model closure ages of the A16 RB: these data are shown in Table 1 listed as Model 1. These ages suggest that the ancient A16 RB represent lithification of immature regoliths throughout the period of lunar basin formation from 4.5-3.93 Ga [5,7,8], and therefore provide a window to regolith formation processes and the nature of bombarding projectiles before the formation of the Imbrium basin at ~3.85 Ga.

**New Age Estimates:** Here we readdress the formation time of these A16 RB in light new calibrations of the relationship between trapped $^{40}Ar/^{36}Ar$ vs. sample isotopic age as proposed by Eugster et al. [9]. The model ages derived from this calibration (Model 2 in Table 1) indicate that the ancient A16 RB are not as old as suggested by the Model 1 calibration [5], and that the ancient breccias only sample post-basin regolith processes from 3.67-3.26 Ga (Table 1).

We have further extended the Eugster et al. [9] calibration to include additional data from lunar meteorite Yamoto-86032 [10] and Apollo 16 regolith breccia components [11-12]. Where possible we corrected the Eugster et al. [8] calibration isotopic ages for updates in decay constants [13-14], and we also removed the Apollo 14 samples from the calibration.

Using this new calibration, we determined model ages (Model 3 in column 7 of Table 1) that are more consistent with A16 RB sample isotopic ages and ages of clast components within them (see column 8 of Table 1) than either the Model 1 [5] or Model 2 [9] ages.

**Implications for accessing the record of impacting projectiles:** Our model results indicate that the ancient A16 RB (e.g. 61135 to 60019) were lithified during the last stages of basin formation on the Moon from 3.81 to 3.38 Ga. This suggests that they do not provide a window to pre-Imbrium regolith processes.

The young A16 RB samples (e.g. 63595 to 60256: Table 1) provide an opportunity to investigate the nature of impacting projectiles through ~2.5 to 1.7 Ga. This period is contemporaneous with recent mare basalt eruptions and associated with quiescent impact bombardment. Samples such as 63507 and 65095, which have low trapped $^{40}Ar/^{36}Ar$ ratios, were lithified very recently and are comparable with the impact record preserved in present day Apollo 16 soils [5].

| Sample | $I_s$/FeO | Age | $^{40}Ar/^{36}Ar_{Tr}$ | Model 1 Age (Ga) | Model 2 Age (Ga) | Model 3 Age (Ga) | Age (Ga) |
|---|---|---|---|---|---|---|---|
| 61135,29 | 0.5 | A | 12.5 | 4.56 | 3.67 | 3.81 | 3.819 |
| 60016,165 | 0.5 | A | 12.2 | 4.52 | 3.64 | 3.78 | 3.8 |
| 66075,76 | 0.5 | A | 11.7 | 4.44 | 3.59 | 3.72 | 3.83 |
| 65715,11 | 0.6 | A | 11.3 | 4.38 | 3.55 | 3.68 | |
| 66035,32 | 0.5 | A | 10.5 | 4.25 | 3.46 | 3.59 | |
| 66036,10 | 0.4 | A | 10.4 | 4.23 | 3.45 | 3.58 | |
| 61516,8 | 0.05 | A | 9.5 | 4.07 | 3.35 | 3.47 | |
| 61195,57 | 0.1 | A | 9.3 | 4.03 | 3.32 | 3.44 | |
| 60019,110 | 0.2 | A | 8.8 | 3.93 | 3.26 | 3.38 | |
| 63595,5 | 0.4 | Y | 4.4 | 2.67 | 2.44 | 2.53 | |
| 61175,206 | 8 | Y | 4.25 | 2.61 | 2.4 | 2.48 | |
| 61295,47 | 6 | Y | 4.1 | 2.55 | 2.35 | 2.44 | |
| 61536,8 | 9 | Y | 3.9 | 2.46 | 2.29 | 2.38 | |
| 60275, 56 | 4 | Y | 3.8 | 2.41 | 2.26 | 2.35 | |
| 61525,9 | 3 | Y | 3.7 | 2.36 | 2.23 | 2.31 | |
| 63588,6 | 0.4 | Y | 3.3 | 2.15 | 2.1 | 2.17 | |
| 60255, 93 | 17 | Y | 2.25 | 1.46 | 1.64 | 1.7 | |
| 63507,15 | 48 | VY | 0.55 | -1.09 | -0.02 | -0.02 | |
| 65095,78 | <0.1 | VY | ~0 | 0 | 0 | 0 | |

**Table 1.** Ages and maturity of the Apollo 16 regolith breccias. Sample number and corresponding $I_s$/FeO value and trapped $^{40}Ar/^{36}Ar$ ratio taken from [5]. Age classifications modified from [5] where A = ancient, Y = young and VY = Very young regolith breccia. Model 1 ages determined from relationship shown in Fig. 6 of [5]. Model 2 ages determined from relationship shown in Table 9 of [9]. Model 3 ages determined from ages and $^{40}Ar/^{36}Ar_T$ ratios (i) of 15005, 60006, 67601, 74001, 74261 as listed in [9]; (ii) recalculated age [13] of clast components in 61135 [14], 60016 [11] and the bulk age of 66075 [12]; and (iii) the Yamoto-86032 lunar meteorite [10].

**References:** [1] Yaniv A. and Heymann D. (1972) *LSC* III, 1967-1980. [2] Hörz F. et al. (1991) Chapter 4. *The Lunar Sourcebook.* pp. 61-120. [3] McKay D. D. et al. (1991) Chapter 7. *The Lunar Sourcebook.* pp. 265-356. [4] Lucey P. et al. (2006) Chapter 2. *Reviews in Mineralogy & Geochemistry*. 60, 83-219. [5] McKay D. D. et al. (1986) *LPS* XVI, D277-D303. [6] Wentworth S. J. and McKay D. D. (1988) *LPS* XVIII, 67-77. [7] Korotev R. L. (1996) *M&PS*, 31, 403-412. [8] Simon et al. (1988) EPSL. 89, 147-162. [9] Eugster O. et al. (2001) *M&PS*, 36, 1097-1115. [10] Eugster O et al. (1991) *GCA*, 55, 3139-3148. [11] Weber H. W., and Schultz L. (1978) *LPS VIX*, 1234-1236. [12] Oberli F. et al. (1979) *LPS X*, 37. [13] Koppers A. A. P. 2002. *Computer and Geosciences,* 28, 605-619. [14] Schaeffer G. A., and Schaeffer O. A. (1977). *LSC VIII*, 2253-2300.

**THE RIES CRATER AND THE INTERPRETATION OF EJECTA DEPOSITS AT IMPACT CRATERS ON MARS.** T. Kenkmann[1], A. Wittmann[2], [1]Institut für Geowissenschaften, Albertstrasse 23-b, Universität Freiburg, 79104 Freiburg, Germany. Thomas.kenkmann@geologie.uni-freiburg.de; [2]Lunar and Planetary Instiute, Houston, TX, USA.

**Introduction:** Terrestrial impact stuctures provide field evidence for cratering processes on planetary bodies with an atmosphere and volatiles in the target. The Ries crater with its preserved deposits is the ideal object on Earth to investigate the effect of atmosphere and target volaties on ejecta deposition.

**Ejecta deposits of Martian craters:** Martian impact craters reveal morphological characteristics like fluidized ejecta with ramparts that are different from ejecta blankets on the Moon. Ejecta morphologies such as single layer ejecta, double layer ejecta, and multiple layer ejecta [1] depend on crater size, geographic location, altitude, terrain, and time of formation [2]. The different layers have sharp boundaries. The inner layers are often sutured with radial grooves and concentric furrows and ridges. The characteristics of Martian ejecta blankets have been explained by either emphasizing the role of subsurface ice and water ('subsurface volatile model') [3] or atmospheric turbulences during the cratering process ('ring vortex model')[4].

**Ries crater:** The ~26 km diameter Ries crater formed ~14.3 Ma ago in a target that is composed of ~650 m of partly water-saturated and subhorizontally layered sediments (limestones, sandstones, shales) underlain by crystalline basement rocks (gneisses, granites, amphibolites).

Its continuous ejecta blanket is the Bunte Breccia, a polymict lithic breccia that is mainly composed of sedimentary target clasts and reworked surficial sediments. It only contains 5-10% crystalline rocks, while local and crater derived materials are thoroughly mixed on all scales. The ratio of primary crater ejecta to local substrate components in the Bunte Breccia decreases with increasing radial range [5]. It is interpreted as a "cold", non-cohesive impact formation [6], however, internal shear planes do occur locally within the preserved ejecta blanket. The Bunte Breccia exhibits sharp contacts to the underlying substrate, even if it is formed by unconsolidated sands [7]. Still, because no paleosols were retained, none of the contact horizons of the Bunte Breccia with the target represent the land surface prior to the impact. A radial flow of the ejecta is indicated by striations on contact surfaces but obstacles of the pre-existing paleorelief locally deflected it by up to 30°.

Upper target layers beneath the ejecta blanket around the crater were decoupled along incompetent, fluid bearing clay and marl beds. Near-surface spallation together with dragging [8] by the ejecta curtain and/or the ejecta blanket flow, induced subsequtent outward shearing of target strata.

Bunte Breccia is locally overlain by 10-25 m thick patches of Suevite, which indicate far higher temperatures and degrees of shock metamorphism and are mainly composed of clasts and melt particles derived from the crystalline basement. Suevite is the dominant type of ejecta in the inner crater, where it reaches a thickness of ~300 m. Outside the crater, the bulk volume of Suevite is only 5-10% of that of the Bunte Breccia. The Suevite - Bunte Breccia contact is very sharp but locally, dm-thick transition zones with reworked and mixed Suevite and Bunte Breccia occur. The contact plane has a strong relief with partly vertical walls and several meter deep grooves .

**Discussion:** The Ries crater's ejecta blanket is tested for the hypothesis of fluidization during emplacement. Initial interpretations of the Bunte Breccia assumed analogies to the Moon: (I) ballistic emplacement, which triggered a ground hugging debris surge, or (II) a rolling and gliding surge under high localized confining pressures. Water saturation in the target sequence of the Ries suggests it more likely formed analogous to Martian rampart craters [8]. Sedimentological evidence from the Bunte Breccia supports this hypothesis. Near-surface volatiles may have been liberated from a variably thick cover of poorly consolidated Tertiary sediments and underlying sedimentary rocks during the impact and deposition of ejecta. This likely caused at least localized fluidization. The existence of volatiles within the Bunte Breccia can be demonstrated by the presence of ductily deformed clays and venting pipes that originate from the interface between Bunte Breccia and Suevite. These venting pipes suggest vaporization of water at the Bunte Breccia's surface during the emplacement of Suevites.

The presence of two distinct ejecta layers is probably the most intriguing analogy between Martian impact craters and the Ries. The mechanism by which the separation of both ejecta layers occurred is still a matter of debate and will be discussed.

**References:** [1] Barlow, N.G. et al. 2000. JGR 105: 26733-26738. [2] Mouginis-Mark, P.J. 1979. JGR 84: 8011-8022. [3] Clifford, S.M. 1993. JGR 98: 10973-11016. [4] Barnouin-Jha, O.S. & Schultz, P.H. 1998. JGR 103: 25739-25756. [5] Hörz, F., Ostertag, R., & Rainey, D.A. (1983) *Rev. Geophys. Space Phys. 21,* 1667-1725. [6] Stöffler, D. (1975) Fortschr. Miner., 52, 385-387. [7] Hörz F. et al. (1977). Roddy, D.J, Pepin, R.O., & Merill R.B. (eds.), p. 425-448. [8] Kenkmann, T. & Schoenian, F. (2006). MAPS 41, 1587-1604.

**EXPLORING KEY LUNAR STRATIGRAPHIC UNITS REPRESENTING 4 BILLION YEARS OF LUNAR HISTORY WITHIN SCHRÖDINGER BASIN.** T. Kohout[1, 2], K. O'Sullivan[3], K. G. Thaisen[4] and D. A. Kring[5], [1]Department of Physics, University of Helsinki, Finland, tomas.kohout@helsinki.fi, [2]Institute of Geology, Academy of Sciences of the Czech Republic, Prague, Czech Republic, [3]Department of Civil Engineering and Geological Sciences, University of Notre Dame, Notre Dame, IN, USA kosulli4@nd.edu, [4]University of Tennessee, Knoxville, TN, USA, [5]Lunar and Planetary institute, Houston, TX, USA.

**Introduction:** To test the lunar cataclysm hypothesis and anchor the beginning of the basin-forming epoch on the Moon, we evaluated potential landing sites within the Schrödinger Basin [1]. This impact site is the second youngest basin-forming event and lies within the South Pole-Aitken Basin (SPA), which is the oldest and largest impact basin on the Moon. Thus, landing sites within Schrödinger should provide access to impact lithologies with ages of each event, providing a bracket of the entire basin-forming epoch and resolving both of the leading science priorities [2]. Additionally, the floor of Schrödinger Basin has been partially covered by younger mare and pyroclastic units. The volcanic materials, as well as impact-excavated and uplifted units, will provide chemical and lithologic samples of the lunar crust and potentially the upper mantle. Collectively, the impact and volcanic lithologies will provide calibration points to the entire lunar stratigraphic column.

**Landing site selection:** We propose a landing site for manned or robotic exploration on a relatively smooth terrain within the inner ring of Schrödinger – either on the exposed melt sheet or on one of the basaltic units.

Based on geological mapping [3] and Clementine images, we evaluated three landing sites (Fig. 1) where most of the scientific objectives can be accomplished. The white circles in Fig. 1 outline a 10 and 20 km radius of an EVA range.

**Conclusions:** The Schrödinger Basin provides a diverse suite of scientific opportunities because of the proximity of different geologic units and its relatively good preservation. Any one of three possible landing sites will provide the first samples of basin melts of undisputable basin origin and potentially melts of SPA origin. In addition, at least two types of younger volcanism (and magmatic source regions) can be studied in the area.

**Acknowledgements:** This work is part of the 2008 Lunar Exploration Summer Intern Program at the LPI, Houston, and co-sponsored by the NASA Lunar Science Institute. We thank the LPI staff for their help and support.

**References:** [1] O'Sullivan K. et al. (2010) *GSA Special papers*, in print. [2] NRC (2007) *The Scientific Context for Exploration of the Moon*. [3] Shoemaker E. M. et al. (1994) *Science, 266,* 1851–1854.

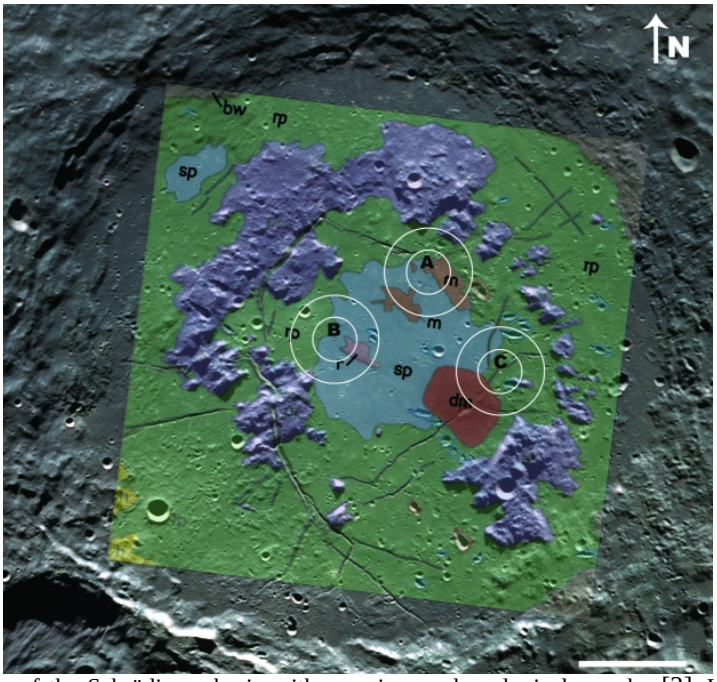


**Figure 1:** Clementine image of the Schrödinger basin with superimposed geological map by [3]. White bar is 50 km long, white dots are landing sites, and white circles are 10 and 20 km radii. The main units are smooth plains material (sp), rough plains material (rp), basin wall material (bw), hummocky material (h), peak ring material (pr) mare material (m), dark explosive volcanic material (dm), and ridged terrain (r). The sp unit is interpreted to be Schrödinger impact melt, and the rp unit to be Schrödinger impact melt breccia.

**WHAT CAN ASTRONAUTS LEARN FROM TERRESTRIAL IMPACT CRATERS FOR OPERATIONS ON THE MOON AND MARS?** David A. Kring[1,2], [1]Center for Lunar Science and Exploration, USRA – Lunar and Planetary Institute, 3600 Bay Area Blvd., Houston TX 77058 (kring@lpi.usra.edu), [2]NASA Lunar Science Institute.

**Introduction:** Virtually any step an astronaut makes on the Moon will be in an impact crater. The excavated cavities, uplifted rims, and distributed ejecta of impact craters dominate the lunar landscape. Impact processes are even responsible for the lunar soil. Learning how to operate in that type of environment will be critical to the success of exploration. Impact craters are also our most treasured scientific sites for lunar exploration. These same observations apply to many regions of Mars.

**Science Lessons to be Learned:** A concentration of *c*. 3.9-4.0 Ga Apollo sample ages suggest there may have been a spike in the impact flux in an event called the lunar cataclysm. Not only did the bombardment affect the geologic evolution of terrestrial planets, it may have also influenced the origin and evolution of life on the Earth and potentially Mars. Because the impact flux to the inner solar system is both accessible and uniquely preserved on the Moon, additional samples to evaluate the impact flux are among the highest lunar science priorities. To complete that task, crew will need to study analogue sites to learn about crater morphology, associated structural elements, the distribution of impact lithologies, and how to locate samples suitable for determining the ages of craters.

Astronauts also need to be taught that complex craters and multi-ring basins are excellent probes of the lunar interior. Normal faults in the modification zones of these craters expose subsurface lithologies and their stratigraphic relationships. Uplifted central peaks and peak rings expose even deeper levels in the Moon's crust. Furthermore, clasts of subsurface lithologies are entrained in impact melt breccias deposited within the crater and beyond its rim. Thus, by combining observations of modification zones, central uplifts, and impact breccias, one can generate cross-sections of the lunar crust that may be kilometers to 10's of kilometers deep. The volume of material beneath an impact site that is melted extends to an even deeper level than the material that is excavated. Thus, while collecting melt samples to determine the impact flux, crew will also be collecting samples of the lunar interior.

Large craters may have formidable crater walls, so some missions may be limited to the crater interior, while others may be limited to the crater ejecta blanket. Learning how to conduct radial sampling of an ejecta blanket to probe the subsurface stratigraphy exposed in the crater interior will be another key training objective at terrestrial craters.

**Exploration Lessons to be Learned:** The expanded geographic scale of future lunar surface operations will be a new challenge. Excursion distances will be far greater than those of Apollo and even some of the topographical features have greater dimensions than those encountered during Apollo. The 1.25 km diameter Meteor Crater of Arizona is a perfectly good proxy for Apollo 16's North Ray Crater. It is even a good analogue for many of the morphological features of Shackleton Crater at the lunar south pole. However, the size of Shackleton Crater (20 km diameter and 3 times deeper than the Grand Canyon) may require training activities at Sierra Madera Crater (13 km) and the Ries Crater (24 km) to capture the operational (e.g., communication, rover mobility, and supply) issues that are affected by greater distances.

**Crew Perspective:** Apollo astronauts found field training and traverse exercises to be the most important component of their EVA preparation. Charlie Duke said "The geology field trips were outstanding. The monthly trips that we did from the time we started on the crew were just right." John Young added that a field exercise "helps you to get a team work pattern and I think that's real important. You are not very effective unless you're working as a team up there. Otherwise you're just going to be spinning your wheels on the Moon and that's not where they want you to spin them."

Fig. 1. Gene Shoemaker training Apollo astronauts at Barringer Meteorite Crater (aka Meteor Crater) in 1965. (NASA photograph S65-23562).

**SHOCK METAMORPHISM AT THE RIES AND IMPLICATIONS FOR LUNAR ROCKS AND MARTIAN METEORITES.** F. Langenhorst[1], [1]Bayerisches Geoinstitut, University of Bayreuth, D-95440 Bayreuth, Germany; Falko.Langenhorst@uni-bayreuth.de.

Before 1960 suevite from the Ries was interpreted by most scientists as a volcanic tuff and the Ries structure itself was considered as the product of a volcanic eruption. The impact origin of the Ries structure was established in 1960 by Shoemaker and Chao [1] who discovered coesite in crystalline fragments of suevite from the Otting quarry. Subsequent petrographic and mineralogical investigations of suevite breccias resulted in the discovery of further diagnostic impact effects such as planar microstructures, diaplectic glasses, and stishovite [2,3]. These investigations led also to the definition of the progressive stages of shock metamorphism and the classification of impact rocks [4, 5]. The knowledge obtained during this early time of impact research was provided to the Apollo 14 astronauts during a NASA field training in the Ries, which was regarded as the "best-known lunar terrain on planet Earth".

Studies of shock metamorphism at the Ries experienced a revival in the mid 90ies by the discovery of impact diamonds [6], which were interpreted to have formed by condensation from the vapour plume. Subsequent studies showed however that the diamonds exhibit a tabular shape (Figs. 1 and 2) that can only be explained by a solid-state transformation of precursor graphite in target rocks [7].

Since the discovery of diamond a number of other new high-pressure phases have been found in the Ries including the new high-pressure polymorphs of $TiO_2$ [8, 9]. These discoveries have been enabled by the use of modern characterization techniques with high lateral resolution such as Raman spectroscopy and transmission electron microscopy (TEM). The latter technique has particularly improved our knowledge of the nature und formation of shock effects in terrestrial, lunar and Martian rocks.

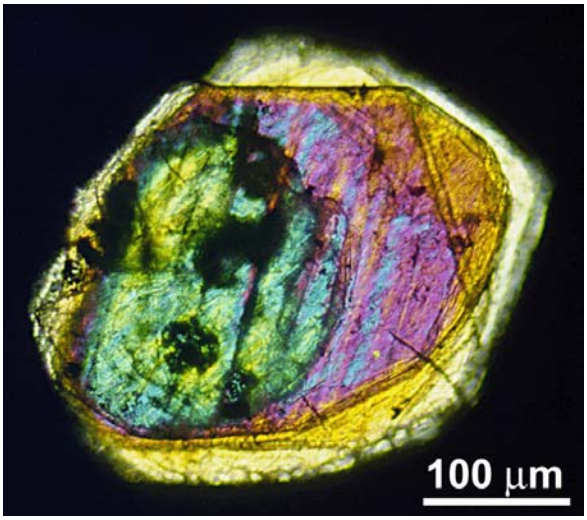


Fig. 1. Optical micrograph of an impact diamond from the Ries, crossed Nicols.

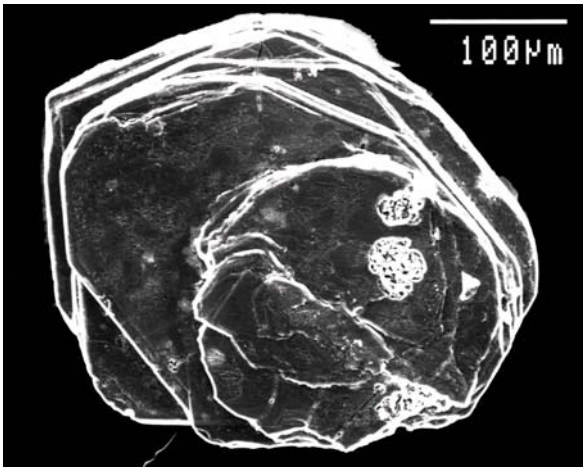


Fig. 2. Secondary electron image of the diamond platelet shown in Fig. 1.

**References:** [1] Shoemaker E. M. and Chao E. T. C. (1961) *JGR, 66,* 3371. [2] von Engelhardt W. (1972) *Contr. Min. Petrol, 36*, 265. [3] Stöffler D. (1972) *Fortschr. Min.,49,* 50. [4] von Engelhardt W. and Stöffler D. (1968) in French B. M. and Short N. M., Monobook Corp., 159-168. [5] Stöffler D. (1971) *JGR, 76,* 5541. [6] Hough R. M. et al. (1995) *Nature, 378,* 41. [7] Langenhorst et al. (1999) *Geology, 27,* 747 [8] El Goresy et al. (2001) *Science, 279*, 1467. [9] El Goresy et al. (2001) *EPSL, 192,* 485.

**Mistastin impact structure, Labrador: A geological analogue for lunar highland craters.**

Marianne M. Mader*[1]; Gordon R. Osinski[1]; Cassandra Marion[1]; Rod Dammeier[1], Bhairavi Shankar[1], Paul Sylvester[2]; [1] Centre for Planetary Science and Exploration, Dept. of Earth Sciences, University of Western Ontario, 1151 Richmond Street, London, ON, Canada, N6A 5B7, [2] Department of Earth Sciences, Memorial University of Newfoundland, St. John's, NL, Canada

**Introduction:** On the Moon, meteorite impact craters are the dominant geological landform. Key sites of scientific and exploration interest for early return missions to the Moon lie in the South Pole-Aiken basin, a region dominated by anorthositic rocks. Geological relationships between specific craters and their impactites (i.e., rocks affected by impact events) on the Moon are complex and relatively poorly constrained.

Geological analogue sites on Earth, which are similar to South Pole lunar craters, include impact structures developed in anorthositic target materials, with preserved impactites of similar lunar mineralogy and outcrop characteristics. Typically, impact ejecta deposits are rare on Earth due to post-impact erosional processes, therefore, finding an appropriate analogue site for comparative studies is difficult.

**Mistastin Lake Impact Structure:** The Mistastin Lake impact structure, in northern Labrador, Canada (55°53'N; 63°18'W) represents an exceptional lunar analogue site which includes both an anorthositic target and newly-discovered ejecta deposits. This intermediate-size crater (28 km diameter) formed by a meteorite impact ~36 million years ago, and still exhibits a distinct rim and central uplift [1]. It is comparable to many of the larger impact craters on the Moon (150-200 km in diameter) when scaled for gravity differences.

The target rocks at Mistastin consist of anorthosite, mangerite and granodiorite. A suite of impactites include: shocked and/or fractured target rocks, monomict breccia, polymict lithic breccia, impact melt-bearing breccia ("suevite") and impact melt rocks.

**Preliminary Results:** An initial 10-day reconnaissance investigation of the Mistastin Lake impact structure was carried out in September, 2009. Detailed field studies primarily focussed on the banks of creeks where contact relationships between units are best exposed. Some preliminary examples of geological lunar analogues at Mistastin Lake include:

1) Anorthosite in a variety of impact settings (i.e., shock levels): as shocked rocks in the central uplift, low-shock lithic (i.e., melt-free) impact breccias, and as clasts within the high-temperature impact melt sheet.
2) An exceptional ~80 m thick unit of impact melt rock within the crater rim (Fig. 1).
3) Impact melt-bearing breccias ("suevites"): rock with fine-grained light grey matrix with abundant plagioclase clasts and inclusions of melt fragments.
4) Impact ejecta deposits inside the crater rim and overlain by impact melt rock, potentially analogous to "double layer ejecta" craters on the Moon in which impact melt ponds overlie the blocky ejecta blanket (Fig. 1).

Figure 1: Left: 80 m high cliff section of impact melt. Right: Impact melt (orange with horizontal fractures) overlying impact breccias of the ejecta blanket.

The discovery of impact ejecta deposits at Mistastin are particularly important. While they lie within the rim of the original crater, they lie outside the initial transient crater and are, therefore, by definition ejecta (cf., many surficial suevite occurances at the Ries crater, Germany [2]). Ejecta deposits are only preserved at one other Canadian impact crater – the Haughton impact structure, Devon Island [3] – so the Mistastin outcrops provide an important new site at which to understand the origin and emplacement of impact ejecta.

**Conclusions:** Impact cratering is considered the most important surface process on the Moon. With limited lunar samples, planetary scientists look to terrestrial craters for comparative studies. The Mistastin Lake impact structure, Labrador offers a unique opportunity to understand the effects of shock on impacted materials; and to understand the origin and emplacement of impact ejecta.

**Acknowledgements:** We thank funding from the Canadian Space Agency's Canadian Analogue Research Network (CARN), NSERC Discovery Grant and Northern Research Supplement Program.

**References:** [1] Grieve R. A. F. (1975) *Geol.Soc.of America Bull. 86*, 1617-1629. [2] Engelhardt, W. v. (1990) *Tectonophys*. *171*, 259 – 273. [3] Osinski, G. R., Spray, J. G., and Lee, P., (2005) *Meteoritics & Planetary Sci. 40*,1789–1812.

**LITHIUM ISOTOPES IN TEKTITES – TALES OF SOURCES, HISTORIES AND IMPACTS.** T. Magna[1], A. Deutsch[2], R. Skála[3], K. Mezger[4], L. Adolph[2], H.-M. Seitz[5], J.T. Wasson[6], J. Mizera[7] and Z. Řanda[7], [1]Inst. Mineralogie, Universität Münster, Germany (tomas.magna@uni.muenster.de), [2]Inst. Planetologie, Universität Münster, Germany, [3]Inst. Geology, Academy of Sciences, Czech Republic, [4]Inst. Geologie, Universität Bern, Switzerland, [5]Inst. Geowissenschaften, Universität Frankfurt, Germany, [6]Dept. Earth Space Sciences, UCLA, USA, [7]Nuclear Physics Inst., Academy of Sciences, Czech Republic.

**Introduction:** Tektites are glassy materials formed by hypervelocity impacts providing enough energy to melt (and probably vaporize) target material completely. These melts are ejected from the impact site and transported ballistically for several hundreds of kilometers (e.g., moldavites ejected from the Ries crater, Ivory Coast tektites originating from the Bosumtwi crater and bediasites, ejected from the Chesapeake Bay crater). Other tektites may have remained in situ after their formation as, for example, Muong Nong-type tektites and the tektite-like Libyan Desert glasses (LDG).

Lithium (Li) have proven useful in tracking continental weathering [1], seafloor alteration [2] or high-temperature fractionations [3-5]. Whereas at low temperatures Li isotopes fractionate significantly, at magmatic temperatures these variations are nearly absent [3,4] or very limited [4,5]. Investigations of other elements of distinct geochemical affinities have shown small (Zn, Cu) [6,7] or absent (Mg) isotope variations [8]. We have therefore studied several occurrences of tektites and impact glasses in order to reveal (i) possible Li isotope fractionation induced by hypervelocity impact, (ii) a possible preserved signature of the source materials of tektites and impact glasses and, (iii) whether there are effects of impact excavation discernible in Li isotope systematics.

**Results and discussion:** The various glasses show large range in Li abundance (5.5–58 ppm) and $\delta^7$Li (-3.0 to 26.0‰). Whereas majority of samples broadly mimic Li systematics of upper continental crust (UCC, [9]), Libyan Desert glass deviates significantly in having both low Li and high $\delta^7$Li. Impact-glasses from the Zhamanshin crater also show elevated $\delta^7$Li relative to moldavites, ivorites, bediasites and Australasites.

Overall, high-temperature events have been shown to be incapable of fractionating Li isotopes significantly [5]. This view is further strengthened by our results. Although there are some $\delta^7$Li variations among moldavites, these do not reflect the different strewn subfields. New data from sedimentary lithologies from the Ries target area (OSM, OMM) and analogs from the S Bohemia tend to have lower Li contents whereas their $\delta^7$Li are identical to those of moldavites. This suggests that Li isotopes do not fractionate during high-T melting events. However, Li seems to be enriched in melts either by partitioning into the vapor phase or by incorporating Li-rich vegetation cover.

Given the near-absent Li isotope fractionation during the impact, source signatures may be preserved even after the flash melting. Whereas tektites formed in areas with evolved continental crust and varied sedimentary cover do not show deviations from $\delta^7$Li recorded in crustal magmatic and sedimentary lithologies [4], notable diversity of several target sites may result in distinctively different Li systematics. This is envisaged from isotopically heavy LDGs that record the earlier fluvial transport of their parental sands [10]. Higher-than-crustal $\delta^7$Li found in zhamanshinites and irghizites may reflect incorporation of large portions of basaltic lithologies, that form part of the target in the Zhamanshin area. Isotope fractionation of Zn and Cu has been modelled by means of evaporation during the heating event [6,7] whereby Rayleigh fractionation was ruled out. The new Li data, however, show that the latter process may still be viable in situations where both the upper (tektite) and bottom (source) layer are sampled.

It seems that Li in impact glasses record the signature of parental lithologies without any detectable shifts in $\delta^7$Li. This is important when considering meteoritic samples from Mars, Moon and Vesta, generated through impact events. We conclude, therefore, that these meteorites may faithfully record the intrinsic Li isotope signatures of their target areas.

**References:** [1] Ushikubo et al. (2008) *Chem. Geol., 272*, 666–676. [2] Chan et al. (1992) *EPSL, 108*, 151–160. [3] Tomascak et al. (1999) *GCA, 63*, 907–910. [4] Magna et al. (2006) *EPSL, 243*, 336–353. [5] Wunder et al. (2006) *Contrib. Mineral. Petrol., 151*, 112–120. [6] Moynier et al. (2009) *EPSL, 277*, 482–489. [7] Moynier et al. (2010) *GCA, 74*, 799–807. [8] Esat (2006) *GCA, 52*, 1409–1424. [9] Teng et al. (2004) *GCA, 68*, 4167–4178. [10] Fudali (1981) *Meteoritics, 16*, 247–259.

**OMEONGA (WEMBO-NYAMA): iSALE HYDROCODE SIMULATIONS.** E. Martellato[1], G. Cremonese[2], M. Massironi[1,3] and G. Monegato[3]. [1]CISAS, University of Padova, Via Venezia 15, 35131, Padova, Italy (e-mail: elena.martellato@oapd.inaf.it); [2]INAF-Osservatorio Astronomico di Padova, Vic. Osservatorio 5, 35122, Padova, Italy; [3]Geoscienze Department, University of Padova, Via Giotto 1, 35127, Padova, Italy.

**Introduction:** The study of Earth impact craters may be difficult because of modifications caused by the cumulative effects of erosion, transport, deposition and weathering caused by vegetation in warm climate.

**Description of the structure:** Omeonga (Wembo-Nyama) is located in Central Africa, and more precisely, in the Eastern Kasai province (R.D. Congo), centered at 3°37'50"S, 24°31'00" (Fig. 1). It is recognizable from satellite images for the perfect roundness of the ring underlined by the Unia River, a tributary river of the Lomani River. This structure was interpreted as an impact structure from geological observations [1].


***Fig. 1:*** *GoogleEarth image of the Ring of Omeonga (Wembo-Nyama).*

Omeonga, with its diameter up to 36-km, pinpoints to a major event happened during Cretaceous-Cenozoic time span. Considering the minimum diameter of 36 km, the crater should be a real peak-ring basin and the relative diameter of the impactor should have been of about 2 km. According to Melosh (1989) [2], most of the ejecta should be limited to a deposit extending up to 5 crater-radius away from the basin. Hence, in our case, a blanket of 90 km from the rim is expected, even if a larger spread of ejecta may be possibly taken into account (e.g., ejecta blanket up to 250 km away from the 36 km-diameter Manson crater, Iowa [3]).

**iSALE simulations:** We are using the iSALE hydrocode to model the Omeonga crater formation and support the geological data in favour to an impact origin [4, 5]. In this work, we will present the preliminary results of these simulations, that are included into the scientific activity of support of the STC channel of the SIMBIO-SYS camera in the project of ESA BepiColombo mission.

We hypothesize a rock projectile, about 2 km in diameter, that strikes the target with the typical velocity on Earth's orbit (25 km/s for asteroids) and perpendicular with respect to the surface. Since almost every impact occurs obliquely, with 45° as the most probable impact angle [6], we take into account a lower impact velocity to simulate a more reliable initial condition. However, impact angle and direction may have a minor effect on crater morphology, while crater size and ejecta curtain are influenced by it. This impact event should have excavated material from the basement (Fig. 2), made up by a 800 m sandstone layer that overlies about 30 km granite upper crust.

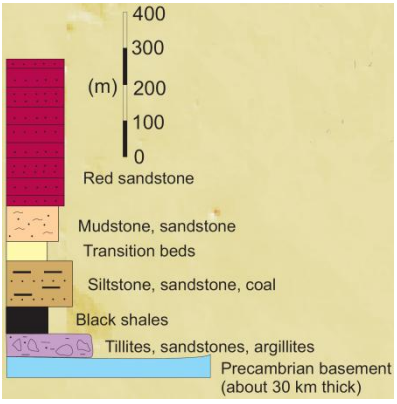


***Fig. 2:*** *Stratigraphy of Permian-Jurassic succession of Karoo Basin in Congo (Lukuga), mod. after Catuneanu et al. 2005 [7].*

**References:** [1] Monegato et al. (2010), *XLI LPSC* 1601. [2] Melosh (1989) *Impact Cratering:a geological prcess. Oxford Univ*, 245 pp. [3] Inzett et al. (1993), *Science*, 262, 729-732. [4] Collins et al. (2002), *Icarus*, 157, 24-33. [5] Wünnemann and Ivanov (2003), *PSS*, 51, 831-845. [6] Shoemaker (1962) In: Kopal Eds., Physics and Astronomy of the Moon, Academic Press, 283-359. [7] Catuneanu et al. (2005) *J. Afr. Earth Sci.* 43, 211-253.

**STRATIGRAPHY OF THE RIES SUEVITE, GERMANY, FROM STEREOMETRIC ANALYSIS.**

C. Meyer[1], D. Stöffler[1], M. Jébrak[2], and W.-U. Reimold[1], [1]Museum of Natural History - Leibniz Institute at the Humboldt University Berlin, Germany; email: cornelia.meyer@museum.hu-berlin.de, [2]Université du Québec à Montréal, Canada

**Introduction:** The suevite of the 14.35 Ma old, 25km wide Ries crater in southern Germany occurs in 3 different geological settings: 1) the crater suevite in the central crater cavity inside the inner ring, 2) the outer suevite on top of the continuous ejecta blanket, 3) dikes in the crater basement and in displaced megablocks [1]. The mechanisms of transport of particles in the suevite remains poorly understood. In [2] the following processes are discussed: 1) "aerial" transport in a gaseous medium, 2) ground surging in a turbulent flow, 3) interaction of a temporary melt sheet in the central crater with surface water leading to "phreatomagmatic" explosions and subsequent aerial transport.

We measured the shape and size distribution of particles in several drill core sections (thickness of suevite in parentheses): Nördlingen, inside the inner ring (300m); Enkingen, at the inner ring (80m); Wörnitzostheim, between inner ring and crater boundary (80m); and Otting, outside the crater (9m). The drill cores were studied by digital stereometric analysis. Grain sizes and shapes of lithic clasts and melt particles were measured on the plane surface of the half cores and on thin sections of the same core sections. The following grain parameters were measured in the size range of +2 to -6 phi (0.25 to 63mm): 1) particle content, 2) aspect ratio = minor axis/major axis, 3) maximum grain size = mean of the ten largest particles, 4) particle size distribution represented as fractal dimension [3].

**Observation and subdivision of the Ries suevite:** The crater suevites can be divided into stratigraphic subtypes. They differ in their stereometric parameters and show distinct differences between the central part and the outer part of the inner crater. The Nördlingen drill core can be subdivided into four suevite units: 1) Upper redeposited suevite (296–314m), 2) "Graded" suevite (314–330m), 3) Melt-rich suevite (331–520m), and 4) Melt poor suevite (520–602m). The Enkingen drill core can be subdivided into four units: 1) Upper suevite (21–40m), 2) Middle suevite (40–66m), 3) Lower suevite with intersection of coherent melt layers (66–86m), and 4) coherent impact melt (below 86m). The Wörnitzostheim drill core can be subdivided into three units: 1) Upper suevite (19–25m), 2) Melt-rich suevite (25–80m), 3) Melt-poor suevite (80–100m). The Otting drill core is homogenous.

A comparison of the characteristics of all drill cores can be summarized as follows: 1) The suevite of Nördlingen shows the lowest content of melt particles decreasing with depth in the lower section, and the highest lithic clast/melt ratio. 2) In the suevites of Enkingen and Wörnitzostheim the maximum grain size and content of melt particles increase with depth. From Enkingen to Otting the maximum grain size of all particles, and especially of the melt fragments, is decreasing with increasing distance from the crater center. 3) The aspect ratio of the lithic clasts is rather similar for all drill cores whereas the aspect ratio of the melt particles increases from Enkingen to Otting. 4) The fractal dimension of the lithic clasts is for small grain sizes always higher than for large ones. Whereas the fractal dimension of the large grain sizes increases from Enkingen to Otting, it decreases for the small grain sizes from Nördlingen to Otting.

**Discussion:** After [5] the grain size distribution of comminuted material formed during the cratering process, should follow a log-normal grain size distribution with the same fractal dimension for all grain sizes. In this case the fractal dimensions of the grain size distribution in ejecta deposits should not depend on the radial distance from the crater center. However, our observations of variations in the fractal dimension indicate that the fragmented and ejected particles were subjected to additional comminution processes. As the fractal dimensions of the larger particles are increasing and the maximum grain size is decreasing with distance, a process is required where the clasts will be comminuted and sorted as a function of their size, density (per volume), and distance to the crater center. As the aspect ratio of the melt particles is also increasing with distance from the crater center a process is required for the transport where particle-particle interactions could occur.

**Conclusion:** Our stereometric results imply a secondary comminution process after the shock wave passage, pressure release, and transient cavity formation. A secondary milling and sorting process in a gas dominated suspension seems to be feasible. Our observations are compatible with the new model for the suevite genesis proposed by [2].

**References:** [1] Stöffler et al. (2009), LPSC, XL, abstr. [2] Artemieva et al. (2009), LPSC, XL, abstr. [3] Rousell et al. (2003) Earth Sc. Rev. 60, 147-174. [4] Houghton \& Schmincke (1989) Bull. Volc. 52, 28-48. [5] Melosh (1989) *Impact cratering; a geologic process.*

**FORMATION OF PSEUDOTACHYLITIC BRECCIAS FROM THE ARCHEAN GNEISS OF THE VREDEFORT DOME, SOUTH AFRICA.** T. Mohr-Westheide[1], W. U. Reimold[1], R. L. Gibson[2], D. Mader[3] and C. Koeberl[3], [1]Museum für Naturkunde – Leibniz Institute at Humboldt University Berlin, Germany, [2]School of Geosciences, University of the Witwatersrand, Johannesburg, RSA, [3]Department of Lithospheric Research, University of Vienna, Austria.

"Pseudotachylite" is friction melt formed along faults or shear zones. It is produced by frictional heating, which generally requires sliding velocities consistent with seismic slip. The distinction between "impact" and "tectonic" "pseudotachylite" plays an important role in impact settings, as melt breccias in impact structures often closely resemble tectonic friction melt but may have been formed by different processes: (1) shearing (friction melting); (2) shock compression melting (with or without a shear component); (3) decompression melting immediately after shock propagation through the target / related to rapid uplift; (4) combinations of these processes; (5) intrusion of allochthonous impact melt. Resolving this problem requires detailed multidisciplinary analysis in order to comprehensively characterize the nature of these breccias and to identify the exact melt-forming process(es). In order to distinguish between bona fide "pseudotachylite" and breccias of similar appearance in impact structures of still debated origin we refer in the latter case to "pseudotachylitic breccia" (PTB).

PTB are the most prominent impact-induced deformation in the central uplift of the Vredefort Impact Structure [1, 2]; similar breccias occur in abundance also at Sudbury, Canada [e.g., 3,4]. We present chemical data for small-scale (1 mm – 3 cm) PTB from mafic (dioritic) and granitic host rocks and compare with the chemical compositions of their respective host rocks.

Electron microprobe analysis of PTB groundmass in comparison to XRF bulk chemical analysis of pseudotachylitic breccias and their host rocks revealed that PTB generally displays a close chemical relationship to the adjacent host rock. This confirms that melt was formed from material of the same composition and for mm to cm wide breccia veinlets is of local origin. In granitic environments, the refractory behavior of quartz seems to be the main reason for the slight chemical differences between PTB and host rock. Our first chemical investigations of < 0.5 cm PTBs in mafic host rocks revealed, overall, good agreement between PTB composition of EMPA DFB analysis and host rock composition of XRF. Where notable deviations occur, it is possible to explain this by preferential melting of either plagioclase or hydrous ferromagnesian minerals of different proportions. PTB seemingly occur preferentially in amphibole-rich host rock portions – an observation that confirms the macroscopic observations of [5,6,]. Thus, PTB genesis in mafic host rock seems to be controlled by the mineralogical composition of the target rock. A further factor is likely the melting temperature of minerals involved that determines the ratio at which feldspar and mafic minerals are melted.

None of the analyzed veinlets has yielded any textural evidence supporting a significant influence from shearing /faulting. Our PTBs of up to 1 m width all contain clast populations that represent local lithologies only, with distinct differences between clast population and host rock mineral abundances likely the result of different mechanical behavior and different melting temperatures of the various minerals.

[1] Dressler B.O. & Reimold W.U. (2004) *Earth-Science Rev.* 67, 1–60. [2] Reimold W.U. & Gibson R.L. (2006) *GSA SP* 405, 233-253. [3] Dressler B.O. (1984) *Ontario Geol. Surv.*1, 97-284. [4] Lafrance B. et al. (2008) *Precambri.. Res.* 165, 107-119. [5] Reimold, W.U. & Colliston, W.P. (1994) *GSA SP* 293, 177-196. [6] Reimold W.U. (1991) *N. Jhrb. Mineral.* 161, 151-184.

**LUNETTE: ESTABLISHING A LUNAR GEOPHYSICAL NETWORK WITHOUT NUCLEAR POWER THROUGH A DISCOVERY-CLASS MISSION.** C.R. Neal[1], W.B. Banerdt[2], L. Alkalai[2], and the Lunette Team, [1]Dept. of Civil Engineering & Geological Sciences, University of Notre Dame, Notre Dame, IN 46556 neal.1@nd.edu, [2]Mail Stop 264-422, Jet Propulsion Laboratory, 4800 Oak Grove Drive, Pasadena, CA 91109.

**Introduction:** Following the Vision for Space Exploration [1] "The Scientific Context for the Exploration of the Moon" [2] designated understanding the structure and composition of the lunar interior (to provide fundamental information on the evolution of a differentiated planetary body) as the second highest priority lunar science concept that needed to be addressed. To this end, the Science Mission Directorate formulated the International Lunar Network (ILN) mission concept that enlisted international partners to enable the establishment of a geophysical network on the lunar surface. NASA would establish the first four "anchor nodes" in the 2018 time frame. These nodes are envisioned to use radioisotope power systems to allow operation of each node for at least 6 years. Each anchor node will contain a seismometer, magnetometer, laser retroreflector, and a heat flow probe [3] and will be distributed across the lunar surface to form a much more widespread network that the Apollo passive seismic, magnetometer, heat flow, and the Apollo and Luna laser retroreflector networks. (Fig. 1). It is planned that the four anchor nodes will be launched on an Atlas 5 launch vehicle and the cost is estimated to exceed that for a current New Frontiers mission.

**Lunette Mission Concept:** What we present here is an alternative to the ILN architecture that would deploy three geophysical nodes on the lunar surface that are widely spaced (3,000-5,000 km), but at a much lower cost (within a Discoverymission cap) [4,5]. This concept uses new power management technology to offer a non-nuclear alternative [3]. This mission will provide detailed information on the interior of the Moon through seismic, thermal, electromagnetic, and precision laser ranging measurements, and will substantially address the lunar interior science objectives set out in "The Scientific Context for the Exploration of the Moon" [2] and "The Final Report for the International Lunar Network Anchor Nodes Science Definition Team" [3].

Each node will contain: a very broad band (VBB) seismometer that is at least an order of magnitude more sensitive over a wider frequency band than the seismometers used during Apollo; a short period (SP) seismometer; a heat flow probe, delivered via a self-penetrating "mole" device; a lowfrequency electromagnetic sounding instrument, which will measure the electromagnetic properties of the outermost few hundred km of the Moon; and a cornercube laser retroreflector for lunar laser ranging. These instruments will provide an enormous advance in our knowledge of the structure and processes of the lunar interior over that provided by Apollo-era data, allowing insights into the earliest history of the formation and evolution of the Moon

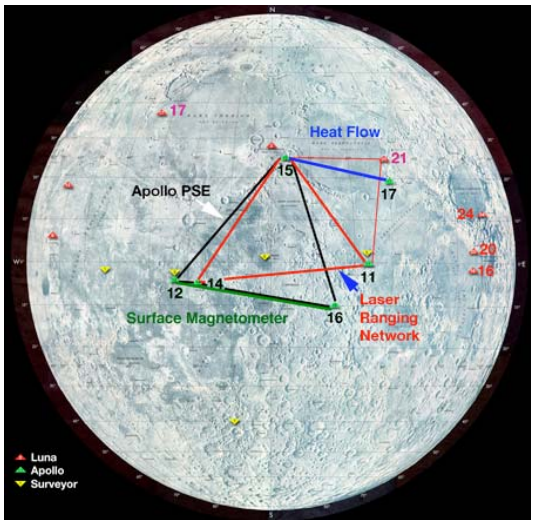


**Fig. 1:** Landing sites on the Moon and geophysical networks established by the Apollo and Luna landings.

**International Collaboration:** The only way this mission can fit within a Discovery mission cost cap is through international collaboration. Therefore, a multinational team has been put together with the VBB seismometer being contributed by a European consortium headed by France, along with Germany and Switzerland; the SP seismometer is being contributed by Japan, the heat flow probe is being contributed by Germany, with the laser retroreflector and EM sounding instruments being supplied by the USA.

**References**: [1] The Vision for Space Exploration (2004) NASA (http://history.nasa.gov/sep.htm) [2] The Scientific Context for the Exploration of the Moon, Final Report. National Academies Press, 121 pp. [3] ILN Final Report: Science Definition Team for the ILN Anchor Nodes, NASA, 45 pp (http://ntrs.nasa.gov/archive/nasa/casi.ntrs.nasa.gov/20090014121_2009013378.pdf. [4] Elliott J. & Alkalai L. (2008) *Proc. Internat. Astro. Congress*, **59**. [5] Elliott J. & Alkalai L. (2009) *Proc. Internat. Astro. Congress*, **60**. [6] Kiefer W.S. et al. (2010) Ground-Based Geophysics on the Moon Workshop abstract, Tempe Arizona.

**COMPARISON OF MID-SIZE COMPLEX TERRESTRIAL IMPACT STRUCTURES.** G. R. Osinski[1], and R. A. F. Grieve[1,2], [1]Dept. Earth Sciences/Physics and Astronomy, University of Western Ontario, London, ON N6A 5B7, Canada (gosinski@uwo.ca), [2]Earth Sciences Sector, NRCan, Ottawa, ON K1A 0E4, Canada.

**Introduction:** Despite the ubiquitous nature of impact craters in the solar system, some important second-order aspects of the processes and products of their formation remain incompletely understood. One such aspect are the parameters and processes controlling the final morphology and morphometry of impact craters For this reason, the systematic study of mid-size impact structures was one of the three main recommendations for future research resulting from the first Bridging the Gap conference in 2003 [1] and provides the motivation for this study. This builds upon an initial comparative study of the Haughton, Ries, and Mistastin that focused on impact melt products [2]. We expand this study here to include other craters (Table 1) and different aspects of these craters.

**Discussion:** We focus here on 3 main aspects of terrestrial impact craters.

*Diameter.* A fundamental question to be asked at the outset is what exactly the various listed diameters for these craters actually represent. Do they represent the *rim* (or final crater) *diameter* or *apparent crater* diameter (see discussion in [3])? It has been suggested for Haughton that the commonly quoted diameter of 23 km is actually the apparent diameter and a robust estimate of 16 km has been suggested for the rim diameter [4]. At the more eroded craters (Mistastin and Rochechouart), the listed diameter is clearly an apparent diameter. It is not so clear, however, for Ries and Boltysh – which both retain much or their original morphology – what the listed diameter represents.

*Impactites.* One of the most notable differences between these various craters is in their allochthonous impactites. Early suggestions that impacts into sedimentary targets do not produce impact melt-bearing lithologies have now largely been superceded by the realization that the volumes of melt produced within craters formed within different target lithologies are similar [2, 5]. It is apparent, however, that even in craters developed purely in crystalline targets, there are substantial differences in the characteristics of the allochthonous crater-fill materials. At Mistastin, a large coherent melt sheet was generated but impact melt-bearing breccias ("suevites") also underlie the melt sheet and intrude into the crater floor [6]. At Boltysh, suevites underlie and overlie the melt sheet [7]; whereas, at Rochechouart, it appears that no coherent clast-poor melt sheet is preserved (or formed?) but rather a series of more heterogeneous melt-bearing breccias. This begs the question of why, given the seemingly similar target lithologies?

*Central uplift.* There are also notable differences in the surface expressions of the central uplifts at these structures. Rochechouart and Mistastin are too eroded to make any definitive affirmations regarding their original uplift morphology. Boltysh possesses a central peak that is emergent through the crater-fill deposits [7]; whereas at Haughton, uplifted lithologies (with a diameter of 12 km) were buried under allochthonous crater-fill impactites such that an emergent uplift would not have been visible in the pristine crater [4]; erosion has since exposed a small part of the uplift. Like Haughton, the Ries structure also lacks a central emergent topographic peak. Instead, an "inner ring" of uplifted basement material is present [8]. Some workers suggest this is equivalent to the central uplift, while others suggest it represents part of the collapsed transient cavity rim. These different hypotheses have very different implications for interpreting cratering processes. We note that the diameter of the central uplift at Haughton and the "inner ring" at Ries are both ~12 km, which potentially suggests a common origin.

**Concluding remarks:** It is most credible to reason that target strength (e.g., sedimentary versus crystalline) played a role in the noted morphological differences and the presence of volatiles played a role in impactite differences. While this may be the case, it is not clear how these different parameters resulted in achieving these differences and further compartive studies are required and encouraged.

**References:** 1. Herrick R.R. and Pierazzo E. 2003. *LPI Contribution No. 1162*. Houston: LPI. 156. 2. Osinski G.R., et al. 2008. *Meteor. Planet. Sci.* 43:1939-1954. 3. Turtle E.P., et al. 2005. Geological Society of America Special Paper 384. GSA: Boulder. p. 1-24. 4. Osinski G.R. and Spray J.G. 2005. *Meteor. Planet. Sci.* 40:1813-1834. 5. Wünnemann K., et al. 2008. EPSL 269:529-538. 6. Grieve R.A.F. 1975. *GSA Bull.* 86:1617-1629. 7. Masiatis V. 1999. *Meteor. Planet. Sci.* 34:691-711. 8. Pohl J., et al. 1977. In Impact and Explosion Cratering. Pergamon Press: New York. p. 343-404. 9. *Earth Impact Database (Accessed: 12/04/2010)*.

**Table 1.** Initial craters investigated for this study and their important attributes*.

| Crater | Age (Ma) | D (km) | Target |
|---|---|---|---|
| Boltysh | 65 | 24 | C |
| Haughton | 39 | 23 | S |
| Mistastin | 36 | 28 | C |
| Ries | 14.3 | 24 | M |
| Rochechouart | 214 | 24 | C |

* Abbreviations: D = Diameter as listed in the Earth Impact Database [9]. C = crystalline. S = sedimentary. M = mixed crystalline–sedimentary target.

**THE RIES IMPACT DIAMONDS: THEIR SPECTROSCOPY, CO-EXISTING PHASES AND ORIGIN.** N. Palchik[1], S. Vishnevsky[1], [1]Inst. Geol. & Mineral., Novosibirsk, 630090, RUSSIA (svish@uiggm.nsc.ru).

***Introduction:*** Ries impact diamonds, RIDs, and their apographitic paramorphs, AGPs, in first turn, are described in [1]. Other RIDs features are summarized here. Origin conditions and open or still poor-studied questions of RIDs are also presented.

***Data on Raman-spectroscopy:*** Most (~90%) of the AGPs are Raman-invisible due to a strong optical fluorescence irrespective of their color. The rest show 2 broad bands at 1305-1334 (see the frequency shift of the main diamond band, MDB) and 1560-1575 $cm^{-1}$ [2]. The shift, extra 1560-1575 $cm^{-1}$ band and broadening of the both may reflect the nanosize of the diamond domains. Alternatively, the MDB broadening may be due to lonsdaleite [3], and the band 1560-1575 $cm^{-1}$ may indicate for the diamond-like amorphous carbon or chaoite [2]. Some AGPs contain local (2-4 μ in size) irregularities exhibiting intense broad band at 1400-1460 $cm^{-1}$, attributed to diamond-like amorphous carbon or chaoite [2]. Surprisingly (a lack of lonsdaleite?), the MDB at 1332 $cm^{-1}$ on in situ AGPs from shocked gneisses [4] has no broadening and is narrow; these diamonds contain also strongly-disordered graphite domains evident from the broad Raman bands of low intensity at 1350 and 1580 $cm^{-1}$ frequencies. Description of co-existing carbon minerals see below.

***Other spectral and EPR-data:*** These data reflect AGPs phase composition, structural features and dislocations. Yellow to orange (depending on grain color) AGPs ultraviolet luminescence spectra contain 590 nm and broad 625-775 nm bands showing lonsdaleite (>20 %) [5]. Electron Paramagnetic Resonance revealed in a single g-line 2.003 at ΔH~250 A/m indicative for the crystal defects and lonsdaleite impurity [5]. Infra-red data [6] show defect-induced vibrations referable to symmetric+asymmetric C-H stretching modes (bands 2852 and 2925 $cm^{-1}$) and to other H-related features (bands at 1650, 1555, 1405 and 1390 $cm^{-1}$) but no defects of Nitrogen-reach types IaA to Ib diamond. Cathodoluminescence, CL, [7] shows a lot of bands (at 2.8-2.9 eV, 443-427 nm, and 1.8 eV, 688 nm) related to dislocations and their vibronic effects and, possibly, to amorphous carbon (peaks at 2.23 eV, 556 nm, 2.32 eV, 534 nm, and 2.39 eV, 519 nm). The bands at 1.8, 2.23 & 2.32 eV are typical for the impact diamonds only. Data on CVD-diamonds [1] are very scarce.

***Association with other carbon phases*:** The Ries AGPs, especially dark-colored ones, show a close association with other carbon phases. Parental or new-generated graphite, G, is the most common here, forming X-ray detectable impurities and lamellae (often with chaoite [5, 8]) or Raman-detected nanocrystalline domains [2]. Diamond-like amorphous carbon, AC, or chaoite is also found in some AGPs [2]. In situ AGPs from shocked gneisses contain highly-disordered and fine-grained Gs and dense hard carbon phase (AC or an unknown crystalline species?) [4]. CL-detectable AC is also found in Ries AGPs [7]. To this we can add that Popigai AGPs from shocked gneisses also contain X-ray detectable strongly-disordered G together with chaoite, cubic diamond and lonsdaleite [9]. Skeletal CVD-RIDs show epitaxial intergrowth with SiC [10].

***Origin conditions of RIDs:*** Following to experiments (by De-Carli, Hannemann, et al.) and observations in astroblemes, the P-T origin range for AGPs is from ~30 GPa (in shocked gneisses) to 140 GPa (in partially-vaporized impact melt) and from ~700 to 4000 K [3, 4, 11]. Due to a prolonged natural shock, the P-T conditions are valid in origin of both the cubic and hexagonal diamonds. They arise by the martensitic (in a solid state) or diffusion (in liquid/amorphous state of the shocked graphite) way [12]. Chaoite (natural carbine) is supposed to form at high, >2500 K, temperatures [11]. A number of high P-T carbon phases, both confirmed and supposed, is listed in [11]; some of the phases can be of shock origin. Recent data [4] contribute in this promising but still poor-studied field of carbon shock mineralogy. Data on CVD-RIDs are scarce.

The brief review on RIDs made here and in [1] is filled up by a number of still open/poorly-studied questions on the topic we shall present at Annual Meteoritical Society Meeting, July 26-30, 2010, New York.

**References:** [1] Vishnevsky S., Palchik N. (2010) *Nördlingen-2010, Print-only section*. Abstract #7006. [2] Lapke C., et al. (2000) *MAPS, 35,* A95. [3] Vishnevsky S., et al. (1997) *Impact Diamonds: their features, origin & significance.* Novosibirsk: SB RAS Press. 110 p. (in Russian & English). [4] El-Goresy A. et al. (2001) *American Mineralogist, 86,* 611-621. [5] Valter A., et al. (1998) *Mineralogichesky Zhurnal, 20,* 3-12 (in Russian). [6] Pratesi G., et al. (2002) *18th IMA Meeting, Edinburg, Scotland, Session 20,* Abstract B20-3. [7] Pratesi G., et al. (2003) *American Mineralogist, 88,* 1778-1787. [8] Siebenschock M., et al. (1998) *MAPS, 33,* A145. [9] Vishnevsky S., Palchik N. (1975) *Soviet Geology & Geophysics, 16 (1),* 55-61. [10] Hough R., et al. (1995) *Nature, 378,* 41-44. [11] Valter A., et al. (1992) *Shock-metamorphic carbon minerals.* Kiev: Naukova Dumka. 172 p. (in Russian). [12] Khomenko A., et al. (1975) *Syntheticheskie almazy, 3,* 3-7 (in Russian).

**COMPOSITIONAL VARIATIONS & PETROGRAPHY OF METALLIC SPHERULES IN MELT ROCK AT MONTURAQUI CRATER, CHILE.** D. W. Peate[1] I. Ukstins Peate[1], L. Chung Wan[1] and C. Kloberdanz[1], [1]Department of Geoscience, University of Iowa, 121 Trowbridge Hall, Iowa City, IA 52242, USA, david-peate@uiowa.edu

**Introduction:** Small impact craters (< 1-2 km dia.) have unique features that raise the possibility of using chemical studies to constrain the nature of physical processes that occurred during impact. Such craters are almost exclusively formed by iron meteorite impactors, with low enough kinetic energy that not all the projectile is vaporized and lost from the impact site. Fragments of unmelted meteorite material can survive, and droplets of FeNi metal are often found dispersed around the impact site and mixed with melted and fragmented target rocks. Studies of these 'spherules' show they are compositionally variable in terms of Fe-Ni-P-Co and different in composition from unaltered iron meteorites [1,2,3]. Several models have been proposed to explain compositional variations in spherules at different impact sites: vaporization-condensation, vapor fractionation or selective volatilization of Fe, selective oxidation processes, selective shock-melting of sulphide-metal intergrowths at meteorite grain boundaries, ionic-radius-controlled mobility of certain elements [2]. One way to determine the relative importance of these different possible mechanisms this is to look at variations in other elements that have different behaviours during processes such as vaporization and oxidation. We are carrying out a petrographic, SEM, electron microprobe and LA-ICP-MS compositional study of individual metallic spherules from the Monturaqui impact crater to address these issues.

**Background:** The Monturaqui impact crater is in the Atacama Desert of northern Chile, 200 km SE of Antofagasta [4]. It is a simple, ~350 m diameter crater, emplaced into Paleozoic granite rocks that were covered by a thin ignimbrite sheet [5]. Its age is ~570-750 ka based on (U-Th)/He zircon/apatite, TL and cosmogenic nuclide methods [6,7]. The impactor is inferred to be a coarse octahedrite of group I based on intensely weathered fragments of iron meteorite ('iron shale') found in and around the crater. Centimetre-sized chunks of impact melt rocks occur scattered around the crater [1,4]. These rocks are comprised largely of glass melt and rock fragments that formed from melting of the granite and ignimbrite rocks present at the target site during the impact. Also present within the glass fragments are small droplets of Fe-Ni metal±sulphides (between < 1 µm and ~2 mm in size).

SEM study of impact melt fragments show that Fe-Ni±S spherules smaller than ~200µm (down to sub-µm) tend to be spherical in shape, while larger areas of Fe-Ni±S have complex irregular shapes, often with hollow centres. The smaller metal spherules are generally homogeneous w.r.t. Fe and Ni contents, with occassional interstitial troilite. The larger patches can show some zonation, typically with Ni-rich margins. The cores of several spherules have been variably replaced by barite during subsequent alteration.

EMP analysis of the glass shows enrichments of Fe w.r.t. target rocks, and significantly elevated S levels (1250±500 ppm), indicative of a S-rich iron meteorite component in the impact melt. However, fine, sub-micron spherules appear to be dispersed completely through the glass matrix, which makes it difficult to analyse metal-free patches of the impact glass by LA-ICP-MS (beam size > 10 µm) to evaluate this further.

Previous studies [1,2] showed significant compositional variations with spherule size: smaller spherules had higher Ni and Co and lower Fe and P relative to the larger spherules. New EMP analyses of spherules (n=100) confirm these variations (see figure), and show that the larger spherules have compositions similar to unaltered fragments of 'iron shale'. We are currently analysing these spherules for other trace elements (Ga, Ge, PGE etc) by LA-ICP-MS, and we will present these data at the meeting.

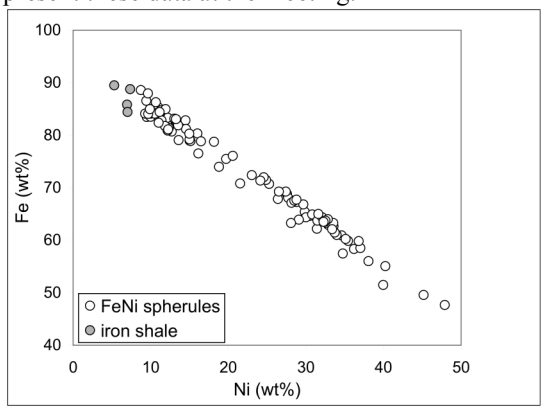


**References:** [1] Bunch T.E. & Cassidy W. (1972) *CMP, 36,* 95-112. [2] Gibbons R.V., Hörz F., Thompson T.D. & Brownlee D.E. (1996) *LPS VII,* 863-880. [3] Mittlefehldt D.W. et al. (2005). *GSA Spec. Paper, 384,* 369-390. [4] Sanchez J. & Cassidy W. (1966). *JGR, 71,* 4891-4895. [5] Ugalde H. et al. (2007). *Meteoritics & Planet. Sci., 42,* 2153-2163. [6] Valenzuela M. et al. (2009) *Meteoritics & Planet. Sci., 44,* A5185. [7] Ukstins Peate I. et al. (2010) *LPS XXXXI,* #2161.

**FUTURE LANDING SITES ON THE MOON: WHAT IS NEW AND WHAT DO WE NEED TO KNOW?** C. M. Pieters, Department of Geological Sciences, Brown University, Providence, RI 02912 USA (Carle_Pieters@brown.edu).

What is new on the Moon? A lot! A host of new data about the Moon have been acquired from modern orbiting spacecraft and are now made available to a hungry planetary science community. SMART-1 [ESA] led the way with an innovative technology demonstration mission to the Moon. An international armada of more complex missions with advanced sensors followed in rapid succession: SELENE [JAXA], ChangE [CNSA], Chandrayaan-1 [ISRO], and LRO-LCROSS [NASA]. The data from these robotic orbital missions are being calibrated, validated, and distributed, and new results and insights are appearing throughout the peer-reviewed scientific literature.

In planning possible future landing sites the new missions provide global data that span diverse spatial resolution, spectral resolution, and spectral range. Although still incomplete, these combined data provide a first order assessment of possible landing sites and the essential overview of geologic context. Perhaps more importantly, they also provide several surprises and unexpected insights about Earth's nearest celestial neighbor.

Rationale for landing at specific sites on the Moon can be portrayed either as a logical and efficient step for human exploration beyond Earth or as a destination that is rich with science return. These are not exclusionary, but have different emphasis. A list of fifty targets across the lunar surface was developed as part of the Constellation Program as example regions of interest for human exploration [1, 2]. Possible landing sites that emphasize expanding our scientific understanding from lunar samples is found in [3] and reinforced by [4].

One of the highest scientific priorities remains obtaining samples from the enormous South Pole-Aitken Basin on the lunar farside [4, 5, 6] because it provides a key to understanding the earliest 600 My of terrestrial planet evolution. Interest in both polar regions remains high because their unusual environment may trap diverse materials (especially volatiles) and because they exhibit potential for long-duration solar power [e.g., 1, 2]. Exploration and sampling the young basalts seen on the lunar nearside is also of high science priority since these basalts are key to constraining the thermal evolution of this small planetary body [1,2,3]. Of course, there are also countless individual targets that are both interesting and perplexing. One class of mysteries has important implications for all airless silicate bodies: the enigmatic swirls, small graceful albedo markings in diverse terrains that are often associated with magnetic anomalies and may hold the key to understanding dust movement on the surface [7].

The unexpected surprises that come from the new data are scientifically thrilling, but also beg for more detailed information. Foremost among these is the discovery of widespread surficial $OH/H_2O$ across the surface of the Moon [8]. Unfortunately, the data are not sufficient to determine key parameters that constrain the abundance, origin, distribution, and fate of this volatile material. Furthermore, discovery of *new* spinel-rich rock types on the Moon [9,10] challenge concepts of crustal evolution and call for new methods of forming and concentrating minerals to be considered.

*References*. [1] Gruener J. E. and Joosten B. K. (2009), Lunar Reconnaissance Orbiter Science Targeting Meeting, #6036. [2] Lucey P. G. et al. (2009) Lunar Reconnaissance Orbiter Science Targeting Meeting, #6022. [3] Shearer C and L. Borg (2006) Chemie der Erde 66, 163–185. [4] NRC (2007) *Scientific Context for Exploration of the Moon: Final Report*, Washington, D.C. [5] NRC (2003) New Frontiers in the Solar System, an Integrated Exploration Strategy. *NAS Decadal Survey, Solar System Exploration*, 248p., Washington, D.C. [6] Jolliff et al., (2010), LPSC41 #2450. [7] Garrick-Bethell et al. (2010), LPSC41 #2675. [8] Clark R.; Sunshine et al.; Pieters et al.; (2009) Science 326, 562-572. [9] Pieters et al.. (2010), LPSC41 #1854. [10] Sunshine et al. (2010), LPSC41 #1508.

**CHARACTERIZATION OF POLYMICT CRYSTALLINE BRECCIAS, RIES CRATER, GERMANY.**

A. Pontefract[1], G. R. Osinski[1,2], R. Flemming[1], and G. Southam, [1]Department of Earth Sciences, University of Western Ontario, 1151 Richmond St., London, Ontario, Canada, N6A 5K1, [1]Physics and Astronomy, University of Western Ontario, London, ON N6A 5B7, Canada. Emails: apontefr@uwo.ca, gosinski@uwo.ca

**Introduction:** First recognized by Shoemaker and Chao in 1961, the Ries Crater of Southern Germany is one of the most studied impact structures in the world. This is owed mainly to the relatively young age of the crater (~14.4 Ma), resulting in very little erosion. The impact facies are also further protected by thick paleolacustrine deposits formed by the post-impact lake [1]. Some of the most thorough studies of Ries Crater have been by von Engelhardt (e.g., see review in [2] and references therein), characterizing the various allochthonous impactites, including the crater suevite, surficial suevite ejecta, and Bunte Breccia. Though suevites overlay the Bunte Breccia in most regions of the crater, in some instances, the suevite is said to overlay polymict crystalline breccia (PCB). "They form either veins in crystalline blocks in the Megablock Zone… or larger masses in the Inner Ring (Maiers Keller at Nordlingen… and outside the southeastern rim (Itzing)." [2]. PCB are categorized as "highly shocked", to Stage I or II, which correlates with pressures ranging anywhere from 10–30GPa [2]; although few detailed studies have been carried out.

Petrographic analysis of these PCB, as well as microXRD reveal the shock and strain features, resulting in a re-categorization of shock level for the samples. A comparison is also made between clasts and groundmass of both PCB and surficial suevites, with special attention paid to shock features, mineral composition, and alteration phases.

**Analysis:** The texture of the PCB is quite heterogeneous. Clast size ranges anywhere from 0.5mm to several meters in size and does not show any preferred orientation or sorting of grain size. Clasts are angular, and frequently show suture lines, where two separate clasts have been crushed together. The matrix is fine grained micro-crystalline, and is difficult to distinguish with a petrographic microscope. In some instances, larger crystals are visible (~10um), though these occurrences are random.

*Composition of PCB:* Compositional analysis was completed through the use of a petrographic microscope, micro X-Ray diffraction (XRD) analysis and back-scattered electron detection (SEM-BSE). In accordance with the origins of the PCB [2], analysis of thin sections revealed the presence primarily of quartz, plagioclase end-members (anorthite and albite), K-feldspar and calcite. In some sections biotite had a distinct presence within clasts, sometimes comprising up to 50% of the clast. MicroXRD analysis further revealed the presence of other alteration phase minerals such as chamosite and flourite, as well as a strong iron presence in combination with calcium, possibly indicating ankerite. SEM-BSE detection confirmed the presence of $TiO_2$, in the form of rutile inclusions, which were frequently associated with biotite, as well as the presence of garnets.

*Shock Level:* Many of the crystals within the PCB did show a certain level of strain and fracturing associated with the impact event. However, only in larger quartz clasts was it possible to discern any diagnostic shock features. Prelimnary analysis revelaed that approximately 10% of clasts show planar fracturing (PFs), and an even smaller number reveal planar deformation features (PDFs). Only slight kink-banding was observed in some of the mica. The presence of glass clasts was observed in some samples, but was not incorportated within PCB clasts. This indicates that the glass was incorporated into the breccia during emplacement, and is not representative of shock level within the sample. It should be further noted that classification of the PCB as "highly shocked" is somewhat misleading, as the limited presence of PDFs as well as lack of diaplectic glass phases indicate shock levels generally below ~10 GPa [3].

*Suevites:* In contrast to the polymict breccia, suevites – though equal in the level of heterogeneity among clast orientation, composition and size – represent a much higher shock level. Features such as toasted quartz, PDF's, kink-banding in micas, diaplectic glass as well as glass bombs all point to incorporation of more highly shocked phases.

**Discussion and further work:** The location of the PCB within the crater is quite sporadic in comparison with other ejecta, such as the Bunte Breccia. Composition of the PCB suggests that it originated within the pre-Varisican gneisses [2], which may explain the limited surface occurrence of the rock-type. This is in contrast to the extensive deposits of megablocks and monomict crystalline breccia, which have a primarily granitic origin, and the Bunte Breccia which comprises large amounts of upper Jurassic limestone [2], indicating much shallower origins. Further diagnostic work on these samples must be completed to fully understand their origins and anomalous presence within the Ries Crater.

**References:** [1] Dennis, J.G. (1971) *JGR, 76,* 5394-5406. [2] von Engelhardt, W. (1990) *Tectonophysics, 171,* 259-273 [3] Stöffler, D. (1971) *JGR, 76,* 1344–1345.

**DETAILED INVESTIGATIONS OF THE SUBO 18 (ENKINGEN) DRILL CORE FROM THE RIES CRATER, SOUTHERN GERMANY.** W.U. Reimold[1], B.K. Hansen[1], I. McDonald[2], C. Koeberl[3], J. Jacob[1], D. Stöffler[1], and C. Meyer[1], [1]Museum für Naturkunde, Leibniz-Institute at Humboldt University Berlin, Invalidenstrasse 43, 10115 Berlin, Germany (uwe.reimold@mfn-berlin.de), [2]School of Earth and Ocean Sciences, Cardiff University, Park Place, Cardiff CF10 3YE, U.K; [3]Department of Lithospheric Research, University of Vienna, Althanstrasse 14, A-1090 Vienna, Austria.

The Ries Crater is one of the best preserved and best studied impact structures in the world, especially with respect to its preserved impact breccia crater fill and extensive deposits of extra-crater breccias (Bunte Breccia, suevite, and distal tektite deposits). Furthermore, a series of boreholes has made the impact breccia deposits accessible for 3D investigations. In 2008, a further cored hole was sunk near the village of Enkingen (SE Ries) by the Bavarian Department of Environmental Studies, accessing the crater breccias at the inner slope of the crystalline ring. The SUBO 18 drill core was initially obtained to investigate the cause of a significant local magnetic anomaly [1] but proved to be a valuable addition to the Ries core record. The 100 m drill core comprises 21.2 m crater sediment above impact breccia (suevite to -86.24 m with varied contents of melt fragments, above a rather massive impact melt rock to end-of-hole).

Core logging recorded, inter alia, the downhole variation of groundmass, melt particle, and crystalline/sedimentary clast proportions, and their average grain sizes. General increases of melt proportion, and melt particle size, as well as the concomitant increase of maximum crystalline clast size with depth became obvious. Only the lowermost section contained a notable but very small component of sedimentary clasts.

The suevite package is characterized by significant variation in melt particle content, with local accumulations of densely packed and frequently sub horizontally aligned melt particles. These can become so densely packed locally that they can hardly be separated visually and to the less careful observer may resemble massive impact melt rock. Similarly it appears that the lowermost massive, melt dominated section also contains thin seams of what appears like remnant stringers of suevitic groundmass. Thus, a complete transition from melt-poor to melt-rich and melt-agglomeratic impact breccia was intersected.

A detailed study by ASEM of the finest-grained materials in the submicroscopic groundmass in suevite samples from throughout the package in SUBO 18 showed that it is composed of secondary phyllosiliate and carbonate. However, textural evidence from clasts in melt-poor, melt-rich, and melt-dominated sections demonstrates that thermal effects are limited in the former, enhanced in the second, and dominant in the latter type of breccia. This is interpreted to indicate that typical melt-poor suevite has a groundmass dominated by unaltered clastic material, whereas the other two types contain more and more melt both in the clast content and in the fine-grained to submicroscopic groundmass. Micro-clasts and -melt particles are well separated. No evidence to suggest that suevite groundmass could represent a melt matrix was detected, in contrast to recent postulates [2,3].

For selected samples from the Enkingen core modal analyses, including a record of shock degrees for quartz and feldspar clasts, were obtained. Overall, it can be concluded that the target volume excavated and mixed into these impact breccias was dominated by crystalline basement-derived material, with only a minor sedimentary component. This is consistent with the macro- and mesoscopic observations made and on drill cores. No trends in modes and clast populations against depth in the borehole could be established. In contrast to the Nördlingen 1973 drill core where a distinct occurrence of accretionary lapilli was noted in the uppermost suevite part (around 296.5 m), no such particles were observed in the Enkingen drill core. The Enkingen suevites are seemingly rather similar, also with regard to dominant shock degree of the microclast fraction. These statistics do not provide any hint at different processes related to the formation and deposition of different levels of this suevite package.

Finally, representative samples of impact breccias from the Enkingen core were subjected to major and trace element analysis by XRF and INA analysis. No significant variation with respect to any major element abundances is noted for the entire length of core investigated. Nickel sulfide fire assay with ICP-MS was used to investigate PGE abundances and patterns/ratios in selected samples from the core. Four samples show Ir (0.37-0.88ppb) and Ru (0.56-1.08ppb) significantly above background (Ir <0.1ppb, Ru <0.24ppb) and with chondritic Ru/Ir, suggesting that a small chondritic projectile component (~0.1%) could be present. This is obviously in contrast to previous findings where in the absence of a meteoritic signature an achondritic projectile was favored for the Ries impact [4, and refs therein]. Further data reduction is in progress.

**Refs:** [1] Pohl, J. et al., GSA SP 465, in press; [2] Osinski, G.R., 2004, EPSL 226, 529-543; [3] Osinski, G.R. et al., 2004,MAPS 39, 1655-1684; [4] Tagle, R. & Hecht, L., 2006, MAPS 41, 1721-1735.

**ENIGMATIC TUBULAR TEXTURES HOSTED IN IMPACT GLASSES FROM THE RIES IMPACT STRUCTURE, GERMANY.** H. M. Sapers[1*], G. R. Osinski[1], and N. R. Banerjee[1]. [1]Centre for Planetary Science and Exploration & Dept. of Earth Sciences, University of Western Ontario, London, ON, N6A 5B7, Canada. [*]E-mail: hsapers@uwo.ca.

**Introduction:** Impact cratering is a ubiquitous geological process on solid planetary bodies. Any hypervelocity impact into a $H_2O$-rich target has the potential to generate hydrothermal systems [1]. Recent research suggests that such impact-induced environments may be conducive to microbial colonization [e.g., 2]. In volcanic environments, bioalteration of basaltic glasses produces characteristic tubular and granular aggregate textures [e.g., 3, 4]. Such bioalteration textures preserved in Archean greenstone belts constitute one of the oldest records of life on Earth [5]. Our examination of glasses from the Ries impact structure, Germany, revealed tubular textures with remarkably similar morphologies to textures observed in volcanic glasses.

Here we present preliminary data characterizing the putative bioalteration structures hosted within the Ries impact glasses.

**The Ries impact structure:** The 14.3 $\pm$ 0.2 Ma [6] Ries impact structure, southern Germany, was formed in a two-layer target comprised of Mesozoic flat lying siliciclastic and carbonate sedimentary rocks that unconformably overlie crystalline Hercynian basement [7]. Ries is a complex crater with a diameter of ~24 km [7]. Impactite (crater-fill and ejecta deposits) are well preserved: surficial "suevite" comprises one of four main proximal ejecta deposits [8].

The surficial "suevites" (impact melt-bearing breccias) are divided into two distinct lithological units: 1) the dominant main suevite that represents a clast-rich particulate impact melt rock or impact melt-bearing breccia [8, 9]; 2) subordinate basal suevite [10]. Four main glass types occur within the main suevite both as groundmass phases and as discrete glass clasts [11]. Glass clasts are typically vesiculated, schlieren-rich mixtures containing abundant mineral and lithic fragments [8]. The glass clasts hosted within the suevite have been classified based on composition and microtextures [11]. Type I glasses are the most abundant in the Ries suevites, contain Al-rich pyroxene quench crystallites and have average $SiO_2$ contents ~63%, and contain the highest concentrations of FeO and MgO of all 4 glass types [11]. Type II glasses have a similar $SiO_2$ content as type I; however, they contain only plagioclase crystallites as well as a generation of dense, micron-scale vesicles. Type III glasses have low $SiO_2$ contents, are hydrated relative to the other glasses, and contain relatively little FeO, MgO, and $K_2O$, while having high $Al_2O_3$, CaO, and $Na_2O$ contents. Type IV glasses have very high $SiO_2$ contents commonly >90%.

**Enigmatic tubular textures:** Tubular textures have only been observed in type I and II Ries glasses and can be organized into 3 classes based on morphology and distribution. Class A tubules are commonly observed in both type I and II glasses, are either randomly distributed or concentrated around glass rims or vesicles, and have a relatively simple morphology with few complex curves. Class B tubules are observed only in type I glass, are concentrated along fractures or clast margins, form radiating aggregates, and have complex morphologies including spirals, and other complex curvatures. Class C tubules are observed only in one sample of type I glass. Class C tubules have significantly larger length to width ratios than other tubule classes and form straight, linear features in the glass.

Class B tubules display various complex morphologies. Approximately two-thirds do not display distinct segmentation. These smooth-walled tubules typically display complex curvatures forming a morphological continuum between loose undulating curves and spirochete morphology. Curvature appears random, non-oriented and specific to individual tubules. Non-segmented tubules have diameters ~1um and commonly have length to width ratios >5. Approximately a third of class B tubules are clearly segmented. Segmented tubules typically display less curvature than non-segmented tubules. Individual segments have length to width ratios approximately 1:2. Segmented tubules vary in diameter from ~1um to approaching 3um. Rare segmented tubules with large (~3um) diameters have segments with length to width ratios approaching 1:6. Additional metrics describing tubule morphology may allow for specific subclassification of class B tubules.

Class A tubules are likely the optical expression of vesicle generation within the type I and II glass clasts comprising the 'hair-like' structures described by [11]. Type C tubules may represent quench crystallites; although the curved morphology is unusual. The complex morphologies of type B tubules, however, lack a parsimonious abiotic or mineralogical explanation and are reminiscent of microbial alteration textures observed in submarine basaltic glasses [4].

**References:** [1] Naumov, M V. (2005) *Geofluids, 5*, 165-184. [2] Cockell, C. S., Lee, P. (2002) *Biological Reviews, 77*, 279-310. [3] Furnes, H. *et al.* (2007) *Precambrian Res. 158*, 156-176. [4] Banerjee, N. R., Muehlenbachs, K. (2003) *G3 4*(4) 1037-1059. [5] Banerjee, N. R. *et al.* (2007) *Geochim. Cosmochim. Acta. 71*, A58. [6] Buchner E. *et al.* (2003) *Int. J. Earth Sci. 92*, 1–6. [7] Pohl J. *et al.* (1977) In *Impact and explosion cratering.* Ed. Roddy D. J., *et al.* NY: Pergamon Press. pp. 343–404. [8] Engelhardt W. v. (1990) *Tectonophysics 171*, 259–273. [9] Osinski G. R. *et al.* (2004) *MAPS 39*, 1655–1683. [10] Bringemeier D. (1994) *Meteoritics 29*, 417–422. [11] Osinski G. R. (2003) *MAPS 38*(11), 1641-1667.

**HOW 'DRY' WAS THE RIES-STEINHEIM IMPACT EVENT?** M. Schmieder[1] and E. Buchner[2,1] [1]Institut für Planetologie, Universität Stuttgart, Herdweg 51, D-70174 Stuttgart, martin.schmieder@geologie.uni-stuttgart.de. [2]HNU Neu-Ulm University, Wileystrasse 1, D-89231 Neu-Ulm, Germany.

**Background:** The ~24 km Ries crater and the ~3.8 km Steinheim Basin, S Germany, likely struck by a binary asteroid ~14.5 Ma ago in the Miocene, count among the best-preserved impact structures on Earth [1;2]. Both impact structures are hosted by a thick sequence of Mesozoic to Cenozoic sedimentary rocks (Ries: ~620 m of Lower Triassic to Miocene rocks; Steinheim: ~1180 m of Lower Triassic to Upper Jurassic rocks [1]) that overlie the Variscan crystalline basement and build up the karstified plateau (~200-300 m of Upper Jurassic limestones and marls) of the Swabian-Franconian Alb (SFA). In addition to the proximal Ries ejecta blanket (lithic Bunte Breccia, impact melt rocks, and suevites), distal ejecta define the Central European tektite strewn field ~200-450 km to the NE [1] and the more proximal 'Brockhorizont' [3]. The Ries and Steinheim impact structures thus provide unique insights into cratering mechanics, ejecta emplacement, and impactite petrogenesis under continental conditions. Despite the continental (i.e., presumably rather 'dry') environment at the time of impact, lines of evidence are presented that suggest a comparatively 'wet' Ries-Steinheim scenario [4].

**Discussion of Paleoenvironmental Conditions:** Miocene shales and black pebble-bearing pisolithic-onkolithic limestones (e.g., Stubersheim) that once covered larger parts of the SFA before and after the time of impact indicate limnic-palustrine surface conditions in a wide area surrounding the Ries and Steinheim impact sites. These sediments are to variable degrees incorporated into Bunte Breccia (e.g., Harburg or Demmingen) and post-impact (e.g., the 'Rezat-Altmühl paleolake' deposits), which further suggests that the pre-, syn-, and post-impact landscape was surficially water-saturated. Host to the Brockhorizont (e.g., Biberach or Ziemetshausen), fluvial to limnic siliciclastics including paleosoils suggestive of water-logging make up large parts of the Upper Freshwater Molasse in the North Alpine Foreland Basin [5].

Slight SE-ward inclination of the South German terrane in response to the Alpine orogeny caused the Jurassic limestones and deeper parts of the SFA to progressively emerge. Karstification of the SFA might have commenced in the Cretaceous but has been penetrative since the Paleogene [6]. A high karst groundwater level within the SFA is in accord with a high global sea level and a subtropical-humid regional paleoclimate in the Miocene. The high supply of groundwater in the Ries-Steinheim area is, moreover, substantiated by the spontaneous inflow of water and the formation of the Ries and Steinheim crater lakes, pronounced degassing [7] and fluvial reworking [8] of Ries ejecta, and the precipitation of freshwater limestone deposits [9] at both craters soon upon impact (e.g., Wallerstein at the Ries; Steinhirt at Steinheim).

Ries and Steinheim impact ejecta petrology is, furthermore, compatible with elevated water contents in the target. Strong dispersion of impact melt, as well as the formation of accretionary lapilli in the Ries suevite [10], might suggest water-saturated target rock conditions. Ries impact glasses are known to contain comparatively high amounts of water [11], and surficial suevites are intensely altered to clay minerals [12]. Likewise, impact melt particles in the largely carbonatic Steinheim impact breccia have been transformed into hydrous phyllosilicates [13].

As a nearby volcanic event 'analog', the roughly contemporaneous (~13-17 Ma) volcanism at the Urach volcanic field, a ~1,500 km³ olivine melilititic volcanic province comprising more than 350 tuff breccia-bearing maar-diatremes set in the sedimentary succession of the central Swabian Alb and its foreland, demonstrates the strong impact of groundwater in contact to magmatic heat [14]. Explosive phreatomagmatism characterized by (multiple) eruptions at variable levels of the host rock and the subsequent formation of maar lakes (e.g., the Randecker Maar) indicate deep groundwater saturation of the SFA in Miocene time.

**Conclusions:** The Ries-Steinheim impacts occurred in a water-saturated paleoenvironment, maybe best described as a landscape of rivers, wide swamplands, and lakes. In addition to surficial waters [4], the deeply karstified plateau of the SFA provided substantial amounts of subsurface water that probably influenced the formation and emplacement of Ries and Steinheim impact ejecta.

**References:** [1] Stöffler D. et al. (2002) *MAPS, 37*, 1893-1907. [2] Buchner E. et al. (2010) *MAPS* (in press). [3] Buchner E. et al. (2007) *Icarus, 191,* 360-370. [4] Artemieva A. (2009) *MetSoc, 72,* abstr. #5049. [5] Maurer H. and Buchner E. (2007) *ZDGG, 158,* 271-285. [6] Strasser M. et al. (2009) *Geomorphology, 106*, 130-141. [7] Newsom H. et al. (1986) *JGR, 91*, E239-E251. [8] Buchner E. and Schmieder, M. (2009) *MAPS, 44*, 1051-1060. [9] Arp G. (2006) SEDIMENT Göttingen field guide, p. 213-236. [10] Graup G. (1981) *EPSL, 55*, 407-418. [11] Osinski G. R. (2003) *MAPS, 38*, 1641-1667. [12] Muttik N. et al. (2008) *MAPS, 43*, 1827-1840. [13] Schmieder M. and Buchner E. (2010) *LPSC, 41*, abstr. #2103. [14] Kröchert J. et al. (2010) *ZDGG, 160*, 325-331.

**THE FAYA BASIN (N CHAD) REVISITED – STRUCTURAL INSIGHTS FROM CENTRAL PEAK MORPHOLOGY AND POTENTIAL MARTIAN ANALOGS.** M. Schmieder[1] and E. Buchner[1,2], [1]Institut für Planetologie, Universität Stuttgart, Herdweg 51, D-70174 Stuttgart, martin.schmieder@geologie.uni-stuttgart.de. [2]HNU Neu-Ulm University, Wileystrasse 1, D-89231 Neu-Ulm, Germany.

**Introduction:** The ~2 km Faya basin (18°10' N, 19°34' E) is an enigmatic circular (slightly polygonal) feature in the desert of the Borkou-Ennedi-Tibesti, northern Chad. With an elevated 'crater' rim, a deep annular moat, a prominent central 'peak', some possible rim slumps/terraces, as well as a set of concentric annular faults, the Faya basin bears a striking morphological-structural resemblance to small, complex impact structures [1]. The Faya basin is hosted by flat-lying Devonian sandstones of the Borkou plateau, which constrains the maximum age of the structure. The confirmed impact structures of Aorounga (16 km), Gweni Fada (22 km) [2], and the nearby Mousso structure (3.8 km) of possible impact origin [3] are located in the same region. Due to the aftermath of the civil war in Chad and serious political instability, field studies of the Faya basin are currently impossible.

**Remote Sensing:** Earlier studies on the Faya basin [1] were based on Landsat-7 ETM+ satellite images (15/30 m/pixel) of rather poor ground resolution. Recent SPOT-5 satellite imagery (2.5 m/pixel) provides higher-resolution data.

**New Observations and Discussion:** A close-up view of the Faya basin still exhibits the characteristic morphological-structural features described earlier [1] (Fig. 1A). However, SPOT-5 data reveal some conspicuous internal features within the central peak of the Faya basin (covering an area of ~250x150 m). The peak represents a slightly triangular, complex 'ridge-shaped' topographic high, characterized by apparent ~SW-NE-trending bilateral symmetry of crests of hills and elongation (Fig. 1B-C). The divergent arrangement of (sandstone) crests of hills in the complex central peak of the Faya basin suggests that the sedimentary rocks are locally steeply inclined, in turn suggesting stratigraphic uplift within the central peak. Similar morphological features occur at the central uplifts of some impact craters on Mars (Fig. 1D-E). Our observations, together with potential Martian morphological-structural analogs, support the theory that the Faya basin could be a small, complex impact structure. Shock-metamorphic studies would be desirable in order to substantiate the impact hypothesis.

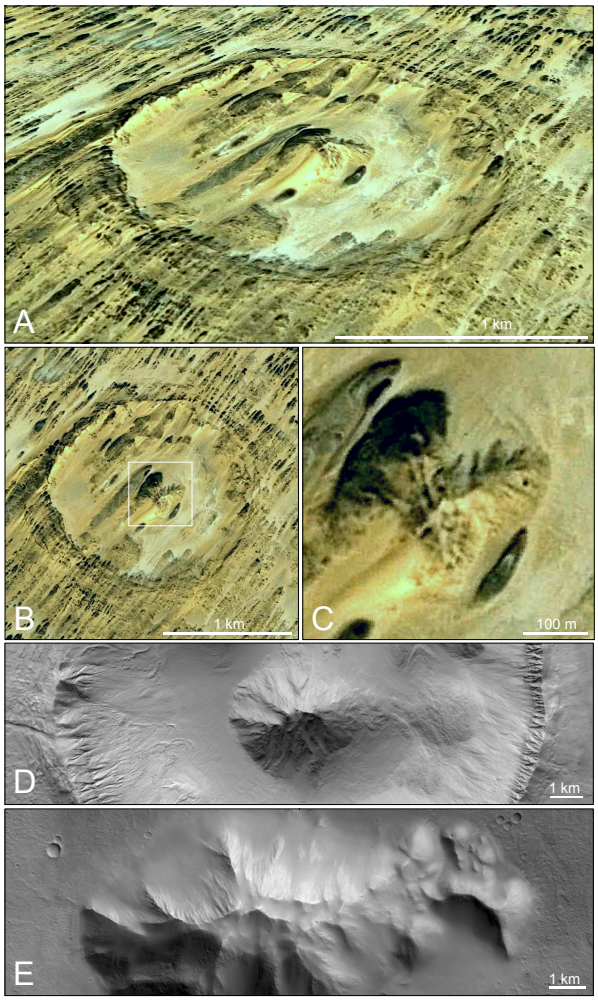


**Fig. 1:** The Faya basin and potential Martian analogs. **A**: Perspective view of the Faya basin; note the distinct elevated 'crater' rim, an annular moat partially covered by desert sands and salts, the prominent central peak, concentric faults, as well as NE-SW-trending yardangs (see [1] for details; 3-fold vertical exaggeration; North is top). **B**: Satellite image scene of the Faya basin (compare A). **C**: Close-up of the central peak (see white box in B for position); A-C: CNES SPOT-5 image; Google Earth. **D**: An unnamed ~19 km complex Martian impact crater (38.5°N, 99.2° E) exhibiting a complex, 'ridge-shaped' central uplift (HiRISE image PSP_007845_2190_RED). **E**: Central uplift of the ~115 km Pickering crater on Mars (33.5°S, 132.7° W; HiRISE image PSP_006865_1460_RED); HiRISE image source: NASA/JPL/University of Arizona.

**References:** [1] Schmieder M. and Buchner E. (2007) *J. African Earth Sci., 47,* 62–68. [2] Koeberl C. et al. (2005) *Meteoritics & Planet. Sci., 40,* 1455-1471. [3] Buchner E. and Schmieder M. (2007) *J. African Earth Sci., 49,* 71–78.

**MULTI-SCALE LUNAR IMPACT CRATER TOPOGRAPHY FROM LROC WAC/NAC STEREO DATA.**

F. Scholten[1], J. Oberst[1,2], and M .S. Robinson[3], [1]German Aerospace Center, Institute of Planetary Research, Rutherfordstr. 2, D-12489 Berlin, Germany, (frank.scholten@dlr.de), [2]Technical University Berlin, Institute for Geodesy and Geoinformation Sciences, Berlin, [3]School of Earth and Space Exploration, Arizona State University, USA.

**Introduction:** From the mean LRO orbit altitude of 50 km the Lunar Reconnaissance Orbiter Camera (LROC) [1,2] provides image data with cross-track and along-track stereo data from which we derive digital terrain models (DTM) of the lunar surface. We adapted the DLR photogrammetric processing system, which has been used operationally for DTM generation from Mars Express HRSC [3,4] and other stereo imagery, to LROC data processing. While LROC WAC images are used for the derivation of global topography [5], LROC NAC data (~0.5 m/pxl) allow for local topographic mapping [6]. DTMs from stereo typically support the topographic analysis of contiguous areas and surface features (e.g. craters), at least as long as DTMs derived from laser altimetry suffer from significant gaps between adjacent tracks.

**WAC Stereo DTM Generation:** From a polar orbit, the Wide Angle Camera (WAC) of the Lunar Reconnaissance Orbiter Camera system (LROC) provides image data with substantial cross-track stereo coverage (50% overlap and 30° stereo angle at the equator). The LROC WAC consists of a 1k x 1k CCD frame which is split up into sub-frames for seven different spectral bands, two ultraviolet bands and five bands in the visible spectrum. Each band consists of 14 lines/subframe, while subframes form an image strip using the pushbroom principle ("push-frame"). WAC's IFOV is about 5.1 arcmin, its ground scale from 50 km orbit altitude is about 75 m/pxl. For the stereo processing we used WAC data of the visible bands, which comprise 704 pxl/line. Within the overlap of WAC images from adjacent orbits we carry out area-based image matching. Ground points are derived by 3D forward ray intersection and finally a 200 m DTM grid with a vertical accuracy of a few tens of meters is interpolated..

**NAC Stereo DTM Generation:** LROC NAC consists of 2 pushbroom scanners, NAC-L and NAC-R, both with an IFOV of 2 arcsec (0.5 m ground scale from 50 km orbit altitude) and 5,000 pxl/line. We use NAC data from 2 subsequent orbits for stereo. DTMs are derived as described for WAC. The typical DTM grid is 2 m with a vertical accuracy of a few decimeters.

**Crater Topography:** We will present a multi-scale series of DTMs and profiles from NAC stereo data, describing the horizontal and vertical structures of small craters (few tens of meters in diameter, e.g. Fig. 1), as well as WAC DTMs of larger craters up to tens of kilometers in width, impact basins like the South Pole-Aitken basin, and finally topography of entire hemispheres (e.g. Fig. 2).

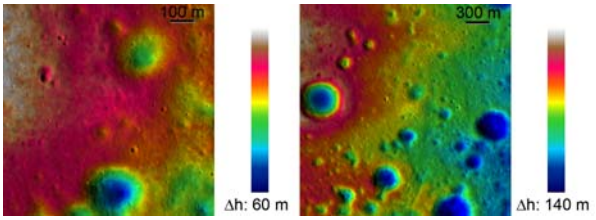


Fig. 1: Subsets of local LROC NAC DTMs (near the Apollo 17 landing site).

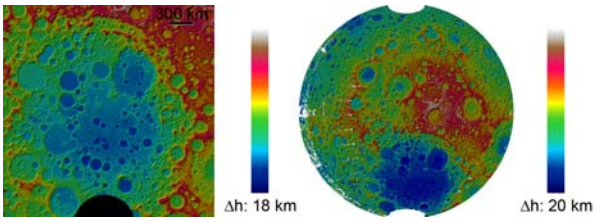


Fig. 2: Regional and global LROC WAC topography of the South Pole-Aitken basin (left) and the lunar far side (right)

**References:** [1] Robinson M. S. et al. (2005) *LPS XXXVI,* Abstract #1576. [2] Chin G. et al (2007) *Space Sci. Rev., 129,* :391–419, doi 10.1007/s11214-007-9153-y. [3] Gwinner K. et al. (2009) *PE&RS, 75(9),* 1127-1142. [4] Gwinner k. et al. (2009) *Earth Planet. Sci. Lett*., doi:10.1016/j.epsl.2009.11.007 (in press). [5] Scholten F. et al. (2010) *LPS XLI* , Abstract #2111. [6] Oberst J. et al. (2010) *LPS XLI* , Abstract #2051.

**THE CHICXULUB EJECTA BLANKET AND ITS BEARING ON SAMPLE RETURN MISSIONS TO MARS.** F. Schönian[1], T. Kenkmann[1,2] and D. Stöffler[1], [1]Museum für Naturkunde, Leibniz-Institute for Research on Evolution and Biodiversity at the Humboldt University Berlin, Invalidenstr. 43, D-10115 Berlin, Germany, frank.schoenian@mfn-berlin.de, [2]Institute of Geosciences, University of Freiburg, Alberstr. 23-b, D-79104 Freiburg, Germany, thomas.kenkmann@geologie.uni-freiburg.de.

**Introduction:** The ejecta blanket of the Chicxulub crater (Ø 180 km, 65 Ma) is one of the few examples for a well preserved ejecta blanket of large impact structures on Earth. It extends up to 5 crater radii from the center [1,2]. Due to this large runout it has been considered since its recognition as a primary example for comparative studies with Martian impact craters [2, 3, 4].

**Distribution and characteristics:** The Chicxulub ejecta blanket is widely distributed over the Yucatán Peninsula. While it is covered with Cenozoic deposits close to the crater, it crops out at the surface on the Central and Southeastern Peninsula (Fig. 1). It can be subdivided into three radial zones [5]. *The inner ejecta blanket* is represented by breccias recovered from the UNAM 7 drill core, 105 km from the impact center (Fig. 1). It is characterized by a two-fold succession of a thick sedimentary megabreccia with rare melt particles overlain by melt-rich suevites with abundant basement clasts [5]. The contact between these units is transitional. *The intermediate ejecta blanket* is typically composed of locally eroded bedrock material. Altered impact melt is very rare and basement clasts and shocked minerals are absent. Some abraded clasts and rarely shear planes do occur in its lower parts [5]. *The outer ejecta blanket* again contains mainly components eroded from the subsurface. However, altered impact melt and crystalline basement clasts are present and occur together with shocked quartz mixed with the local material. Clasts do often display abrasion features and subhorizontal shear planes with slickensides are abundant [2].

**Discussion:** These characteristics have been explained by a combination of the two processes involved in the ejecta emplacement on planets with an atmosphere and subsurface volatiles: The lower inner and the intermediate ejecta have been deposited by *Ballistic Sedimentation*, while in the outer part *Atmospheric Ring Vortices* overrode the ejecta curtain and deposited crater material that later became eroded by the secondary ejecta flow (Fig. 1, [5]). In order to assess these processes on Mars a “double layer ejecta” (DLE) or “multiple layer ejecta” (MLE) crater preferably on sedimentary terrain should be sampled from its proximal to its distal ejecta blanket.

**References:** [1] Ocampo A. C. et al. (1997) *LPS XXVII,* Abstract #1861. [2] Kenkmann T. and Schönian F. (2006) *MAPS. 41(10),* 1587-1603. [3] Pope, K. O. and Ocampo A. C. (1999) *LPS XXX,* Abstract #1380. [4] Schönian F. et al. (2004) *LPS XXXV,* Abstract 1848. [5] Schönian F. et al. (2008) *LMI IV,* Abstract 3100.

**Fig. 1:** Sketch of the Yucatán-Peninsula during the final stage of ejecta emplacement (elevation not to scale).

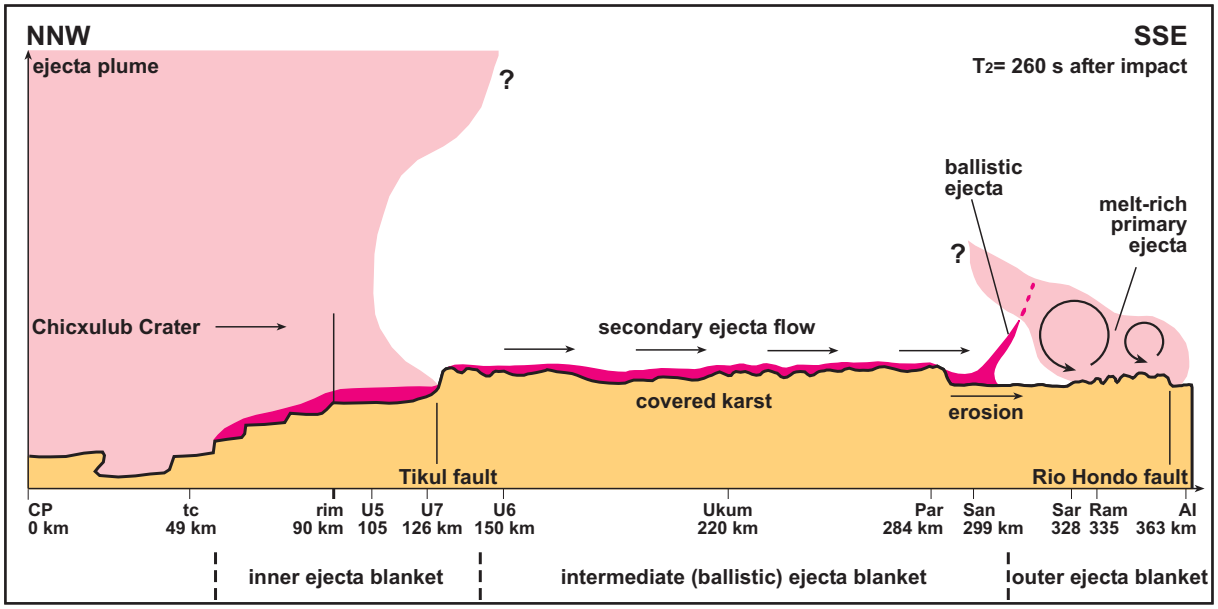

**THE IMPACT OF RIES CRATER RESEARCH ON THE RECOGNITION AND CLASSFICATION OF IMPACT-METAMORPHOSED PLANETARY ROCKS.** D. Stöffler[1] and W. U. Reimold[1], [1]Museum für Naturkunde – Leibniz Institute at the Humboldt University Berlin, Research Department / Mineralogy Section, Invalidenstrasse 43, D-10115 Berlin, Germany; dieter.stoeffler@mfn-berlin.de

**Introduction:** The Ries crater (Ø = 25 km) is the best preserved and best studied mid-sized complex terrestrial impact crater formed in a target with ~ 700 m of Mesozoic sedimentary rocks on top of crystalline rocks. The 14.35 m.y. old [1] crater displays an uplifted inner ring and a two-layer ejecta blanket with a discontinuous layer of suevite on top of a continuous polymict megabreccia ("Bunte breccia") [2].

**Five decades of Ries research:** Modern research prompted by the discovery of coesite in 1960 [3] has been continuous, intensive, interdisciplinary, and international within 5 decades. It has been repeatedly stimulated by progress in the exploration of terrestrial planets, but it also fostered related studies of other cratered landscapes and impact-metamorphosed rocks.

**Major messages from Ries research:** Studies of the Ries crater and its rocks have been fundamental for many outstanding issues of planetary impact cratering research. The most conspicuous issues are: (a) Properties, geological setting, stratigraphy, and classification of allochthonous and autochthonous impact formations including distal ejecta (tektites) [4,5,6,7]. (b) Recognition and systematics of progressive shock metamorphism of rocks [8,9] including the identification and geologic setting of metastable high pressure minerals [e.g., 10,11,12]. (c) Discovery and interpretation of impact-induced geophysical anomalies [4,5,6]. (d) Ground-truth for the model of secondary mass wasting on planetary surfaces induced by the ejecta deposition [13]. (e) Ground-truth for post-impact hydrothermal activities in "hot" impact formations such as suevite with applications to Mars (14,15). (f) Recognition and genesis of different types of suevite [6,16] and most recent attempts for a new genesis of suevite by "quasi-phreatomagmatic" explosions based on the concept of "fuel-coolant"-interaction [17]. (g) Modern quantitative structural geology of impact craters [18].

**Currrent systematics of planetary impactites:** Ries crater studies have been instrumental for the development of a comprehensive classification and nomenclature of (1) impact-induced rock types (impactites), and (2) progressive shock metamorphism of rocks including meteorites [19,20,21,22]. Earlier classification attempts were taken up by the IUGS Subcommisssion on the Systematics of Metamorphic Rocks [9,23]. The IUGS proposal applicable to all terrestrial planetary bodies, involves: (1) Impactites from single impacts, and (2) impactites from multiple impacts. Type 1 is subdivided into "proximal" and "distal". Proximal impactites are: (1) Shocked rocks, (2) impact melt rocks, and (3) impact breccias. Impact breccias are subdivided into (3.1) monomict breccias, (3.2.) lithic breccias (without cogenetic melt particles), and (3.3.) suevite (with cogenetic melt particles) with 3.2 and 3.3 being polymict breccias.

**Conclusion:** For future sampling activities of astronauts or robots on planetary bodies it appears mandatory to educate them on macroscopic properties of terrestrial impactites and their parental craters.

**References:** [1] Buchner E. et al. (2003), *Int. J. Earth Sci. Geol. Rund. 92*, 1-6. [2] Stöffler, D. and Ostertag, R. (1983) *Fortschritte Mineralogie 61, Bh 2*, 71-116. [3] Shoemaker, E.M. and Chao, E.C.T. (1961), *JGR 66*, 3371-3378. [4] Pohl, J. et al. (1977) in Roddy, R.O. et al. (eds.) Impact and Explosion Cratering, Pergamon Press, N.Y., 343-404. [5] Bayer. Geol. Landesamt (ed.) (1969) *Geologica Bavarica 61,* 478 pp. [6] Bayer. Geol. Landesamt (ed.), (1977) *Geologica Bavarica 75,* 470 pp. [7] Engelhardt, W. v. (2005) *Geochim. Cosmochim. Acta 69*, 5611-5626. [8] Stöffler, D. (1971*) JGR 76,* 5541-5551. [9] Stöffler, D. and Grieve, R.A.F. (2007) in Fettes, D. and Desmons, J. (eds.) *Metamorphic Rocks,* Cambridge Univ. Press, 82-92, 111-125, and 126-242. [10] Schmitt, R. et al. (2005) in Kenkmann et al. (eds.) *Geol Soc. of America Special Paper 384*, 299-314. [11] El Goresy et al. [2001] *Science 293*, 1467-1470. [12] Stähle, V. et al. (2010) Contrib.Min.Petrol, in press. [13] Hörz et al. (1983) *Rev. Geophys. Space Phys. 21*, 1667-1725. [14] Newsom, H. E. et al. (1986) *JGR 91, B13,* E239-E251. [15] Muttik et al. (2008) *Meteoritics & Planet. Sci., 43,* 1827-1840. [16] Stöffler, D. et al. (2009) *LPS XL,* Abstract #1504. [17] Artemieva, N.A. et al. (2009) *LPS XL,* Abstract #1526. [18] Kenkmann, T. and Ivanov, B.A. (2006) *EPSL, 252*, 15-29. [19] Stöffler, D. et al. (1980) in Papike J.J. and Merrill, R.B. (eds.) *Proc. Conf. Lunar Highland Crust*, Pergamon Press, N.Y., 51-70. [20] Stöffler, D. et al. (1991) Geochim. Cosmochim. Acta *55*, 3845-3867. [21] Stöffler, D. et al. (2006) and [22] Hiesinger, H. and Head, J. (2006) both in Joliff, B. L: et al. (eds.), *New Views of the Moon, Rev. Mineral. Geochem., 60,* Mineral. Soc. America, 519-596 and 1-81, resp.. [23] Fettes, D and Desmons, J., eds. (2007) *Metamorphic Rocks,* Cambridge Univ. Press, 244 pp.

**MODERN DATA ON THE GEOLOGICAL STRUCTURE OF ILYINTSI ASTROBLEME – IMPORTANT GEOLOGICAL AND ARCHAEOLOGICAL MEMORIAL IN UKRAINE.** A.Valter, A.I. Pisansky, Institute of Applied Phys. Acad. of Sci. of Ukraine, dep.50. Av. Nauki, 46, apt.201, Kiev-03028, Ukraine; avalter@iop.kiev.ua

**Introduction.** The outcrops of Ilyintsi astrobleme impactites known since 1851 are the geological and cultural memorial in Ukraine of national significance.

The impact nature of this structure was identified in 1973 and the first simplified geological map was published in 1975 [see reviews in 2,3]. The astrobleme is sheard near 400 m.

Since the IIIrd century AD, for about one thousand years, glass poor suevites from the Ilyintsi outcrops have been worked out for producing hand millstones [4,5].

The artefact from the deer antler [6] found in the ancient quarry contributes to data revealing the commercial connections in Kievan Russia at that time [7].

This paper presents new results on the Ilyintsi astrobleme geology.

**Methods, results and discussion.** In 1953-1984 the structure was the object of the geological survey and prospecting for Ni, U, nonferrous metals, diamonds, etc. by core drilling. We collected 3040 samples from 76 drill-holes with a full description of the whole core.

We examined this collection and all the geophysical data. The 2D-distribution of different types of rocks over the Pre-Cenosoic area and across the cut were constructed taking into account the relief. The 2D-image was obtained by digitization of the data using the original software and GIMP graphics (fig.1).

The Ilyintsi astrobleme is usually considered to be a structure elongated in the NW-SE direction with the degree of ellipticity 1,4 -1,5 as illustrated in [2,8,9].

The results obtained (fig. 1) show the structure ellipticity to be considerably less: $1{,}17\pm0.02$ with E-W elongation.

In the case of circular approximation the average diametr of the suevite cover is $4{,}8\pm0{,}1$ км (inner circle in fig. 1). The outer circle (d=6,1 km) reflects the spread of the autigenic breccia and relicts of the crater sediments.

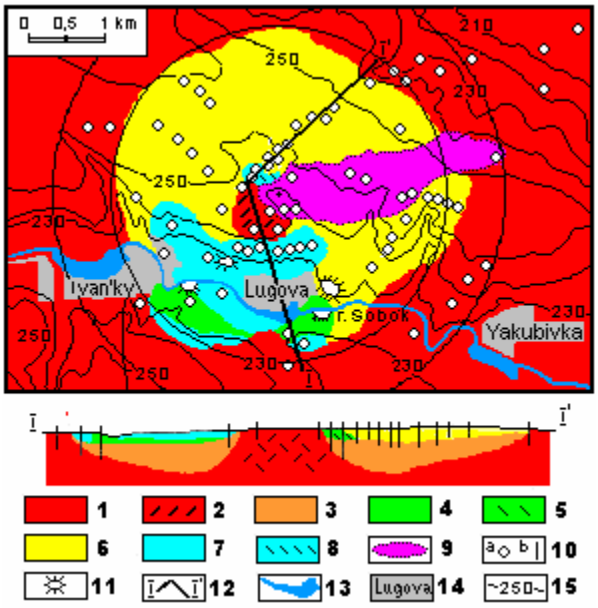


Fig. 1. Simplified map and cut across Ilyintsi astrobleme (coordinates of the center: $49^0 07'$N; $29^0 07'$E)

1 – Basement granitoids; 2 – Bracciated granitoids of Central uplift; 3 – Impact breccia, partly allogenic; 4 – Massive glassy impactites (tagamites by V.L. Masaitis); 5 – region of impactite glassy dykes in suevites (in the cut); 6 – Glassy poor suevites; 7 – The area (in the map) of tagamite layer spreading under the glassy poor and glassy rich suevites; 8 – The area (at the map) of tagamite veins spreading in suevites; 9 – The relicts of crater sediments ($S_2$-$D_1$); 10 – Drill holes; a – in the cut; b – in the map; 11 – Outcrops; 12 – The cut line; 13 – The Sobok river and ponds; 14 – Villages; 15 – The horizontal lines above the sea level.

**References:** [1] Tarasenko V.E. (1898) About the effusive rock from Lipovetz district of Kiev province. Kiev, 15p. [2] Gurov E.P. et al. (1997) *Meteoritics & Planet. Sci., 33,* 1317-1333. [3] Valter A.A. et al. (2000).*Proc. CAMMAC-99.*Vinnytsa, 1999, 367-380 (in Russian). [4] Havl'uk P.I (1973) *Archaeology (Kiev), 9, 34-40 (in Ukrainian).* [5] Klimovsky S.I., Gurov E.P (2001) */http:arheology.kiev.ua /journal/*(in Russian). [6] Valter A. (2009) *Vernadsky-Brown Microsymposium 50. Abstract m50_56.* [7] Valter A., Pisanski A.I. (2010) *LPS XXXXI,* Abstract #1069. [8] Danilin A.N. In:*Masaitis et al. Geology of astroblemes. Leningrad, 1980, 321p. 37-44* (in Russian). [9] Gurov E.P. et al. (2006) *Geological Journal (Ukraine), N4, p.105-116* (in Russian).

**MICROSCOPIC IMPACT FEATURES IN THE CENTRAL UPLIFT OF SERRA DA CANGALHA.** Marcos A.R. Vasconcelos[1,2], Wolf U. Reimold[2], Alvaro P. Crósta[1] and Thomas Kenkmann[3], [1]Institute of Geosciences, University of Campinas, Campinas, SP, Brazil. (vasconcelos@ige.unicamp.br, alvaro@ige.unicamp.br),[2] Museum für Naturkunde, Leibniz Institute at Humboldt University Berlin, Berlin, Germany (uwe.reimold@mfn-berlin.de),[3] Institut für Geowissenschaften, Albert-Ludwigs-Universität Freiburg, Freiburg, Germany.

**Introduction:** The Serra da Cangalha (SdC) structure is the second largest Brazilian impact structure with a 13.7 km diameter and a central uplift of 5.8 km diameter [1]. It is located in Tocantins state, northeastern Brazil, and formed in undisturbed Phanerozoic sedimentary rocks of the Parnaíba Basin. Impact features, such as shatter cones and PDFs, had been described in SdC rocks in the 1980s [2, unpublished]. In the early 1970´s, the Brazilian Department of Mineral Production (DNPM) carried out mineral exploration in the central part of the structure. This resulted in three boreholes that all reached depths of 200 m. During a field campaign to SdC in 2009 we collected samples at outcrops within and outside of the central uplift, and studied additional drill core samples. Our preliminary analysis by optical microscopy resulted in the discovery of some diagnostic shock deformation features, thus confirming the meteorite impact origin of the Serra da Cangalha structure.

**Petrographic analysis:** The three principal lithotypes occurring in the Serra da Cangalha structure comprise siltstones, sandstones and impact breccias. We observed a strong microdeformational contrast among the rocks from the central uplift and from outside of the central uplift. The samples from outside of the central area are characterized by quartz grains that are mostty coarse-grained and rounded, and practically without any deformation features. There are no planar microdeformations and only minor brittle deformation (fracturing) could be registered. The samples from the center are derived from blocks of sandstone, as well as from monomict and polymict breccias, which were found in close proximity to locations showing shatter cones. Both, breccias and shatter cones, were only found within the inner depression of the central uplift, which corresponds to the area of occurrence of the lowermost stratigraphic unit, the Longá Formation shale. The main characteristic of quartz shocked in the 10-30 GPa pressure regime is the presence of planar microdeformations, which include planar fractures (PFs) and planar deformation features (PDFs). The formation of PFs starts at low shock pressure(< 8 GPa), whereas PDFs are formed at higher pressures (>8 GPa) [3].

Preliminary analysis of thin sections from the central uplift showed that sandstones exhibit intense cataclasis of quartz and feldspar grains. In general, the grains exhibit angular margins and are often fractured internally. Especially samples of breccias and shatter cones show intense fracturing with distinctive PF development, with up to three sets of different orientations in quartz grains. PFs are also frequent in sandstone samples from the collar along then outside of the central depression, and also in quartz of drill core samples. The drill core samples comprise fine-grained sandstones, shales, siltstones, and breccias. One of the samples, from approximately 90 meter depth, exhibits strong brittle deformation with extensive PF development. Thin section analysis of the lithologies from the central uplift also revealed the presence of feather features with planar fractures mostly parallel to (0001) in quartz. Furthermore, we found intersecting sets of PDF in quartz. According to these observations we can determine general isopachs representing shockm levels attained by the rocks of the Serra daCangalha impact structure. The strata exposed in the central region was subjected to considerable shock pressure of 10-30 GPa, whereas the collar rocks experienced <10 GPa pressures, and the samples from exposures in the annular basin and crater rim only having experienced weak brittle deformation, likely <1-2 GPa.

**Conclusions:** Only the presence of diagnostic shock-metamorphic effects, such as shatter cones and PDF, are generally accepted as unambiguous evidence for an impact origin [4]. Our preliminary study allowed to identify some these diagnostic impact features in the field (shatter cones) and at the microscopic scale. The recognition of these features allows to conclude beyond doubt that Serra da Cangalha was formed by a meteorite impact event. This event subjected the strata of the central region of Serra da Cangalha to shock pressures in excess of 10-30 GPa.

**References:** [1] Kenkmann, T. et al. (2010) 41st LPSC, abstract #1237. [2] McHone, J. F. Jr. (1986), PhD thesis. University of Illinois at Urbana-Champaign, 210 pp. [3] Stöffler, D. & Langenhorst, F.(1994), *MAPS* 29:155-181. [4] French, B.M. and Koeberl, C. (2010) *Earth-Sci. Rev.* 98, 123-170.

**THE RIES IMPACT DIAMONDS: DISTRIBUTION, MICROSCOPY, X-RAY AND SOME OTHER DATA.**

S. Vishnevsky[1] & N. Palchik[1], [1]Inst. of Geology & Mineral., Novosibirsk, 630090, RUSSIA (svish@uiggm.nsc.ru).

***Introduction:*** First find of Ries impact diamonds, RIDs, was made 35 years ago (Special report 15350-15, 1975, unpublished, [1]), and licenced for press [2] but was out of interest for a long time until the finding was repeated [3] and attracted the attention of western colleagues. Since the moment, a broad international study of RIDs was started, with a peak of the activity in 1995-2003. Various teams [3–11**,** and refs. therein] described a number of RIDs features, including their 2 principally-different genetic types, namely: i) shock-induced apographitic paramorphs, AGPs, (*Greek,* after graphite) [2, 3, 6], and ii) carbon-vapor-deposition, or CVD-diamonds, in terms of [4], derived from the Ries plasma fireball. The data obtained are rather interesting for the shock mineralogy of the carbon system and impact cratering as well. Nevertheless, some questions are still open and need a further study.

***Spatial distribution of RIDs:*** AGPs are found in both fallout and fallback suevites from many points of crater and its surrounding (Altebürg, Aumühle, Hainsfarth, Heerdorf, Hohenaltheim, Otting, Seelbronn, Zipplingen, drill hole Nördlingen-1973 [2, 3, 5–11]), and in glass-bearing bottom breccia dyke Unterwilfringen [9]. The main AGP carriers are the glass bombs and shocked gneiss fragments. The AGP concentrations in the rocks are as 0.06÷0.7 ppm. A lack of the diamonds in Ries massive impact melt rocks [9] looks like unusual: their equivalents, tagamites, are diamond-bearing in Popigai and some other sites. CVD RIDs are found in Otting suevite glass, but are supposed to be of a broad extent both in Ries and other impact sites [4].

***Optical & SEM/TEM microscopy of RIDs:*** AGPs, ranging in size from <50 to 300 μ, are mainly flat ones of 5÷40 μ in width [2, 6]; grains of <5–10 μ in size are also known in shocked graphite [3, 10]. Many of AGPs are pseudo-hexagonal elongated para-crystals resembling morphology of the precursor graphite, including its various twinning features. The platelet intergrowth is the most common among the features [3, 6]. Some grains are kinked or bent; xenomorphic grains are very rare [9]. Both primary (inherited PG features) and secondary (planar deformation elements formed together with the AGPs) hatching [6], of one to several systems per grain, is common for some flattened diamonds. The hatching is well-expressed in luster, color and relief [5, 6]. Many of APG grains show various intensity of surface etching which took place in the hot impact melt by the action of K, Na and $OH^-$ components. The color of APGs varies from white or colorless to yellow, brown, gray and black. Lamellar or hatching fabric can control the distribution of dark masses (graphite or amorphous carbon?) within the AGPs. Light-colored grains are transparent and birefringent [2, 3, 6]. Birefringence, 0.007÷0.020, is correlated with lonsdaleite content (25÷75 %, respectively, data by [6]). CVD-diamonds [4] are the skeletal aggregates of cubic diamond crystallites, of 0.01÷2 μ in size, showing the epitaxial intergrowth with SiC crystallites of up to 1 μ in size.

***X-Ray data on AGPs composition:*** Following to these data, the grains are fine to superfine polycrystalline aggregates made up of cubic+hexagonal diamond phases mixed up in various proportions, from entirely cubic ones to those with up to 75 % of lonsdaleite [6]. The size of the crystallites is varying from 10÷100 nm to ~1 μ [2, 3, 6]; at this, the cubic phase is more "coarse" in respect to hexagonal one [3, 6]. Laue patterns of crystallites show their preferred orientation, but its degree can vary from moderate to well-expressed one, up to that which is equal to the state of "mono-crystal". Dark-colored AGPs and grains with black lamellae inclusions show X-ray detected graphite impurity [6, 8]; sometimes, d-spacing equal to chaoite (lines of 0,43 and 0,403 nm) is also present [6].

***Density and carbon isotopy of RIDs:*** Density dispersion, <3.28÷3.48 g/cm$^3$, is found for AGPs, correlating with their color (the darker the color the lower the density [3]). Following to [8], $\delta^{13}C$ of RIDs is either –16‰ to –17‰ or –25.2‰ to –26‰, indicating heterogeneous sources of C; at this, the “lighter” Otting AGPs are equal to the basement graphites.

***Summary:*** The data presented above, describe the RIDs main features. Other features and still open problems on the topic are shown in [12] and refs. therein.

**References:** [1] Vishnevsky S. (2007) *Astroblemes.* Novosibirsk: Nonparel Press. 288 p. (in Russian). [2] Rost R., et al. (1978) *Doklady AN SSSR, 241,* 695-698 (in Russian). [3] Masaitis V., et al. (1995) *Proc. Russ. Min. Soc., 4,* 12-19 (in Russian). [4] Hough R., et al. (1995) *Nature, 378,* 41-44. [5] Vishnevsky S., et al. (1997) *Impact Diamonds: their features, origin & significance.* Novosibirsk: SB RAS Press. 110 p. (in Russian & English). [6] Valter A., et al. (1998) *Mineralogichesky Zhurnal, 20,* 3-12 (in Russian). [7] Abbot J., et al. (1998) *MAPS, 33,* A7. [8] Siebenschock M., et al. (1998) *MAPS, 33,* A145. [9] Schmitt R., et al. (1999) *MAPS, 34,* A102. [10] El-Goresy A., et al. (1999) *MAPS, 34,* A125-A126. [11] El-Goresy A., et al. (2001) *American Mineralogist, 86,* 611-621. [12] Palchik N., Vishnevsky S. (2010) *Nördlingen-2010, Print-only section*. Abstract.

**Detection of subsurface megablocks in the Ries crater, Germany: Results from a field campaign and remote sensing analysis.** M. Willmes[1], S. Sturm[1], H. Hiesinger[1], T. Kenkmann[2] and G. Pösges[3], [1]Institut für Planetologie, Westfälische Wilhelms-Universität Münster, Germany (malte.willmes@uni-muenster.de), [2]Albert-Ludwigs Universität Freiburg, Germany, [3]Rieskrater-Museum Nördlingen, Germany.

**Introduction:** The Ries impact crater, located in southern Germany, represents one of the best studied impact craters on Earth and is used as an archetype for complex craters across the solar system. However, its geologic structure still poses questions regarding crater formation mechanics. The complex geology of the Ries crater has been studied in detail by many researches over the last 40 years [e.g. 1 and references therein]. The megablock zone is located between the inner crystalline ring and outer crater rim and is characterized by a hummocky morphology. It consists of allochthonous blocks of crystalline and sedimentary material, Bunte Breccia deposits and parautochthonous sedimentary blocks that slumped into the crater during the modification stage [2, 3]. Analysis of Google Earth image data has revealed possible megablock structures in the near subsurface that have not been mapped in detail before (Fig. 1). They can be observed in fields with spare vegetation and show structures that are similar to megablock outcrops. Their visibility is related to humidity differences in the topsoil that is most likely caused by the different composition and/or permeability of the underlying megablock material.

**Methods:** We used a combination of remote sensing and field analyses to investigate the subsurface megablocks. Google Earth images with an average resolution of 1m/pxl were used to search the megablock zone for possible subsurface megablock structures. The mapping was done using ArcGIS software. The remote sensing analysis was followed by a field campaign in which we used shallow drilling devices like Prückhauer and Percussion Piston Corer to verify the observed structures in the near subsurface and to determine their composition.

**Results:** The connection between remote sensing analysis and shallow drilling has proven to be very successful. Most subsurface megablocks are found within a depth of < 5 m. However the shallow drilling was not always successful indicating that some of these blocks might be at greater depth. Weathered material of the megablocks can often be found mixed in with the top soil. This is another tool to locate the approximate location of subsurface megablock in the field. Different albedos were observed in the remote sensing data but connecting these with the depth of the megablock in the sub-surface is not trivial. In fact it depends on many different factors including soil type and humidity.

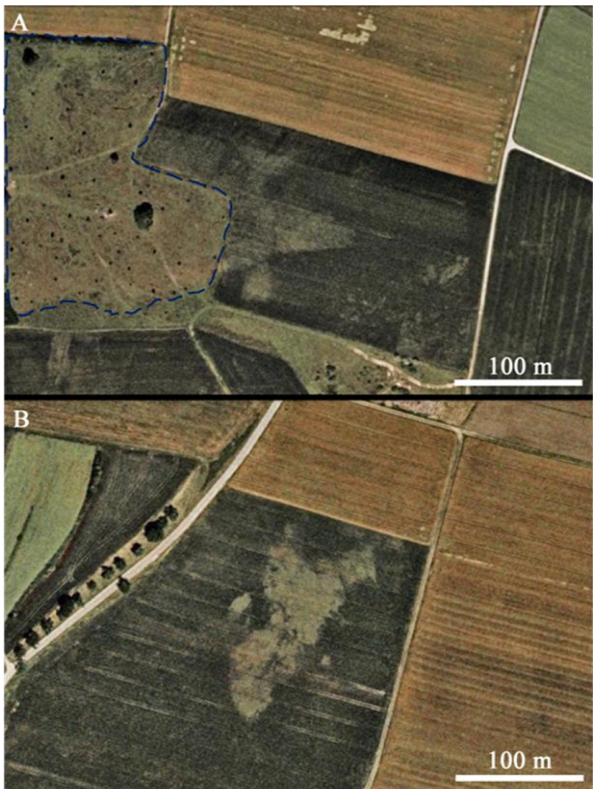


***Fig. 1:*** *Google Earth images showing megablock structures in the subsurface, north is top. (A) Malm limestone megablock outcrop near Hürnheim (marked with blue dots). It dips into the subsurface and can be observed in the dark field on the right side. (B) Crystalline megablock near Marktoffingen that is covered by 40 cm of soil and sand deposits.*

**Outlook:** Further investigation of these features will include the use of a larger drilling device and the analysis of new high-resolution remote sensing images (HRSC-AX) complementing our current database. From the detailed analysis of the megablock zone we hope to gain a more in-depth understanding of the complex geologic history of the Ries crater. In addition this information can be used to better understand the emplacement mechanism of megablock structures in other complex craters on Earth and terrestrial bodies like Moon and Mars.

**References:** [1] Hüttner and Schmidt-Kaler, 1999, Geologica Bavarica, 104, 7-76; [2] Kenkmann and Ivanov, 2006, Earth and Planetary Science Letters, 252, 15-29; [3] Pohl et al., 1977, Impact and Explosion Cratering, Flagstaff, Arizona.

**MODELING THE RIES IMPACT: THE ROLE OF WATER AND POROSITY FOR CRATER FORMATION AND EJECTA DEPOSITION.** K. Wünnemann[1], N. A. Artemieva[2,3], and G. S. Collins[4], [1]Museum für Naturkunde–Leibniz Institute at the Humboldt University Berlin, Germany, [2]Planetary Science Institute, Tucson, AZ 85719 [3]Institute for the Dynamics of Geospheres, Russian Academy of Sciences, Moscow, Russia, [4]Impacts and Astromaterials Research Centre, Dept. of Earth Science and Engineering, Imperial College London, London SW7 2AZ, UK; kai.wuennemann@mfn-berlin.de

**Introduction:** Ries crater is one of the best-studied impact structures in the world. Ries crater is of particular interest for numerical modeling because (1) the crater morphology is relatively pristine in comparison to most other exposed terrestrial complex crater structures; (2) the proximal ejecta deposits are at least partly well preserved (Bunte Breccia, Suevite) and there exist remnants of the distal ejecta (tektite strewn field, Moldavites); (3) a large data set of the subsurface was obtained by geophysical surveys as well as several shallow and one deep drill hole (Forschungsbohrung Nördlingen, 1973). This rich set of observations is unique for the terrestrial complex crater record and serves as an ideal test for numerical modeling of the formation process. Here we summarize briefly the recent modeling attempts of Ries crater formation and the production and emplacement of impactites using the iSALE [1,2] and SOVA [3] hydrocodes.

**Morphology and structural deformation:** Numerical modeling [4,5] shows that the inner part of the crater bounded by a ring of crystalline basement rocks marks approximately the size of the transient crater. Subsequent collapse results in significant structural uplift (which corresponds to the relatively flat inner crater floor) and inward collapsing and slumping of large blocky units of the upper sedimentary layers (forming the so-called megablock zone inside the outer rim). A zone of heavily fractured rocks reaching probably several kilometers below the crater floor is consistent with the observed geophysical anomalies (gravity low, increased electrical conductivity, reduced seismic velocities [6, 4]). The models show that the rheological contrast between the weak sedimentary layers on top of much stronger crystalline basement rocks affected the crater formation processes [5].

**Impact melt** All models predict the production of large quantities of impact melt forming an approximately 200 m thick melt pool in the inner crater. The presence of porous sediments may have even increased the production of impact-melt [7]. The lack of impact melt and the genesis of Suevite that occurs as a 350 m thick layer in the inner crater and as patches on top of the ballistically ejected material outside the crater is still unclear and demonstrates the limitations of current models.

**Distal ejecta (**Tektites): Numerical modeling [8] shows that tektites originate from an extremely thin surficial layer and are ejected with velocities up to 10 km/s at the very beginning of crater formation. The ejected particles are surrounded by high-temperature vapor with similar velocity allowing transportation of the material hundreds of km from the source crater, its devolatalization and solidification in the upper atmosphere. Modeled distribution of particles on the surface resembles the observed fan of Moldavites.

**Proximal ejecta:** Previous assumptions that the outer Suevite may originate from a collapsing impact plume [9, 10] representing some sort of ignimbrite-forming flow [11], or by a low-viscosity melt flow during the crater collapse [12] can be ruled out by our recent numerical modeling studies [13]. Therein we found that (1) ejecta from all stratigraphic units are deposited ballistically without separation; (2) the impact plume above the crater consists mainly of a sediment-derived vapor/melt mixture, with the total thickness of plume deposits inside the crater < 2 m and much less outside.

**Future work:** So far the presence of water was neglected; however the explosive interaction of water with hot melt may initiate additional post-impact explosions (similar to the fuel-coolant interaction or hydromagmatic eruptions). Thus, our working hypothesis is that Suevite is the result of the interaction of the Ries melt pool with an external water source (e.g., rivers). Cooling of the Ries melt pool with an assumed thickness of 200 m to below the glass transition T (~1000 K) and water boiling temperature (373 K) would have taken 0.3 – 3 kyr, during which the crater Suevite fill (and outer Suevite) would have to be produced.

**References:** [1] Amsden et al. (1980) Los Alamos *National Laboratory Report* LA-8095. [2] Ivanov et al. (1997) *Int, J. Impact Eng*. 20, 411-430. [3] Shuvalov V. (1999) *Shock waves 9*, 381–390. [4] Wünnemann et al. (2005), *GSA special paper* 384, 67-83. [5] Collins et al. (2008), *M&PS* 43, 1955-1977. [6] Pohl et al. (1977) *Impact and explosion cratering*, p. 343–404. [7] Wünnemann et al. (2008) *EPSL* 269, 529-538. [8] Stöffler et al. (2002) *M&PS 37*, 1893-1907. [9] Stöffler D. (1977) *Geologica Bavarica 75*, 443-458. [10] Engelhardt W. v. Et al. (1995) *Meteoritics 30*, 279-293. [11] Newsom H.E. et al. (1986) *JGR 91*, E239-E251. [12] Osinski G.R. et al. (2004) *M&PS 39*, 1655-1683. [13] Artemieva N. et al. (2009) *LPSC-40*, abstr. 1526..

# NOTES

# NOTES